



UNIVERSIDADE FEDERAL DE PERNAMBUCO  
CENTRO DE TECNOLOGIA E GEOCIÊNCIAS  
DEPARTAMENTO DE ENGENHARIA DE PRODUÇÃO  
PROGRAMA DE PÓS-GRADUAÇÃO EM ENGENHARIA DE PRODUÇÃO

RAFAEL VALENÇA AZEVEDO

**DEVELOPMENT OF BAYESIAN MULTILEVEL MODELS FOR RELIABILITY  
ASSESSMENT OF UNDER DEVELOPMENT TECHNOLOGIES IN THE OIL AND  
GAS INDUSTRY: CASE STUDIES FOR AN EXPANSIBLE PACKER AND A  
SLIDING SLEEVE VALVE FOR OPEN-HOLE WELLS**

Recife  
2024

RAFAEL VALENÇA AZEVEDO

**DEVELOPMENT OF BAYESIAN MULTILEVEL MODELS FOR RELIABILITY  
ASSESSMENT OF UNDER DEVELOPMENT TECHNOLOGIES IN THE OIL AND  
GAS INDUSTRY: CASE STUDIES FOR AN EXPANSIBLE PACKER AND A  
SLIDING SLEEVE VALVE FOR OPEN-HOLE WELLS**

Dissertação ou Tese apresentada  
ao Programa de Pós-Graduação em  
Engenharia de Produção da Universidade  
Federal de Pernambuco, como requisito  
parcial para a obtenção do título de Doutor  
em Engenharia de Produção.

Área de concentração: Pesquisa  
Operacional.

Orientador (a): Prof. Márcio das Chagas Moura, DSc

Recife

2024

.Catalogação de Publicação na Fonte. UFPE - Biblioteca Central

Azevedo, Rafael Valenca.

Development of bayesian multilevel models for reliability assessment of under development technologies in the oil and gas industry: case studies for an expansible packer and a sliding sleeve valve for open-hole wells / Rafael Valenca Azevedo. - Recife, 2024.

115p.: il.

Tese (Doutorado) - Universidade Federal de Pernambuco, Centro de Tecnologia e Geociências, Programa de Pós-Graduação em Engenharia de Produção.

Orientação: Marcio Jose das Chagas Moura.

1. Completion technology development; 2. Multilevel reliability model; 3. Bayesian reliability; 4. Informative prior distribution; 5. Residual uncertainty analysis. I. Moura, Marcio Jose das Chagas. II. Título.

UFPE-Central



UNIVERSIDADE FEDERAL DE PERNAMBUCO  
PROGRAMA DE PÓS-GRADUAÇÃO EM ENGENHARIA DE PRODUÇÃO

PARECER DA COMISSÃO EXAMINADORA  
DE TESE DO DOUTORADO DE

**RAFAEL VALENÇA AZEVEDO**

***"DEVELOPMENT OF BAYESIAN MULTILEVEL MODELS FOR  
RELIABILITY ASSESSMENT OF UNDER DEVELOPMENT  
TECHNOLOGIES IN THE OIL AND GAS INDUSTRY: CASE  
STUDIES FOR AN EXPANSIBLE PACKER AND A SLIDING  
SLEEVE VALVE FOR OPEN-HOLE WELLS"***

ÁREA DE CONCENTRAÇÃO: PESQUISA OPERACIONAL

A comissão examinadora, composta pelos(as) professores(as) abaixo, sob a presidência do(a) primeiro(a), considera o(a) candidato(a) **RAFAEL VALENÇA AZEVEDO, APROVADO(A)**.

Recife, 09 de Agosto de 2024.



Documento assinado digitalmente  
**MARCIO JOSE DAS CHAGAS MOURA**  
Data: 09/08/2024 15:00:01-0300  
Verifique em <https://validar.itl.gov.br>

Prof. MÁRCIO JOSÉ DAS CHAGAS MOURA, Doutor (UFPE)



Documento assinado digitalmente  
**ISIS DIDIER LINS**  
Data: 09/08/2024 11:15:34-0300  
Verifique em <https://validar.itl.gov.br>

Prof. ISIS DIDIER LINS, Doutora (UFPE)



Documento assinado digitalmente  
**LEANDRO CHAVES REGO**  
Data: 09/08/2024 10:50:15-0300  
Verifique em <https://validar.itl.gov.br>

Prof. LEANDRO CHAVES RÊGO, PhD (UFPE)



Documento assinado digitalmente  
**MANOEL FELICIANO DA SILVA JUNIOR**  
Data: 12/08/2024 09:25:00-0300  
Verifique em <https://validar.itl.gov.br>

Prof. MANOEL FELICIANO DA SILVA JUNIOR, Doutor (PETROBRAS)



Documento assinado digitalmente  
**DANILO COLOMBO**  
Data: 12/08/2024 17:33:26-0300  
Verifique em <https://validar.itl.gov.br>

Prof. DANILO COLOMBO, Doutor (PETROBRAS)

## **ABSTRACT**

The development of new equipment technologies constitutes one of the greatest challenges in the oil and gas industry, particularly for the well engineering area. It is necessary to ensure that new technologies have satisfactory and failure-free performance for high mission times, much longer than the typical and viable durations of qualification and reliability demonstration tests. Furthermore, the development process is complex and iterative, involving different types of data from tests, numerical simulations and multiphysics analyses, from its inception to full-scale operation. In this context, it is essential to have a way to collect and aggregate these different types of data as they become available to monitor and control the technological development process, being able to provide equipment developed with the desired reliability requirements. However, to achieve this objective two key challenges need to be overcome: (i) the heterogeneity of data obtained during development, since tests and analyzes are carried out on different models, components, and stressors; (ii) the low quality of information collected in tests for such long time horizons (such as mission times for completion equipment, which can reach 27 years in Brazilian fields) due to infrastructure, technology and cost limitations. To achieve this, the methodology presented in this thesis proposes the construction of a multilevel reliability model (MRM) and a Bayesian framework that allows the use of heterogeneous data to feed the reliability model of the new technology and aggregate test data with information from other sources. , such as the opinions of experts and databases of similar systems, which are treated as a baseline for the a priori analysis of the reliability of the new technology, being updated by the test results. Two methods for obtaining a priori reliability prediction with simple and intuitive elicitation are proposed and applied to an openhole expandable packer and a sliding sleeve valve, demonstrating the robustness and applicability of the solutions for continuously and non-continuously operated systems. Furthermore, the model allows the aggregation of new information as it becomes available, allowing a residual uncertainty analysis to be carried out at each stage of development and thus providing a powerful reliability monitoring tool throughout the development process of new equipment.

Keywords: completion technology development; multilevel reliability model (MRM); Bayesian reliability; informative prior distribution; residual uncertainty analysis.

## LIST OF FIGURES

Figure 1 – Open hole expansible packer .....	8
Figure 2 – Dual position sliding sleeve mechanical valve.....	8
Figure 3 – Schematic of the open hole completion string with packers and sliding sleeves. ....	8
Figure 4 – General steps of the methodology.....	11
Figure 5 – Example of system breakdown for the DHSV .....	15
Figure 6 – Relationship between failure cause, failure mode and failure effect.....	18
Figure 7 – General rule for selecting failure mechanism's reliability model. ....	21
Figure 8 – Stress-strength modeling .....	23
Figure 9 – Damage-endurance model.....	23
Figure 10 – Damage-endurance model based in stress-strength relationship. ....	24
Figure 11 – Generic Markov-based diagram for system states in methodology. ....	28
Figure 12 – FT diagram for the system failure mode <i>SFM</i> 1.....	30
Figure 13 – Bayesian framework for estimating the MRM parameters.....	33
Figure 14 – Residual uncertainty analysis example. ....	37
Figure 15 – Overview of the proposed methodology and how the contributions of the basic events are computed.....	42
Figure 16 – FT diagram representing the equipment failure during its installation. ...	49
Figure 17 – Example containing illustrative values.....	52
Figure 18 – Estimate of the reliability of the equipment during its installation $R_0$ .....	54
Figure 19 – FT diagram representing equipment failure during well operation.....	55
Figure 20 – Procedure adopted to solve the constrained ME method.....	59
Figure 21 – Estimate of the equipment reliability for 27 years of operation, $R_{27}$ .....	61
Figure 22 – Main steps of the proposed methodology for obtaining an informative Bayesian prior distribution for on-demand equipment based on experts' opinions. ....	65
Figure 23 – Possible status of on-demand equipment. ....	65
Figure <b>24</b> – Elicited values in red boxes and downward propagation methodology; how the contributions of the basic events are computed. ....	67
Figure 25 – The approach applied to define the hyperparameters of the prior distributions. ....	72

Figure 26 – The procedure adopted to solve the constrained maximum entropy method. .....	74
Figure 27 – Fault tree diagram representing the valve failure during actuation, where green and yellow blocks represent basic and intermediate events, respectively. ....	75
Figure 28 – Fault tree diagram representing the valve failure during operation, where green and yellow blocks represent basic and intermediate events respectively. ....	77
Figure 29 – Distribution of the contributions of each basic event, $w_i$ , to actuation failure ( $i = 1$ to 9) and to operation failure ( $i = 10$ to 25). ....	79
Figure 30 – Distribution of probability estimates of (a) failure during actuation for each basic event $p_{it} = 0, d = 0$ ; (b) failure during actuation for each basic event $p_i(t = 0, d = 5)$ ; and (c) failure during actuation for each basic event $p_i(t = 10, d = 0)$ . ....	79
Figure 31 – Distribution of estimates of the probability of failure in 27 years of operation $p_i(t = 27)$ . ....	80
Figure 32 – Example of aggregation result, beta distribution for $E9$ obtained through PVA. ....	81
Figure 33 – Prior reliability distribution of the valve; the vertical red line indicates the target reliability of 90% for 27 years. ....	85
Figure 34 – Gate 0 residual uncertainty analysis for the expansible production packer. .....	86
Figure 35 – Test sequence for producer well .....	87
Figure 36 – Distribution of the samples of $R(27)$ at Gate 1 .....	90
Figure 37 – Distribution of the samples of $R(27)$ at Gate 2 .....	90
Figure 38 – Gate 0-2 residual uncertainty analysis for the expansible production packer .....	90

## LIST OF TABLES

Table 1 – FMECA columns referring to system function breakdown. ....	16
Table 2 – FMECA columns referring to failure identification. ....	17
Table 3 – FMECA columns referring to criticality assessment. ....	19
Table 4 – FMECA columns referring to qualification activities. ....	19
Table 5 – generic example of FMECA. ....	30
Table 6 – Description of basic events of the fault tree diagram for the failure during the packer installation. ....	49
Table 7 – Failure contribution of basic events for the installation FT diagram. ....	52
Table 8 – Prior distributions obtained through MM. ....	53
Table 9 – Description of basic events of the FT diagram for the equipment failure during well operation. ....	55
Table 10 – Completion expansion packer Wellmaster report (operation of similar equipment). ....	57
Table 11 – Responses regarding the contribution of events 15, 16 and 17 to the valve failure ( <i>EVF</i> ). ....	58
Table 12 – Failure contribution of basic events for the operation FT diagram. ....	58
Table 13 – Prior distributions obtained through ME. ....	61
Table 14 – Description of basic events of the FT for the valve failure during actuation. .....	76
Table 15 – Description of basic events of the FT for the valve failure during operation. .....	77
Table 16 – Beta distribution that represents, for each basic event, the probability of the first actuation failure $pit = 0, d = 0$ , the probability of actuation failure after 5 demands in $t=0, pit = 0, d = 5$ , and the probability of the first actuation failure in $t=10$ without demands, $pi(t = 10, d = 0)$ . ....	81
Table 17 – Beta distributions of probability of failure during operation in 27 years for each event. ....	82
Table 18 – Hyperparameters of the prior distribution of the valve actuation failure. ..	83
Table 19 – Hyperparameters of the log-normal distributions of Weibull parameters $\alpha i$ and $\beta i$ . ....	83
Table 20 – Prior reliability of the valve, values in percentage. ....	84



## LIST OF ACRONYMS

PDP	Production Development Project
O&G	Oil and Gas
IWC	Intelligent Well Completion
TQP	Technology Qualification Program
RDT	Reliability Demonstration Testing
PPoF	Probabilistic Physics of Failure
MRM	Multilevel Reliability Model
MCMC	Markov Chain Monte Carlo
MC	Monte Carlo
MATIC	Manufacture, Assembly, Testing, Installation, and Commissioning
MTTF	Mean Time To Failure
DHSV	Downhole Safety Valve
RPN	Risk Priority Number
PoF	Physics of Failure
PFD	Probability of Failure on Demand
ALT	Accelerated Life Testing
ADT	Accelerated Degradation Testing
PH	Proportional Hazard
PDF	Probability Density Function
FT	Fault Tree
SCM	Submarine Control Module
FMEA	Failure Modes and Effects Analysis
RBD	Reliability Block Diagram
MM	Method of Moments
ME	Maximum Entropy
PSO	Particle Swarm Optimization
CDF	Cumulative Distribution Function

## TABLE OF CONTENTS

1	Introduction .....	1
1.1	Initial Remarks.....	1
1.2	Literature Review on reliability prediction of new O&G technologies and the proposed solution .....	3
1.3	Objectives.....	6
1.3.1	General Objective .....	6
1.3.2	Specific Objectives.....	7
1.4	Thesis Structure .....	7
2	The methodology for predicting reliability and uncertainty of new equipment technologies in O&G industry .....	10
2.1	Reliability requirements planning.....	11
2.2	The Multilevel Reliability Model (MRM) .....	13
2.2.1	FMECA for identifying relevant failure mechanisms.....	14
2.2.2	Definition of failure mechanism reliability model .....	20
2.2.3	Modeling the system reliability via fault tree analysis.....	29
2.3	Reliability data collection .....	31
2.4	Bayesian Inference of MRM parameters .....	32
2.4.1	Implementation of Bayesian methodology .....	34
2.5	Reliability Assessment and Residual Uncertainty Analysis .....	36
3	Prior analysis for continuously operated equipment based on generic data and experts' opinion .....	39
3.1	Introduction.....	39
3.2	Methodology .....	41
3.2.1	Overview .....	41
3.2.2	Expert opinion for FT events.....	42
3.2.3	Downward propagation .....	43

3.3	Case Study .....	47
3.3.1	Equipment installation .....	48
3.3.2	Equipment operation .....	54
3.4	Conclusion .....	61
4	Prior analysis for non-continuously operated equipment based on experts' opinion	63
4.1	Introduction .....	63
4.2	Methodology .....	64
4.2.1	Probabilistic Modeling .....	66
4.2.2	Data Source .....	66
4.2.3	Aggregation process .....	69
4.2.4	Prior distribution definition .....	72
4.3	Case study .....	75
4.4	Results .....	78
5	Posterior estimates and residual uncertainty analysis for the Expandable Production packer case .....	86
5.1	Likelihood functions .....	86
5.2	Reliability update and residual uncertainty analysis .....	88
6	Conclusions .....	91
6.1	Impacts of the Thesis .....	93
6.1.1	Economic Impacts .....	93
6.1.2	Social Impacts .....	93
6.1.3	Environmental impacts .....	93
6.2	Limitations and Future Works .....	94

## 1 INTRODUCTION

### 1.1 INITIAL REMARKS

The production development project (PDP) comprises definition and execution of the best technical solution to be employed in an oil and gas (O&G) production field whose declaration of commerciality has been approved. The O&G industries have actively practiced the implementation of remotely monitored and controlled well completions in their PDP's. This technology, referred to as intelligent well completion (IWC), has rapidly advanced over the last few years, showing benefits that include increased recovery and production acceleration (HU et al., 2021). Applications of IWC and their values has been shown in WOSOWEI & SHASTRY (2023), LIU et al. (2022), SCHAEFER & SAMPAIO (2020), EREN & POLAT (2020), AVILA (2020), BRONI-BEDIAKO et al. (2019), AFUEKWE & BELLO (2019), DA SILVA et al. (2017), and RAOUFI et al. (2015).

The employment of IWC has required the development of new equipment technologies that are essential for the system operation. For instance, a new open hole configuration with electric intelligent completion is being developed in Brazil's pre-salt, and some equipment for use in open hole intelligent completion configurations, such as sliding sleeve valve and the open hole expansible packer, have been developed and implemented since 2019 (CARVALHO & DA SILVA, 2022).

The in-progress equipment development projects for electrical completion include electric flow valves, the downhole connection and disconnection system with inductive coupler or electrical contact, the responsible control cards for the management and supply of energy and communication for the well (including sensors and actuators of the various installed equipment). In addition, the roadmap for the electric intelligent completion also foresees the future incorporation of electrically operated gas lift valves, electrically operated well safety valves, intelligent equipment and new opportunities in well sensing, such as those based on fiber optics (CARVALHO & DA SILVA, 2022).

In high-reliability applications such as the O&G production, it is necessary to assure that new products have the required quality before they are put into operation. The time to the first planned intervention may be five years, or even longer, and the

installed system should be able to operate properly during this period. For some IWC equipment, intervention-free operation may be required throughout the well's entire production period (which comprises about 27 years in Brazil). New technologies are often met with skepticism in O&G producing field, since the operators fear that they may fail and lead to production losses, costly repair interventions, and hydrocarbon leakages to the sea (RAHIMI & RAUSAND, 2015). Then, to provide such assurance, a technology qualification program (TQP) has been implemented to reduce the uncertainty for new products development (AMERICAN PETROLEUM INSTITUTE, 2018; DET NORSKE VERITAS, 2017).

Qualification is the process by which systems are examined and evidence is provided to demonstrate that the new technology meets the specified requirements for the intended use (AMERICAN PETROLEUM INSTITUTE, 2017; LLOYD'S REGISTER, 2022). It is therefore an application-oriented process, which means that equipment technology may be qualified for one specific application. The operator will usually specify strict goals and requirements for the new equipment and require the supplier to follow an agreed TQP during the design, development, and manufacturing phases of the system (AMERICAN BUREAU OF SHIPPING, 2017; DET NORSKE VERITAS, 2017). Such requirements typically include regulatory, functional, and technical specifications (AMERICAN PETROLEUM INSTITUTE, 2018). The latter should cover reliability and integrity performances, since they are core business values that O&G companies are seeking to achieve. Reliability requirements to be addressed in a TQP may be (AMERICAN PETROLEUM INSTITUTE, 2017):

- i. Management related goals: specify an analysis (e.g.: Failure Modes and Effects Analysis – FMEA) to be implemented within the scope of technology development process.
- ii. Qualitative: it requires the probability of occurrence of a specific failure mode to be negligible or very low.
- iii. Quantitative: it specifies a level of reliability required for an item.

Most of works found in the literature deal primarily with qualitative requirements and/or management goals for qualifying new technologies in a PDP against reliability requirements as in ABBASZADEH et al. (2022) ARIF et al. (2022), DENNEY (2003), FEDER (2019), KLEYNHANS et al. (2016), MCGEORGE et al. (2019), PATEL et al. (2019), RATNAYAKE et al. (2014), SOLOVYEVA et al. (2023), WILKINS (2018), and

WRIGHT (2017). The same is seen in the industry standards used for qualifying subsea/downhole systems, components and materials, such as ISO 14310 (2008), ISO 23936 (2011), API 17F (2014), API SPEC 14A (2024), ISO 11960 (2020), ISO 15156 (2020), AWES RP 3362 (2017), API 11D1 (2022), API 19G2 (2020), API 5CT (2019b), API 19V (2019a).

In these types of qualification activities, a “pass/fail” test approach is adopted to select materials and validate components designs. Then, if the result satisfies a previously established acceptance criterion, or if some qualitative or management analysis is performed, then the technology is qualified (pass) for the respective requirement (LLOYD’S REGISTER, 2022), but no quantification can be made about the new technology reliability level.

When a quantitative reliability requirement is adopted, it is needed to predict the reliability level of the new system in its future operational context. The procedure requires the development and application of statistical techniques for collecting and analyzing reliability data during the development process.

## 1.2 LITERATURE REVIEW ON RELIABILITY PREDICTION OF NEW O&G TECHNOLOGIES AND THE PROPOSED SOLUTION

Within the investigated literature base, just a few articles were found in the O&G context. RAHIMI & RAUSAND (2013) present a practical approach for failure rate prediction of new subsea systems based on available operational data from similar, known systems from the topside environment and a comparison between the two systems. The author’s procedure however does not use data from the new system itself (e.g.: from test), becoming a highly subjective approach based on the judgement about the impact of the reliability-influencing factors in the new and similar systems.

Also, the recommended practice API 17Q (2018) presents a reliability demonstration test (RDT) approach for planning a test protocol capable of proving that the technology meets some target of reliability with a certain confidence level if it runs successfully according to an acceptance criterion. However, for systems with high reliability, standard RDTs are no longer preferred because test plans often require long test durations and pose high risks to producers and consumers (JIANG et al., 2022). Besides that, an RDT is typically limited to a set of components and failure mechanisms, which can be covered by the single testing protocol. This means that reliability targets

and RDT plans should be defined for each of them in order to demonstrate the reliability of a complex equipment at a system level, or the reliability is assessed only for the prioritized failure mechanisms.

Furthermore, in the technology development, an RDT is typically performed for prototype validation step at an advanced phase of the development process. Predicting system reliability at early stages in the system development process is important due to the high cost of design modifications later in the development process. This risk is relevant if the RDT is the unique way to demonstrate the system reliability level quantitatively. For more about RDT approach, see GRUNDLER et al. (2022).

Therefore, this thesis proposes a methodology for predicting the system reliability, and updating it, along the steps of the development process, by aggregating the available information at each of them. In earlier phases of the development process, a high uncertainty level is expected for the reliability prediction. As new data is gathered and aggregated during the process, the uncertainties are reduced until a satisfactory remaining uncertainty is met according to the defined reliability requirement. By using this reliability evolution all along the process, the decision-makers can take more informed and supported decisions about the project actions, design changes, and continuity of the developing technology.

In the development phases, reliability data from the system itself is only available through reliability tests carried out on prototypes of the equipment or its components. The probabilistic physics of failure (PPoF) methods (MODARRES et al., 2017) have been used, in a general manner, to gathering and analyzing these types of data. Reliability tests are performed, normally in accelerated conditions, to evaluate the system (or component) lifetime for specific failure mechanisms. A PPoF model is formulated to model the system reliability against the failure mechanism and the results of the tests are used to estimate the PPoF model parameters (MUHAMMAD et al., 2020; POURGOL et al., 2018; RANE et al., 2019; REGATTIERI et al., 2017; WEI et al., 2022; XIE & HUANG, 2016; ZAHARIA et al., 2020).

However, the development of an engineering system is a process that evolves from basic research to prototype validation, through concept development and validation, and it is usually characterized by continuing updates and modifications in design specifications in order to overcome observed technical difficulties as well as implement engineering improvements. In this way, from some specific test or analysis performed at each phase, the reliability data are provided for different hierarchical

structure (system, subsystem, module, component, part, material, etc.), in different forms (lifetime, pass/fail data, degradation measure, etc.), and regarding different failure mechanism (fatigue, corrosion, etc.). Classical PPOF models are useful for modeling individual test or analysis. Then, a method for aggregating this heterogeneous data set is mandatory for the objective pursued in this thesis.

In WANG et al. (2013), special consideration is given to the inclusion of accelerated degradation data in conjunction with field data (lifetime) for a specific component. This work is enlarged in WANG et al. (2017), by including the possibility of pass/fail data to be aggregated in the model proposed in 2013. However, despite providing a solution for the multitype data set, these works don't deal with multilevel data problem. On the other hand, multi-level integration methods, such as those proposed in JACKSON & MOSLEH (2016), YONTAY; PAN (2016), and LI et al., (2014), have aimed to solve the problem of evaluating the reliability of a complex system, but they assume that each component has only one data source and/or one data type.

If one wants to integrate multi-source reliability information in a systematic way, Bayesian approach is a natural choice, just as it happened in these above-mentioned papers. However, there is still a gap for a method that aggregates into a unique Bayesian framework data from various sources, in multiples forms and hierarchical level, and relative to different PPOF failure mechanisms models. For that end, a Multilevel Reliability Model (MRM) is built-up in this thesis, and a Bayesian framework is developed to estimate and update the MRM parameters and reliability metrics in each phase of the development process, from the heterogeneous data sources. The MRM and Bayesian framework proposed makes possible the consideration of design changes.

Specifically, prior distributions are a key component for Bayesian analysis, being classified as informative or non-informative. The main idea of non-informative prior is that it should slightly affects the likelihood information. However, when limited data is available, the likelihood constructed is sometimes weak and, using non-informative prior may end in a posterior distribution with high uncertainty. Therefore, it is essential to incorporate every possible information to build the prior distribution (KONG et al., 2020; YANG; GUO; KONG, 2019). Informative prior distributions, in turn, improve the precision of the reliability estimates and, even if they are weakly informative, they help reduce convergence issues for algorithms for the posterior probability calculation, such



as Markov Chain Monte Carlo (MCMC) (GELMAN et al., 2017; WILSON & FRONCZYK, 2016).

It is worth highlighting that difficulties are found for collecting quality reliability data from the tests due to limitations of cost, time, and test infrastructure and technology, besides the possibility of design changes after running a test. Thus, data gathered from reliability tests may characterize "poor" likelihood functions for Bayesian updating and special attention is given for integrating them with other available source such as expert's judgement and data from similar equipment (including previous system design versions) and/or components (some components may have already been used in another project). These alternative sources are treated as a prior information.

Given the need to develop informative prior distributions for reliability parameters of O&G equipment technologies that are under development, we have developed two methods, described in MAIOR et al. (2022) and MACEDO et al. (2023). The former applies to continuously operated O&G equipment, while the latter focuses on non-continuously operated technologies (on demand systems). Both are based on experts' opinion and generic database information and propose an approach to define informative prior distributions for the MRM parameters that does not require direct elicitation of parameters, facilitating the elicitation process.

Finally, from posterior distributions of the MRM parameters, which can be inferred from an MCMC based technique, a Monte Carlo (MC) method will be used for assessing the uncertainty on reliability prediction (and its updates) at each development phase and compared them to the target defined in the reliability requirement planning. The target must be reached at the end of the development process, and then a residual uncertainty analysis is performed whenever an updated measurement is obtained, providing a powerful tool to control the development process by monitoring the uncertainty on the system reliability.

### 1.3 OBJECTIVES

#### 1.3.1 General Objective

This thesis aims to present a methodology for the reliability assessment of O&G systems under development based on various sources of information such as in-house

test data under both accelerated and nominal test conditions, experts' judgments, and observed performance of similar equipments such as the ones recorded in generic databases. Specifically, the methodology is elaborated for well completion systems that are essentially non-repairable equipment, and it encompass continuously and non-continuously (on-demand) operated equipment, by modelling their different operating modes.

### 1.3.2 Specific Objectives

The followings specific objectives are pursued:

- To propose a Multilevel Reliability Model (MRM) that translates the system reliability based on reliability models of the different failure mechanisms.
- To prepare a Bayesian framework capable of estimating uncertainty for the MRM parameters from heterogeneous data sources (multitype and multilevel data).
- To define a methodology for using expert opinions and historic data of similar components to obtain prior distributions for the MRM parameters of continuously operated equipment.
- To define a methodology for using expert opinions and historic data of similar components to obtain prior distributions for the MRM parameters of non-continuously operated equipment.
- To employ MCMC and MC techniques to calculate posterior distributions and uncertainty on the system reliability in order to perform a residual uncertainty analysis about the achievement of the reliability target.
- To apply all above objectives to new technologies of an open hole expansible packer and a dual position sliding sleeve mechanical valve, which are equipment used in recent IWC projects for zonal isolation and control flow.

## 1.4 THESIS STRUCTURE

This thesis is structured as follows: The Multilevel Reliability Model (MRM) and the Bayesian framework are described in Chapter 2. Chapters 3 and 4 present the application of the MRM formulation and the proposed methods for obtaining prior distributions for continuously and non-continuously operating pieces of equipment

respectively, based on the papers published in MAIOR et al. (2022) and MACEDO et al. (2023).

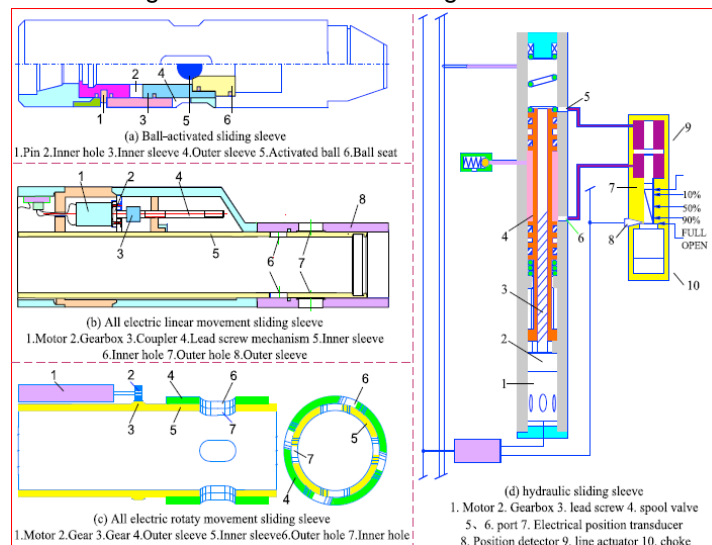
Specifically, the continuously operated system comprises an open hole expandable packer (Figure 1) developed for isolation of production zones, while the non-continuous one embraces a mechanical sliding sleeve valve (Figure 2 shows a traditional sliding sleeve valve) designed to control the in-flow of product from a reservoir zone to the production string. Both systems have been used in recent IWC projects deployed on the pre-salt field in Brazil. Figure 3 illustrates an example of their application in a well completion. Chapter 5 illustrates the Bayesian updates for the results of Chapters 3 and 4, from the tests performed for the systems under analysis. Finally, Chapter 6 gives the conclusions, methodology limitations and suggestions for future works.

Figure 1 – Open hole expandable packer



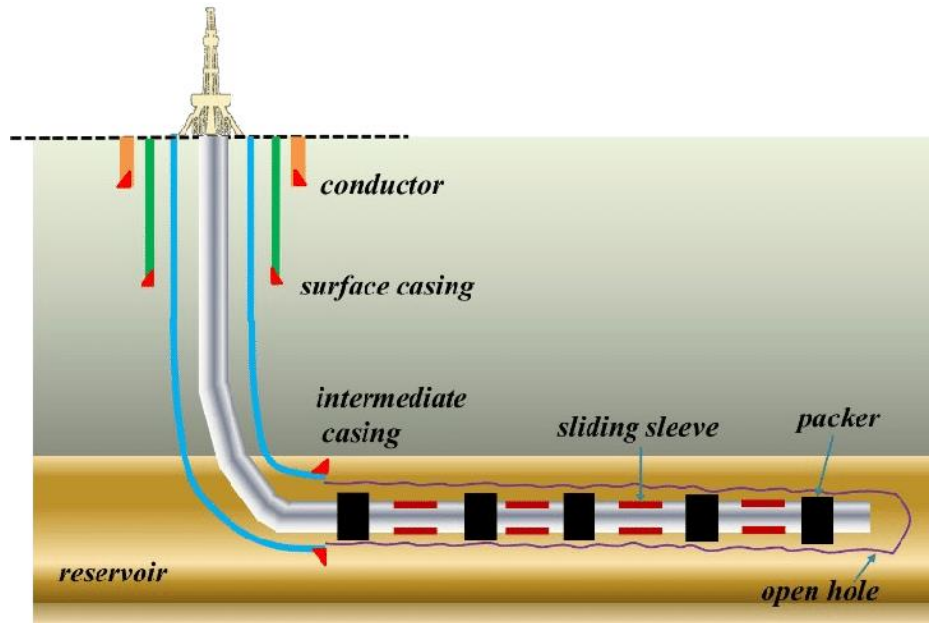
Source: JACINTO et al., (2015)

Figure 2 – Traditional sliding sleeve valve



Source: ZHANG et al (2017)

Figure 3 – Schematic of the open hole completion string with packers and sliding sleeves.



Source: LIANG et al., (2020)

## 2 THE METHODOLOGY FOR PREDICTING RELIABILITY AND UNCERTAINTY OF NEW EQUIPMENT TECHNOLOGIES IN O&G INDUSTRY

This chapter is based on the list of conference papers below (most published in extended abstract format), all of which I co-authored; it is worth noting that the content of this chapter is not limited to the contents of the papers listed below. There is an additional contribution, especially in the details of the models used in each stage of the methodology, which does not occur in the papers cited:

- Methodology for extracting reliability parameters from the qualification standard tests ISO-23936 (AZEVEDO et al., 2023).
- Methodology for Assessing the Reliability of Equipment under Development (AZEVEDO et al., 2022a)
- The use of Weibull-GRP Virtual Age Model for Addressing Degradation due to Demand Induced Stress in Reliability Analysis of On-demand Systems (AZEVEDO et al., 2022b)
- Technical assurance in new technology development projects: a reliability-based approach (AZEVEDO et al., 2020)
- Development of a software tool to implement reliability assessment of developing technologies (SANTANA et al., 2023)
- Proposal of a Test Protocol for Reliability Evaluation of O&G Equipment (MENEZES et al., 2022)
- Reliability-based Guidelines for Elaborating Technical Specifications of New Technologies (SANTANA et al., 2022)
- A Bayesian Prior Distribution for Novel On-Demand Equipment Based on Experts's Opinion: A Case Study in the O&G Industry (MACEDO et al., 2022)
- Physics-Based Accelerated RDT Testing for High Reliable Equipment (MAIOR et al., 2021)

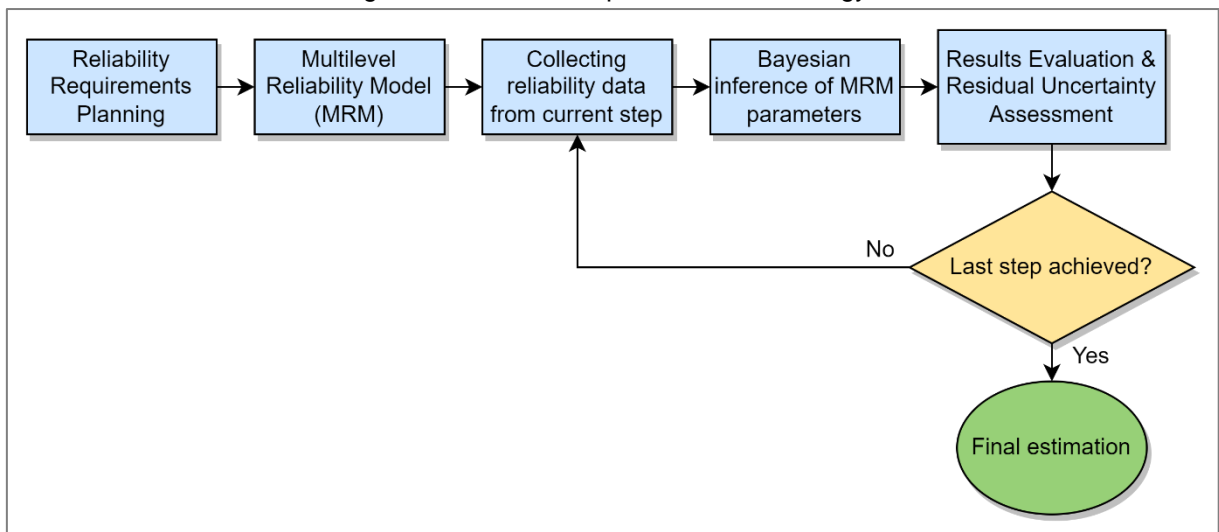
The methodology is designed to make quantitative assessments of the reliability behavior of equipment or systems that are still in the design stage of their life cycle and must be qualified for use in a production development project (PDP). Specifically, it supports qualification against quantitative reliability requirements. Despite the lack of data originating from the equipment operation/test itself, it is often possible to find alternative data sources, such as engineering judgements and operating history or

testing of similar equipment/components (whether heritage or generic ones), that, even though only partially relevant, provide information on which an assessment of the new technology reliability can be based.

The methodology allows incorporating these various types of evidence from the development process, as they become available, to produce reliability prediction and evaluate the residual uncertainty that needs to be reduced to meet the reliability requirement from the earliest stages. One of the main challenges is that these various data may be in different formats (e.g., pass-fail, lifetime, degradation measures) and related to different hierarchical levels (system, subsystem, component) or failure modes and/or failure mechanisms.

Figure 4 shows the methodology steps, and a detailed explanation of its modules is given in the following sections.

Figure 4 – General steps of the methodology.



Source: The author

## 2.1 RELIABILITY REQUIREMENTS PLANNING

The requirements planning process within a qualification program is an activity that involves developing a plan for identifying and validating goals and requirements from stakeholders, as well as agreed-upon criteria for adapting the general definitions of the development activities to the specific technology to be qualified. These requirements should address, but not be limited to, regulatory requirements, function and performance requirements, and technical requirements which includes standards to be used, operational and process conditions, internal and external environmental

conditions, reliability performances, etc. (AMERICAN PETROLEUM INSTITUTE, 2018).

Specifically, the methodology presented in this document is concerned with the definition of the quantitative level of reliability to be reached by the new equipment technology in a specific application. This reliability target works as a parameter for key decisions and test planning along the development process, and it is typically defined by the customer, for example through a reliability allocation procedure (Souza et al, 2022), from the risk analysis of the well configuration selected in the PDP. This thesis does not intend to propose a method for setting the system reliability target, but just indicate how it should be typified in the methodology, as described above. Whatever process is used for planning the reliability requirements, the following points are relevant:

- The target for the system reliability in a mission time and the confidence level should be determined (AMERICAN PETROLEUM INSTITUTE, 2017). For example, the new technology should have a minimum of 90% reliability over 10 years, with 80% confidence level at least.
- The reliability target must be stated at system level and not for specific components or failure mechanisms. However, setting different targets for different system failure modes may be necessary, as their consequences are eventually associated with different severities. For instance, for process shutdown valves, such as the downhole safety valve (DHSV), a higher level of reliability should be required for the failure mode "fail to close when demanded" compared to the failure mode "spurious closing" since the first can result in consequences for the safety of operation.
- The evidence that the equipment will meet the reliability goal should be provided as design/development requirement, for prototype validation and qualification. It means that the target for reliability does not encompass qualification for manufacturing, assembly, testing, installation, and commissioning (MATIC). In the design/development activities, reliability analysis is oriented towards causes of failure related to design uncertainties and expected wear and tear resulting from normal operation of the equipment unit, as described in ISO 14224 (2016). Failures related to fabrication, installation, operation/maintenance errors are not included in the methodology and should not be considered for defining the reliability target.

- Other types of reliability metrics are discouraged in defining the quantitative reliability target. Most of well completion equipment is treated as a non-repairable system, then availability and/or maintainability metrics are not relevant in the methodology. Also, the mean time to failure (MTTF) is not interesting to be used for it does not provide a measure of the equipment's ability to perform its function during mission time.

Naturally, the reliability analysis process depends on the definition of system failure, which in turn will depend on the definition of other specifications for the system such as functional and performance requirements in addition to the operational/environmental conditions. For instance, one functional performance requirement for a DHSV system is to close on demand within a specified time, then, failure occurs if the valve does not close when demanded or if it closes completely after the set time.

Once the reliability target is defined, the next steps of the methodology aim to execute evidence collection and analysis procedures throughout the development process capable of demonstrating that the project will meet the goal, and they are shown in following sections.

## 2.2 THE MULTILEVEL RELIABILITY MODEL (MRM)

This step consists in formulating the reliability model for the new system; this is not performed by simply setting a parametric probability distribution to the time to failure (e.g., Weibull). An important characteristic of the development process integrated in a TQP is that the analyses are made gradually on key parts or components prior to the entire system or subsystem, and from laboratory testing environments (without integration into a broader system) to a simulated environment (e.g. hyperbaric chamber) or actual intended environment (e.g. subsea environment, well-laboratory), and so on. Also, different tests and analysis could cover only specific failure mechanisms due to limitation in test technology and infrastructure.

This means that, data and information about the system reliability are related with different levels in the system breakdown and different failure mechanisms. In this way, the system reliability model must be defined as a function of the reliability models of fundamental failure mechanisms (formulated at the item level), hence the name



“Multilevel Reliability Model”. Failure mechanisms will compete to cause the system failure, and the system reliability is interpreted as the probability that none of them can do that in an interval time  $(0, t]$ . Then, let  $R_i(t|\theta_i)$  be the parametric reliability model for the failure mechanism  $i$ , with parameter  $\theta_i$ ; the system reliability ( $R_s(t)$ ) is formulated as a function of failure mechanisms reliability models, i.e.,  $R_s(t) = g[R_i(t|\theta_i)]$ , with  $i = \{1, \dots, m\}$ , where  $m$  is the number of failure mechanisms and  $g[\cdot]$  models the logical representation among them in the competition to cause the system failure.

The approach to formulate the system reliability as a function of failure mechanisms reliability models brings flexibility to the methodology to be applied for different types of developing equipment (on-demand, continuously running, etc.), and allows updating the model parameters estimate with information from tests on different hierarchical levels. Three tasks are therefore central in formulating MRM: (i) the identification of the failure mechanisms  $i = \{1, \dots, m\}$ , (ii) the definition of the parametric reliability models  $R_i(t|\theta_i)$  of each failure mechanism, and (ii) the modeling of the system reliability as a function of  $R_i(t|\theta_i)$ , i.e., modeling of  $g[\cdot]$ . The following subsections discuss these steps.

### 2.2.1 FMECA for identifying relevant failure mechanisms.

A key tool used in the formulation of the MRM is the *failure modes, effect, and critically analysis* (FMECA). In this section, it is described the format and content of some fields to be covered in the FMECA form. Basically, it will provide details regarding threats and weaknesses that should be considered in the reliability model and prioritized in the testing planning. The FMECA output may also identify design actions and improvements to be made before testing commences.

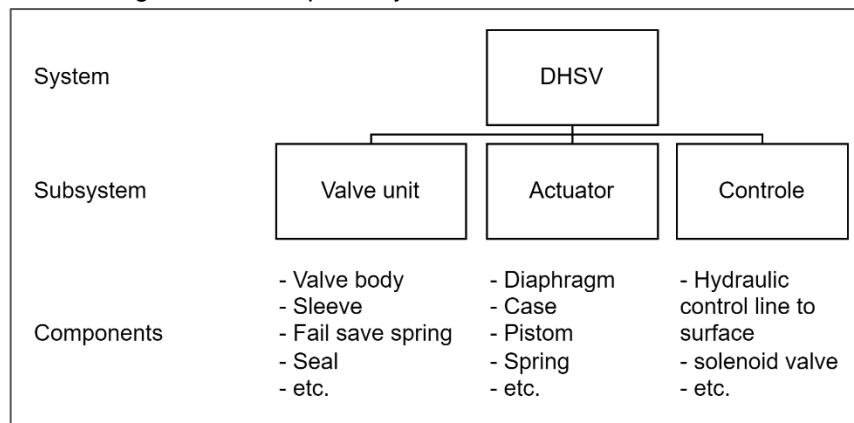
Naturally, the FMECA should be used for other purposes such as manufacturing/operating procedures in order to avoid the occurrence of some failure mechanisms during MATIC activities. A process FMECA (P-FMECA) could be used in this sense (AMERICAN PETROLEUM INSTITUTE, 2017). However, as discussed in Section 2.1, only risks associated with normal use of the hardware design in the specific application are considered. Then a design/hardware FMECA (AMERICAN PETROLEUM INSTITUTE, 2017) must be applied for the methodology purposes.

The format of the fields proposed in this section is based upon existing design-hardware FMECA types with a focus on identifying the logical representation of the system failure modes and the detailed identification of failure mechanisms. The FMECA should be performed at a component function level. The Sections 2.2.1.1 through 2.2.1.4 describe a set of recommended columns for a standard FMECA to be used in the methodology, and Section 2.2.1.5 provide additional recommendations.

#### 2.2.1.1 System Function Breakdown

Breakdown of the system to a level of detail required to discretely identify independent failure mechanisms that are to be verified during reliability qualification activities. The latest level in the system breakdown is the item for which the failure analysis is to be performed. Figure 5 illustrates a general example for the system breakdown of a DHSV project. The system breakdown may also be used to identify combinations of items required for reliability qualification testing as an assembly. This is useful where a specific failure mechanism only applies to an assembled unit or if it is not feasible to test items separately.

Figure 5 – Example of system breakdown for the DHSV



Source: Adapted from ISO 14224 (2016)

Once the items are defined, it is necessary to identify the functions and performance required for each of them within the system functions. This is useful to correlate the identified reliability qualification activities to a specific item function and performance requirement. For example, a DHSV system has the function of closing and keeping closed the production string flow on demand. The seal of the valve unit

(Figure 5) contributes for this system function by sealing the region between the control sleeve and valve body when the DHSV is in the closed position.

Table 1 illustrates the FMECA columns referring to the system function breakdown.

Table 1 – FMECA columns referring to system function breakdown.

<b>System Function Breakdown</b>		
Subsystem	Component (item)	Item function

Source: The author

#### 2.2.1.2 Failure Identification

Identification of all potential failure modes, mechanisms, and root causes for each functional entity examined, addressing potential deviations from performance expectations. The inducing agents (stressors) the inducing agents of the failure mechanisms and the mode of operation in which they occur should be recognized in the form to support tests planning and reliability modeling activities. Also, the technical consequence (effect) should be documented to inform the criticality and risk assessments.

Table 2 shows the fields in FMECA related to the failure identification. The following definitions are useful:

- A failure mode is the description of a failure, i.e., the manner in which failure occurs (ISO 14224, 2016). The failure modes typically refer to not obtaining a desired function (e.g. failure to start) or to a specified function lost or outside accepted operational limits (e.g. spurious stop, high output).
- The failure mechanism is the physical, chemical or other process or combination of processes that leads to the failure (ISO 14224, 2016). It is an attribute of the failure event that can be deduced technically, as an apparent, observed cause of the failure (e.g.: fatigue, corrosion, etc.).
- The cause of failure is the initiating event (“root causes”) in the sequence leading up to a failure of the item, that is, the reason for the occurrence of the failure mechanism process.

- The stressors of a failure mechanism are the failure-inducing agents, i.e., the environmental/operational variables (temperature, humidity shock pressure, etc.) that stress and age the item (MODARRES et al., 2017).

Table 2 – FMECA columns referring to failure identification.

Failure Identification					
Failure Mode	Failure Mechanism	Root Cause	Stressors	Operating Mode	Effect (at system level)

Source: The author

A general picture of the relationship between failure modes, cause, and effect is that a failure mode of an item is one of the failure causes of a failure mode of the item at the next higher level in the system breakdown, and the failure effect of a failure mode of an item corresponds to the failure mode of the item at the next higher level. The failure mechanism is therefore the cause of the failure mode at the lowest items as if it were the failure mode of the materials and the root cause comprises why failure mechanism occurs.

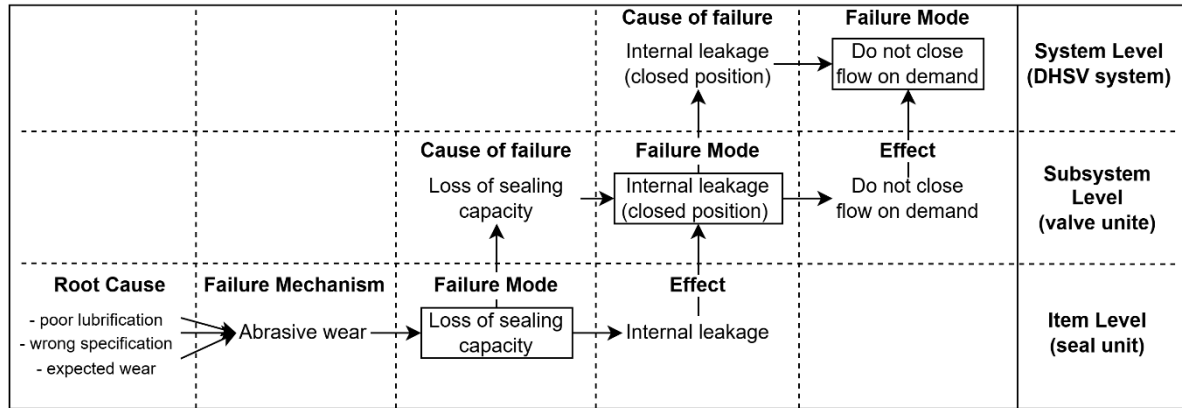
For example, abrasive particles in the fluid can cause seal wear during operation, when DHSV is open. Hard particles can become embedded in soft elastomeric and metal surfaces, leading to abrasion of the harder mating surfaces forming the seal, ultimately resulting in loss of sealing capacity of the seal unit. The loss of sealing capacity of the seal unit will cause an internal leakage on the valve unit when it is in the closed position. Finally, if there is an internal leakage in the valve unit, the DHSV system will not be able to close flow when demanded. The root cause in this scenario could be a poor lubrication during DHSV test/maintenance intervals, a wrong material specification, or even expected degradation during normal operation (impossible to be avoided with certainty by design actions and operating procedures).

This example is illustrated at Figure 6 and will result in the following description in a row of the FMECA:

- *Item*: seal unit
- *Failure mode*: loss of sealing capacity
- *Failure Mechanism*: Abrasive wear
- *Root cause*: (i) poor lubrication (operating error); (ii) wrong material specification; (iii) expected material degradation.
- *Stressors*: fluid flow containing solid particles

- *Operating mode* (in which the failure mechanism occurs): keep flow open (production)
- *Effect* (system failure mode): DHSV does not close flow on demanded.

Figure 6 – Relationship between failure cause, failure mode and failure effect.



Source: The author

### 2.2.1.3 Criticality Assessment

Assessment of each potential failure mechanism to determine means of failure detection and to facilitate categorizing and prioritizing the qualification program. Table 3 presents the content to be included in FMECA for the criticality assessment. The risk priority number (RPN) is a function of the three numeric parameters in the criticality assessment, viz, the probability of occurrence, the severity of the effect of failure, and the ease of detection for each failure mechanism. RPN is calculated by multiplying these three numbers as per the Equation 1 below, where  $O$  is the probability of failure occurrence,  $S$  is the severity of the effect of failure, and  $D$  is the ease of detection (KIRAN, 2017). Values of  $O$ ,  $S$  and  $D$  are defined from a numeric scale built previously. Some works have proposed adequate definitions for these numeric scales in the context of O&G industries (CATELANI; CIANI; VENZI, 2018; NI et al., 2022). This thesis does not intend to propose them. The qualifier or end user risk matrix may be used to assign a severity level to the identified consequences.

$$RPN = O \times S \times D$$

1

RPN may not play an important role in the choice of an action against failure mechanisms but will help in indicating the threshold values for determining the areas

of greatest concentration. In other words, a failure mechanism with a high RPN number should be given the highest priority in the analysis and corrective action.

Table 3 – FMECA columns referring to criticality assessment.

<b>Criticality Assessment</b>				
Detection Mode	Occurrence (by numeric scale)	Severity (by numeric scale)	Detection likelihood (by numeric scale)	Risk priority number (RPN)

Source: The author

#### 2.2.1.4 Activities

Identification of qualification activities needed, which can include design/engineering actions, operational/maintenance procedures and reliability tests (Table 4). Where underlying failure mechanisms and causes are not fully understood, FMECA actions should include investigations including those involving testing and research, to improve knowledge and understanding of failure.

Table 4 – FMECA columns referring to qualification activities.

<b>Activities</b>		
Design/Engineering actions	Operational/Maintenance procedures	Reliability tests

Source: The author

#### 2.2.1.5 Other considerations on FMECA

The following recommendations should be observed in the processes of developing and reviewing the FMECA form:

- For modifications to existing technology, the system breakdown should identify all elements of the technology and be of sufficient granularity to detect which items are affected by the design or application changes.
- Following implementation of identified qualification activities and follow-up actions, the technology assessment and FMECA should be updated and include an update of the RPN associated with each failure mechanism or the addition of a new potential failure mechanism identified in the qualification analysis.

- The FMECA is intended to be a living document throughout the qualification process, and it should be updated as the technology advances in development stages.

## 2.2.2 Definition of failure mechanism reliability model

### 2.2.2.1 General rule

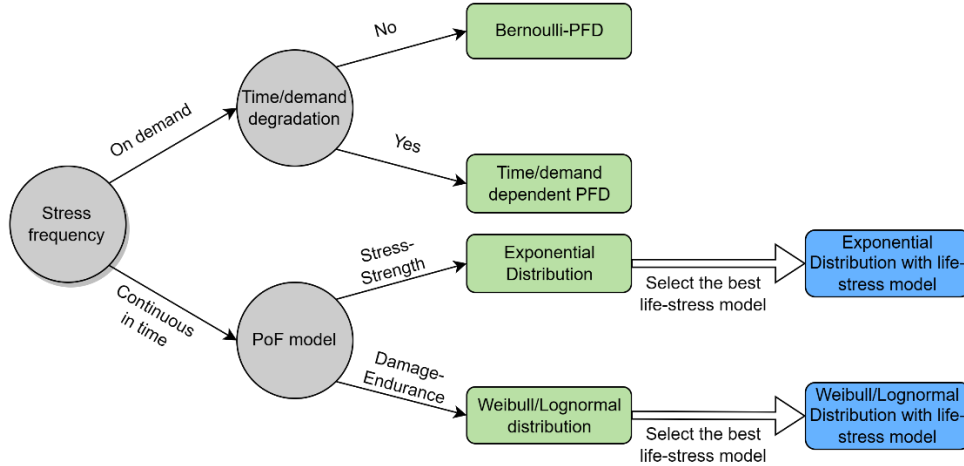
The proposed general rule for selecting the reliability modes of each failure mechanism is based on evaluation of the physics of failure (PoF) model (MODARRES, 2021) and illustrated in Figure 7. At first, the frequency at which the component is subjected to the stressor agent must be evaluated. Demand-induced stresses act “instantaneously” on a component only during a demanded procedure, such as installation, actuations (e.g: open/close valve), interventions, etc. These type of failure mechanisms are associated a probability of failure on demand (PFD),  $\rho$ , which means that when demand occurs the failure mechanism will occur with a probability  $\rho$ . For example, during the installation of an expansible packer, a pressurization procedure is carried out, providing a stress on the metallic expansible sleeve. The expansible sleeve may burst during this procedure with probability  $\rho$ .

Installation-induced stresses comprise demand stresses that occur only once on the system, i.e., at its installation. However, other types of stresses on demand can be repeated throughout the life of the equipment, as long as the causing procedure is demanded again. For example, a mechanical flow valve used for zonal control is under axial force stress every time it is actuated. In this case,  $\rho$  is probability that the failure mechanism, related to the axial force applied, will occur in one actuation procedure, i.e., the PFD. However, if the component degrades over time and/or due to stresses suffered in the actuations, the probability  $\rho$  also increases with time and/or with number of demands. So, a time and/or demand dependent PFD.

The time/demanded-dependent PFD can be formulated as Equation 2 (based on MARTORELL et al., 2017), where  $\rho[d, t_d]$  is the probability of failure mechanism occurrence in the  $d^{th}$  demand occurring at  $t_d$ ,  $\rho_0$  is the residual PFD (i.e. the probability of the failure mechanism in a pseudo first demanded procedure occurring at  $t_0 = 0$ ),  $\varepsilon$  is the demand degradation factor and  $\gamma$  is the time degradation factor. This

formulation models a linear degradation on time and by demand for  $\rho_0$ , but other types of degradation models (logarithmic, power law, etc.) can be easily formulated. Whether a classic PFD or a time/demand-dependent PFD, the reliability against failure mechanism  $i$  in a demand can be modeled by the Bernoulli distribution, according to Equations 3 and 4.

Figure 7 – General rule for selecting failure mechanism's reliability model.



Source: The author

$$\rho[d, t_d | \rho_0, \varepsilon, \gamma] = \rho_0 + \rho_0 \times (\varepsilon \cdot d + \gamma \cdot t_d) \quad 2$$

$$R_i(\text{on demand} | \rho_i) = 1 - \rho_i \quad 3$$

$$R_i(\text{on demand} | \rho_{0_i} \varepsilon_i, \gamma_i) = 1 - \rho_i[d, t_d | \rho_{0_i} \varepsilon_i, \gamma_i] \quad 4$$

For failure mechanisms whose stressors affect continuously the item, or in a high frequency, a time-to-failure distribution is used. This includes environmental variables that constantly act on item (e.g.: temperature, axial loads, pressure differential, vibration, humidity, electrical potential, etc.) causing it to fail due to mechanisms such as fatigue, corrosion, erosion, and so on. The suitable choice for the time-to-failure distribution depends on the form of PoF model that better represents the failure mechanism. The PoF modeling framework is subject to the nature of underlying failure and degradation mechanism. The main ones are described below (MODARRES, 2021):

- *Stress-Strength model*: In this model, the item fails if the applied stresses exceed its strength (see Figure 8). This failure model may depend on environmental conditions, applied operating loads and the occurrence of



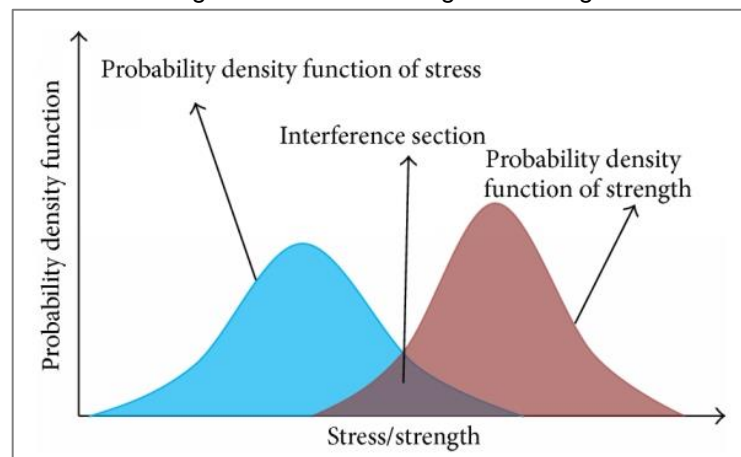
critical events, rather than the passage of time or cycles. Stress and strength are treated as a random variable encompassing variability in all conditions. An example of this model includes a metal item under a tensile stress lower than its yielding point, but which will be randomly subjected to load that exceeds the yielding point over time. The likelihood of failure is estimated from the probability that the stress random variable exceeds the strength random variable, which is obtained from a convolution of the two respective distributions.

- *Damage-Endurance Model:* This model differs from the stress-strength model in that although the stress (load) applied to an item may be below of its strength it brings about a small but accumulating amount of irreversible damage, for example, corrosion, wear, embrittlement, creep, or fatigue. The repeated application of these stresses results in the accumulation of damage, until the damage surpasses the endurance of the item. For example, a crack grows on a structure until it reaches a critical length beyond which the growth will be catastrophically rapid. Accumulated damage does not disappear when the stresses are removed, although sometimes treatments can repair cumulative damage. Figure 9 shows a depiction of this model with multiple traces of damage starting with an uncertain amount of initial damage (shown by a probability density function) and growing until it exceeds the endurance limit. Each damage accumulation trace produces one instance of time to failure. All such instances result in the time-to-failure distribution of the item as shown in Figure 9. At each instant of time, so long as the distribution of cumulative damage does not surpass the endurance limit, no failure will occur. However, when the cumulative damage exceeds the endurance level, a failure will be expected.

The assumption behind the *stress-strength model* for reliability modeling is that so long as the stresses applied to a unit are below its strength, no damage will occur, and it remains as good as new. The overlap between the two distributions represents cases where a random stress value in the high tail of its distribution occurs at some instant of the system life and coincides with the item having a random strength on the weak tail of the strength distribution at that moment. Then it is possible that strength falls short of the applied stress and a failure will occur. This type of failure usually

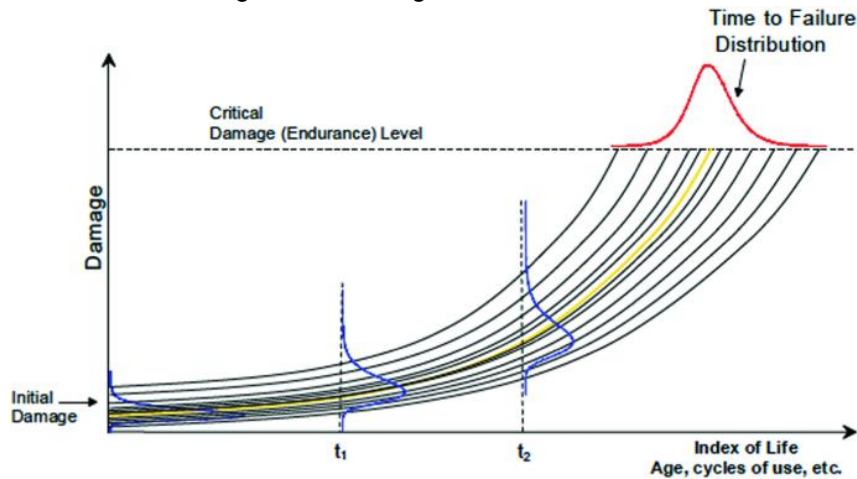
results from temporal random application of high stresses, or from insufficient strength due to poor design, manufacturing or maintenance. Thus, the time until item failure is independent of how long it has already lasted, and the exponential time-to-failure distribution is suitable to model this feature. The reliability model of a failure mechanism  $i$  with an exponential time-to-failure distribution is given in Equation 5, where  $\lambda_i$  is the rate parameter.

Figure 8 – Stress-strength modeling



Source: GAO & XIE (2015)

Figure 9 – Damage-endurance model



Source: MODARRES (2021)

For *damage-endurance model*, the mathematical concept determining the failure of an item at a given time is similar to the *strength-strength* modeling approach, however with the assumption that the strength reduces in time due to the degradation process caused by the cumulative damage (see Figure 10). The endurance limit, therefore, represents the level of accumulated damage at which the strength becomes

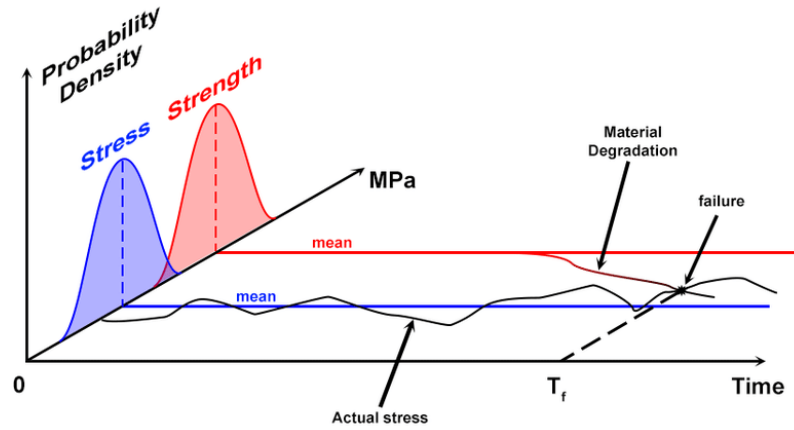
less than the stress. Naturally, in a probabilistic dimension, the endurance limit is uncertain, even because of the stochastic nature of the stress level, but it is possible to realize that the interference section (Figure 8) increases in time. This mean that the rate parameter also increases in time. Weibull and Lognormal time-to-failure distributions are most used for these cases (O'CONNOR et al. 2016). Equations 6 and 7 present the reliability model of a failure mechanism  $i$  with, respectively, Weibull and Lognormal time-to-failure distribution, where  $\alpha_i$  and  $\beta_i$  are the scale and shape parameters of Weibull distribution, while  $\mu_i$  and  $\sigma_i$  are the mean and the standard deviation of the time-to-failure's natural logarithm, and  $\Phi$  is the cumulative distribution function of the standard normal distribution.

$$R_i(t|\lambda_i) = e^{-\lambda_i t} \quad 5$$

$$R_i(t|\alpha_i, \beta_i) = e^{-\left(\frac{t}{\alpha_i}\right)^{\beta_i}} \quad 6$$

$$R_i(t|\mu_i, \sigma_i) = 1 - \Phi\left(\frac{(\ln t) - \mu_i}{\sigma_i}\right) \quad 7$$

Figure 10 – Damage-endurance model based in stress-strength relationship.



Source: PAGGI et al. (2017)

#### 2.2.2.2 The use of life-stress models

Figure 7 previous Section outlined three life distributions (Exponential, Weibull and Lognormal) for modeling the time-to-failure of mechanisms acting continuously in time. However, not rarely, accelerated life testing (ALT) and/or accelerated degradation testing (ADT) are performed during technology development process.

These models not only deal with determining the life distribution at each tested stress level, but more importantly, life distribution conditional on the level of stress and estimation of parameters of the corresponding life-stress relationship. Based on the distribution of life-stress models, we can extrapolate and predict the life distribution and other metrics of interest at the use stress level. For this reason, a distribution of life conditional on the level of stress is used in place of classical statistical distributions.

Basically, a life-stress model relates the life of an item with the level of stress, with respect to a specific failure mechanism. The formulation of the appropriate life-stress model for a failure mechanism is within the scope of PoF analysis. Let  $S$  be the level of stress, Equations 8, 9 and 10 show respectively the exponential, the power, and the Eyring formulation for life-stress models, where  $a, b, c$  and  $n$  are model parameters related to material constants.

$$L(S) = b \cdot e^{\frac{a}{S}} \quad 8$$

$$L(S) = \frac{1}{a \cdot S^n} \quad 9$$

$$L(S) = \frac{1}{S} \cdot e^{-\left(c - \frac{a}{S}\right)} \quad 10$$

The exponential life-stress model (Equation 8) is one of the most common models used in accelerated life testing of items subject to temperature stresses. This model derived from the well-known Arrhenius reaction rate expression (Equation 11), where  $R$  is the reaction rate,  $A$  is thermal constant,  $E_a$  is the activation energy, the energy that a molecule must possess in order to participate in the reaction (i.e., it is a measure of the effect that temperature has on the reaction),  $K$  is Boltzmann's constant ( $8.617385 \times 10^{-5} \text{eV K}^{-1}$ ), and  $T$  is the absolute temperature (in Kelvin). The power life-stress model (Equation 9) is another popular life-stress model, commonly used in applications where the applied stresses are non-thermal in nature (e.g. vibration), and the Eyring life-stress relationship (Equation 10) is a special form of the exponential life-stress model that is commonly used when the acceleration variable is thermal in nature (e.g., temperature or relative humidity).

$$R(T) = A \cdot e^{-\frac{E_a}{KT}} \quad 11$$

Sometimes, the failure mechanism involves two or more stress conditions, each accelerating the degradation and reducing the life. Equation 12 shows the dual-stress exponential life-stress model, which is commonly used in electronics when temperature ( $T$ ) and humidity ( $H$ ) are considered as agents. However, the dual stress exponential model can be used when both variables independently affect life in any application. The power-exponential life-stress model (Equation 13) is used when a combination of temperature  $T$  (or humidity) acceleration variable along with a second non-thermal stress  $S$  (e.g. mechanical or voltage) accelerated variable is used.

$$L(T, H) = c. e^{\left(\frac{a}{T} + \frac{b}{H}\right)} \quad 12$$

$$L(T, S) = c. S^{-n}. e^{\frac{a}{T}} \quad 13$$

Whichever life-stress model best represents the relationship between the failure time and stress level for a failure mechanism; in order to use it with a time-to-failure distribution, it is important to first define the conditional combined model. It can be made by replacing the scale parameter of the time-to-failure distribution with the stress-dependent life model. This comprises the branch of the probabilistic physic of failure (PPoF) analysis, where the relationship between life and stress is given in a probabilistic dimension rather than the deterministic one. Scale parameters for Exponential, Weibull and Lognormal distributions are respectively the  $\lambda$ ,  $\alpha$  and  $\mu$  parameters in Equations 5, 6 and 7. Then these equations can be transformed in the equations bellow by combining a conditional life-stress model with the probabilistic time-to-failure distribution, where  $L_i(S|\delta_i)$  is the life-stress model that better represents the failure mechanism  $i$ , with stress  $S$  and parameter  $\delta_i$  vectors.

$$R_i(t, S|\delta_i) = e^{-L_i(S|\delta_i)t} \quad 14$$

$$R_i(t, S|\delta_i, \beta_i) = e^{-\left(\frac{t}{L_i(S|\delta_i)}\right)^{\beta_i}} \quad 15$$

$$R_i(t, S|\delta_i, \sigma_i) = 1 - \Phi\left(\frac{(\ln t) - L_i(S|\delta_i)}{\sigma_i}\right) \quad 16$$

Another measure of the effect that the stress has on the life distribution can be made by a modifier function to be applied in the hazard rate function of a time-to-failure

distribution. This modifier function can be a combination of different independent life-stress models such as exponential, inverse power law, etc. This type of PPoF model is known as proportional hazards (PH) model. For more about PH models and other PPoF formulations used for failure mechanisms occurring in mechanical and electrical components see MODARRES (2021), MCPHERSON (2019), MODARRES et al. (2017), HAGGAG et al. (2005) and OHGATA et al. (2005).

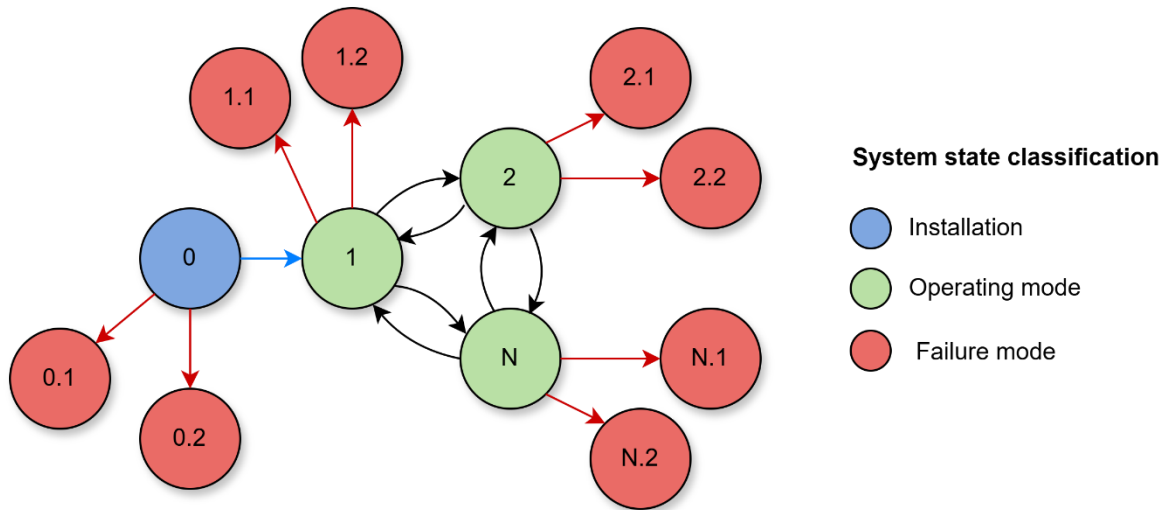
#### 2.2.2.3 Modelling for non-continuously (on-demand) operated systems.

The formulations in previous sections can describe the reliability model of failure mechanism for continuously operated systems. However, when dealing with non-continuously (on-demand) operated systems, the dependence on the operating modes must be considered. For these cases, the time-to-failure distributions and reliability models presented so far only describe the probability of occurrence (or non-occurrence) of the failure mechanism in a time interval since the system is subject to that mechanism in that interval. However, during a period, a failure mechanism only will compete for causing the system failure if the system stays in the operating mode in which it can happen. Therefore, the distributions of the transitions among operating modes should be evaluated, as well as their impact on the probability of failure mechanism occurrence. That can be made by a Markov-based analysis.

Related operating modes for each failure modes are mapped in FMECA. Taking as example the scenario in Figure 6, the loss of sealing capacity (due to abrasive wear) of the sealing unit occurs only during the “keep flow open” operating mode. It is noteworthy that the operating mode in which the component failure mechanism takes place is not always the same as the corresponding one for the system failure mode. For example, the internal leakage (failure mode) resulting of the abrasive wear only appears during the demand for closing (and keep closed) the flow, even though the failure mechanism (abrasive wear) had happened during the “keep flow open” operating mode. It can be said that the system was in a fault state (hidden failure) while it keeps the flow open. The system failure mode state (do not close the flow when demand) only manifests when the operating mode is “keep flow closed”. A Markov-based diagram (LIANG et al., 2020) can be constructed to model failure mechanism as a function of the system states.

Figure 11 illustrates the general Markov-based diagram used in methodology to that end. The first state of a system in field is its installation, represented by node "0" (in blue) in Figure 11. All nodes in red represent failure modes which can happen during each operating mode. Two failure modes may occur during installation (illustrated by the nodes "0.1" and "0.2"). If the installation completes successfully, the system migrates to state "1", the first operating mode immediately after installation. From then on, the system will transition among its  $N$  operating modes (green nodes) until the end of mission time or until a failure mechanism (red nodes) occurs.

Figure 11 – Generic Markov-based diagram for system states in methodology.



Source: The author

It is possible to notice that the reliability models  $R_i(t|\theta_i)$ , presented in previous sections, represent the probability that system does not go to the faulty state (failure mechanism)  $i$  when it is in the operating mode state (0, 1, 2, ..., N) in which the failure mechanism  $i$  can occur. Furthermore, classic parametric probability density functions (PDF), such as the Exponential distribution, can be used to model the transitions among the operating mode states. Then, let  $\Lambda$  be the set of PDF's representing the transitions among operating states, the general formulation for the reliability model of the failure mechanism  $i$ ,  $R_i(t|\theta_i, \Lambda)$ , is given by the probability that the system does not go to the state  $i$  during the interval  $(0, t]$ . Given the complexity of the reliability models  $R_i(t|\theta_i)$  as seen in previous sections, an analytical formulation for  $R_i(t|\theta_i, \Lambda)$  is infeasible and it should be inferred via simulation techniques.

## 2.2.3 Modeling the system reliability via fault tree analysis

### 2.2.3.1 Selecting FMECA scenarios

After analyzing failure scenarios via FMECA, design actions are usually performed to reduce the probability and/or severity of some specific failure mechanisms. Following implementation of these actions, an update to the RPN assessment must take place. Typically, frequency and severity scales (section 2.2.1.3) are defined in such way that some very low RPN values correspond to risks that can be neglected in the operation of the system for the specific application. Then, a lower limit in RPN value should be set to select the failure mechanism to be considered in the quantification. Failure mechanisms with RPN lower than the threshold must be neglected when formulating the reliability model, as if there is sufficient confidence that it is avoided by design, in normal use conditions.

### 2.2.3.2 Fault tree analysis (FTA) to model the system reliability for each failure mode.

As seen in section 2.2.1.2, system failure modes are captured in the “*Effect*” column of FMECA. So, it is possible to identify the failure mechanisms that causes each system failure mode. A fault tree (FT) diagram can be built for a system failure mode where basic events comprise the failure mechanisms resulting in that system failure mode, and the corresponding item failure modes are the intermediate events. Some additional information may be needed to determine the logical gates connecting events of a lower level to the one in the level immediately above. At first, a system failure mode occurs if any of the item failure modes resulting in it happens, which would result in the use of “OR” gate. However, the existence of redundancies and conditionalities must be known to better specify the gates.

If a redundancy for some item is applied in the system design, then it is necessary that all redundant items suffer the failure modes resulting in the same effect to the system. An “AND” gate should be used to connect the failure modes of the redundant items. Sometimes, an item has a safety function and the loss of it does not result immediately in a system failure mode, but it only removes the system protection. Another item failure mode must occur (now, without the protection) for the system to fail. For example, if an anode protection against corrosion is connected to the metal



surface of the casing of a submarine control module (SCM), for corrosion to occur in the SCM, first the anode must lose its protective function, and from then on the casing must fail due to corrosion. The “INHIBITION” or “PRIORITY AND” gates can be used for this case.

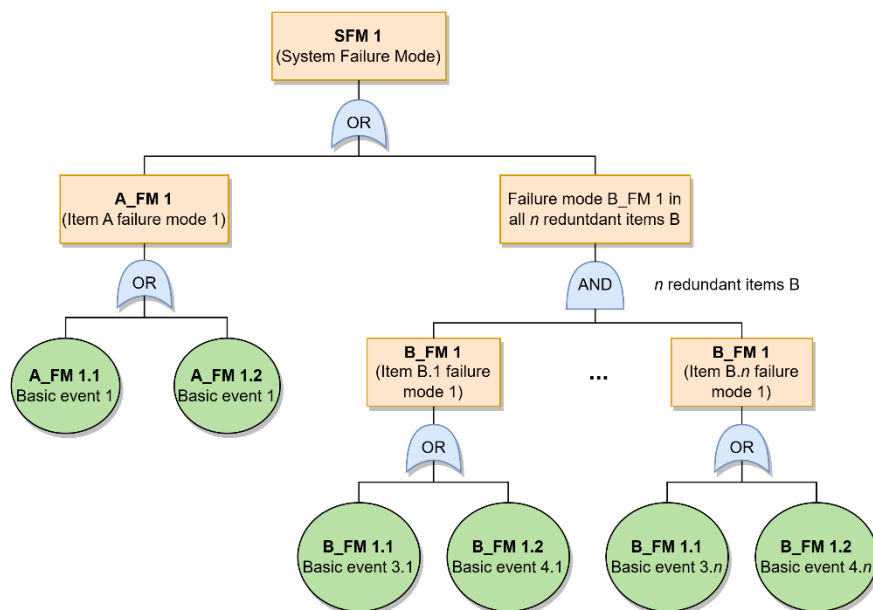
Be the Table 5 a generic example of an excerpt from FMECA, Figure 12 illustrates the resulting FT diagram for the generic system failure mode (system effect) *SFM 1*. Note that the item A failure mode *A\_FM 2* was not included in FT diagram once it doesn't cause the system failure mode *SFM 1*. Also, an “AND” gate connect *n* failure modes *B\_FM 1* due to existing redundancy for item B.

Table 5 – generic example of FMECA.

...	Item	Failure Mode	Failure Mechanism	...	Effect (at system level)	...
...	A	A_FM 1	A_FM 1.1	...	SFM 1	...
			A_FM 1.2	...		...
		A_FM 2	A_FM 2.1	...	SFM 2	...
			A_FM 2.2	...		...
...	B	B_FM 1	B_FM 1.1	...	SFM 1	...
			B_FM 1.2	...		...
...	...	...	...	...	...	...

Source: The author.

Figure 12 – FT diagram for the system failure mode *SFM 1*



Source: The author.

Reliability models of basic events (failure mechanisms)  $R_i(t|\theta_i)$  are formulated according to section 2.2.2. The event top reliability model (system failure mode) can be built as a function of  $R_i(t|\theta_i)$  from the logic gates of FTA. Equations 17 and 18 show how we can obtain the reliability of an intermediate FTA event ( $IE$ ) from the reliability models of the events immediately below considering respectively "OR" and "AND" logic gates, where  $\Delta_{IE}$  is the set of events (intermediates and/or basics) at the next lower level that are connected to the  $IE$  event. Note that  $\theta_{IE} = \{\theta_i, i \in \Delta_{IE}\}$ , this is, the parameter of an FTA event reliability model is formed by the set of reliability model parameters of the basic events that cause it (i.e., a multilevel reliability model - MRM). Then, in a bottom-up perspective, and using the equations below, the reliability model of the FTA top event (the system failure mode) can be obtained. For the FTA in Figure 12, the reliability model of top event would be given by Equation 19, by assuming that reliability models of item B failure mechanisms are the same for any redundant part.

$$R_{IE}(t|\theta_{IE}) = \prod_{i \in \Delta_{IE}} R_i(t|\theta_i) \quad 17$$

$$R_{IE}(t|\theta_{IE}) = 1 - \prod_{i \in \Delta_{IE}} [1 - R_i(t|\theta_i)] \quad 18$$

$$R_{top}(t|\theta_{top}) = R_1(t|\theta_1) \cdot R_2(t|\theta_2) \cdot \{1 - [1 - R_3(t|\theta_3) \cdot R_4(t|\theta_4)]^n\} \quad 19$$

## 2.3 RELIABILITY DATA COLLECTION

During the development of a new system, the reliability tests are the unique direct evidence available for the current system design. However, secondary sources of evidence can be adopted in order to overcome a possible low quality of data arising from the reliability tests due to limitations in cost, time, and infrastructure for performing them. In general, the additional sources of information consist of (i) experts' opinions and (ii) information from similar systems (partially relevant information). The last can include:

- Historical raw data (field or test) on a previous design and from similar heritage systems: Sometimes, the design under development is an improvement of an earlier design and/or comprises the use of commercial components already used in other applications. Although these data sets are

not 100% relevant, they do provide useful background information for the events related to such components.

- Reliability estimates for similar systems/components from generic databases (e.g., Oreda, Wellmaster): Generic databases directly or indirectly provide reliability estimates for a set of equipment previously defined by the user's query. Suppose this set is deemed to be similar to the system under development (in design and application). In that case, the estimate can be used for analyzing reliability of related events/components.

Whatever the source, there is a tough challenge in aggregating the various evidence since they can be presented with significant differences in:

- Type: different types of reliability evidence include pass/fail data, lifetime data, degradation data, and reliability metrics estimates (failure rate, reliability level, MTTF, etc.)
- Hierarchical level: the collected evidence may refer to system, subsystem, component, part, or material level, and only cover a specific set of failure modes or mechanisms.
- Operating conditions: for example, a reliability test can be executed under use or accelerated conditions (ALT or ADT). Also, historic data from similar system usually match to different operational and environmental conditions.
- Timeline: portions of this heterogeneous evidence are usually made available in different stages of the development process.

The use of the heterogeneous evidence presented in this section for estimating the MRM parameters will be described in the next section.

## 2.4 BAYESIAN INFERENCE OF MRM PARAMETERS

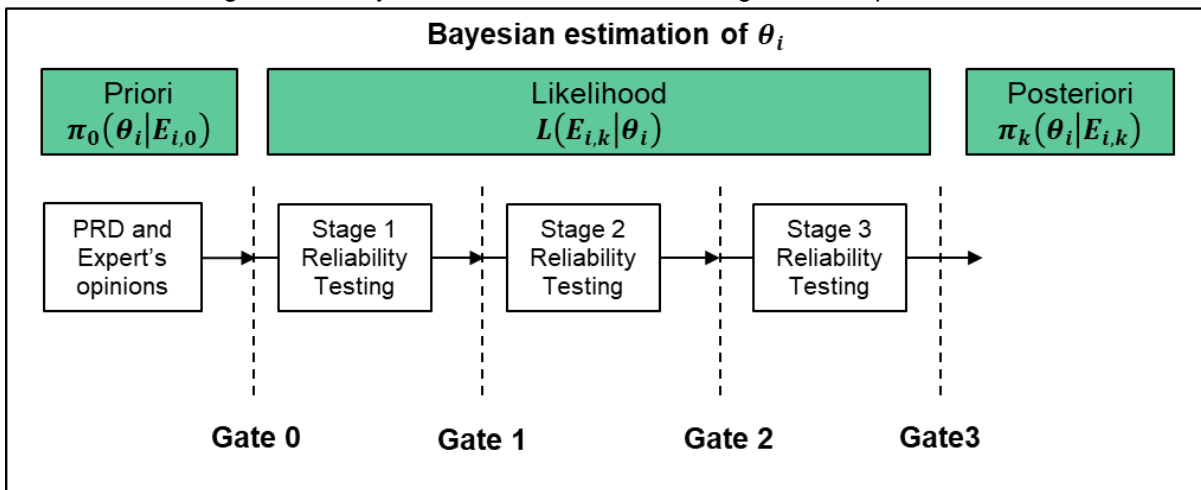
This section depicts of the Bayesian framework proposed to estimate the MRM parameters by using the multitype and multilevel reliability evidence from the sources described in the previous section. The methodology implements an analysis procedure which breaks down the problem into a number of analysis steps that are part of different stages in the system's development process. Each analysis step consists of a

Bayesian updating in a particular stage of the development. Therefore, different posterior distributions for the MRM parameters are estimated at each step in the analysis. The result of the estimation at each step consists of uncertainty distributions over the MRM parameters.

The analysis steps in each of these stages and the data source used are showed in Figure 13. The first step in this analysis flow is to establish prior distributions for MRM parameters. In this moment, no evidence from reliability tests is available and this baseline analysis should be based on partially relevant data and/or expert's opinions. We will use the notation  $E_{i,0}$  to refer to this prior evidence and  $\pi_0(\theta_i|E_{i,0})$  to describe the prior distribution of the set of parameters  $\theta_i$ , related to the failure mechanism  $i$ .

Since the prior distributions are defined, the likelihood functions must be constructed from the test data carried out in the following stages of the development process. Naturally, if the failure mechanism  $i$  is covered by a specific test, then the likelihood of the evidence extracted from that test can be obtained as a function of  $\theta_i$ , based on the reliability model  $R_i(t|\theta_i)$  (see section 2.2.2). Then, let  $T_{i,k}$  be the set of tests performed at stage  $k$  that cover event  $i$  and  $E_{i,k}$  the evidence gathered from each test in  $T_{i,k}$ .  $L(E_{i,k}|\theta_i)$  denotes the likelihood function of the tests run at stage  $k$  that updates the prior distribution of  $\theta_i$ .

Figure 13 – Bayesian framework for estimating the MRM parameters



Source: The author

Then, the posterior distribution of  $\theta_i$  is obtained by applying the Bayesian update Equation 20, where the prior distribution of  $\theta_i$  at stage  $k$  is the posterior

distribution calculated in the previous stage ( $k - 1$ ). Therefore, using the evidence from various sources, an updated distribution for MRM parameters is estimated at each stage in the analysis. Equation 20 shows the Bayesian equation for  $\theta_i$  at stage  $k$ , where  $k = 0$  comprises the stage immediately prior to performing the first reliability test. Some methods to solve Equation 20 include the analytical approach (when a conjugate prior can be obtained for the likelihood functions), and the approximative approach via Markov Chain Monte Carlo (MCMC) and/or Variational Inference (VI) (BLEI; KUCUKELBIR; MCAULIFFE, 2017; ROSSI, 2018; SPADE, 2020).

The chosen between MCMC and VI, in case of approximative approach, normally comprises the precision x scalability analysis. The MCMC method is asymptotically exact but computationally intensive, i.e. given enough time, which can be computationally expensive for high-dimensional problems, it can provide samples that are very close to the true posterior distribution. To the other side, the VI method is faster than MCMC methods and can be scaled to handle large datasets and complex models, however the quality of the approximation depends on the chosen family of distributions, which might not capture all the complexities of the true posterior.

$$\pi_k(\theta_i | E_{i,k}) \propto \pi_{k-1}(\theta_i | E_{i,k-1}) \times L(E_{i,k} | \theta_i) \quad 20$$

#### 2.4.1 Implementation of Bayesian methodology

Two problems arise for implementing the Bayesian framework presented in previous section: (i) the creation of a methodology for getting suitable prior distributions for  $\theta_i$  from expert's opinions and/or PRD, in the O&G context, and (ii) be able to construct likelihood functions as a function of parameter  $\theta_i$  from the data gathered from various separate reliability tests for the components, subsystems, and system in different forms. For (i), two methods are proposed, and a comprehensive literature review are given, in Chapters 3 and 4 respectively for continuously and non-continuously operated systems.

Regarding item (ii), the reliability tests data commonly include the pass-fail, lifetime, and degradation data sets collected for individual components or pass-fail, and lifetime data sets collected for the subsystems, and the overall system, which may be under accelerated or nominal conditions. So, let us consider a basic failure event  $i$

with reliability model  $R_i(t, S|\theta_i)$ , such as in Equations 14-16, those heterogeneous data sets are incorporated through their contributions to the joint likelihood function, if the corresponding test cover the failure mechanism  $i$ , as follow:

- The contribution of pass-fail data: Suppose  $K$  lots of pass-fail tests covering the failure mechanism  $i$ . In each of them,  $n_k$  samples are tested separately, at different observation times  $t_k$ , and stress levels  $S_k$ , where  $k = 1, \dots, K$ . The number of units  $y_k \leq n_k$  that pass each test is observed. The probability that a unit passes the test, against the failure mechanism  $i$ , at time  $t_k$  is determined by its reliability at that time, as  $R_i(t_k, S_k|\theta_i)$ . The likelihood model, as a function of  $\theta_i$ , for that pass-fail data is based on the binomial distribution and described as Equation 21.

$$L(K|\theta_i) = \prod_{k=1}^K \binom{n_k}{y_k} [R_i(t_k, S_k|\theta_i)]^{y_k} [1 - R_i(t_k, S_k|\theta_i)]^{n_k - y_k} \quad 21$$

- The contribution of lifetime data: Suppose  $n$  units are tested at stress level  $S_j$  ( $j = 1, \dots, n$ ), of which  $n^F$  failed due to basic event  $i$  with exact failure time points  $t_k^F$  ( $k = 1, \dots, n^F$ ), and  $n^C$  operated successfully (with no occurrence of basic event  $i$ ) by the end of the test with right-censored time points  $t_k^C$  ( $k = 1, \dots, n^C$ ), where  $n = n^F + n^C$ . Then, the likelihood function for the lifetime data can be obtained as Equation 22, where  $f_i(\cdot|\theta_i)$  is the PDF of the time to failure due to failure mechanism  $i$ .

$$L(t_k^F, t_k^C, S_k|\theta_i) = \prod_{k=1}^{n^F} f_i(t_k^F, S_k|\theta_i) \prod_{k=1}^{n^C} R_i(t_k^C, S_k|\theta_i) \quad 22$$

- The contribution of degradation data: Suppose  $n$  components have been tested at a stress level  $S_k$  and a number of degradation measurements has been taken for each, in relation to the failure mechanism  $i$ , at different time points, from which a set of degradation curves  $Y_k(t|\beta_k^{Deg})$  is get, conventionally assumed to be monotonically increasing, where  $k = 1, \dots, n$  and  $\beta_k^{Deg}$  being the parameter of the degradation curve obtained for the  $k^{th}$

component. The component fails when the degradation curve crosses a predefined threshold value  $Y^D$ , such as in a damage-endurance model (see Section 2.2.2.2). Then, a prediction for the lifetime can be made by finding the time point  $t_l^k$  for which  $Y_k(t_l^k | \beta_k^{Deg}) \geq Y^D$  and the likelihood model of Equation 23 is defined.

$$L(t_l^1, \dots, t_l^n | \theta_i) = \prod_{k=1}^n f_i(t_l^k, S_k | \theta_i) \quad 23$$

Given the measurement error  $\xi_k \sim \text{Normal}(0, \sigma_k)$ , an uncertainty model for the predicted lifetime of the  $k^{th}$  component can be estimated as a Gaussian distribution with mean  $t_l^k$  and standard deviation  $\sigma_k$ . The likelihood function that takes into account the uncertainty about the estimated degradation curve can be obtained by averaging the likelihood functions for each possible realization of  $t_l^k$ , as showed in Equation 24, where  $N(\tau | t_l^k, \sigma_k)$  is the Gaussian PDF for  $\tau$  with mean  $t_l^k$  and standard deviation  $\sigma_k$

$$L(t_l^k, \sigma_k | \theta_i) = \prod_{k=1}^n \int_{\tau} f_i(\tau, S_k | \theta_i) \times N(\tau | t_l^k, \sigma_k) d\tau \quad 24$$

From solutions presented above likelihood functions can be constructed for  $\theta_i$  whatever the type and taxonomic level of the test, as long as the failure mechanism  $i$  is being covered by the test.

## 2.5 RELIABILITY ASSESSMENT AND RESIDUAL UNCERTAINTY ANALYSIS

The result of the posterior distribution is not a point estimate for the  $\theta_i$ 's but a distribution of uncertainty about their real value. A similar distribution of uncertainty for the system reliability can be obtained through Monte Carlo (MC) sampling technique (SINGH & MITRA, 1995), where random samples for  $R_s(t)$  is attained from the samples randomly generated for the  $\theta_i$ 's by calculating the MRM, i.e.,  $R_s(t) = g[R_i(t | \theta_i)]$ ,  $i = \{1, \dots, m\}$ , for a specific time  $t$ . The  $\theta_i$ 's samples are found from the

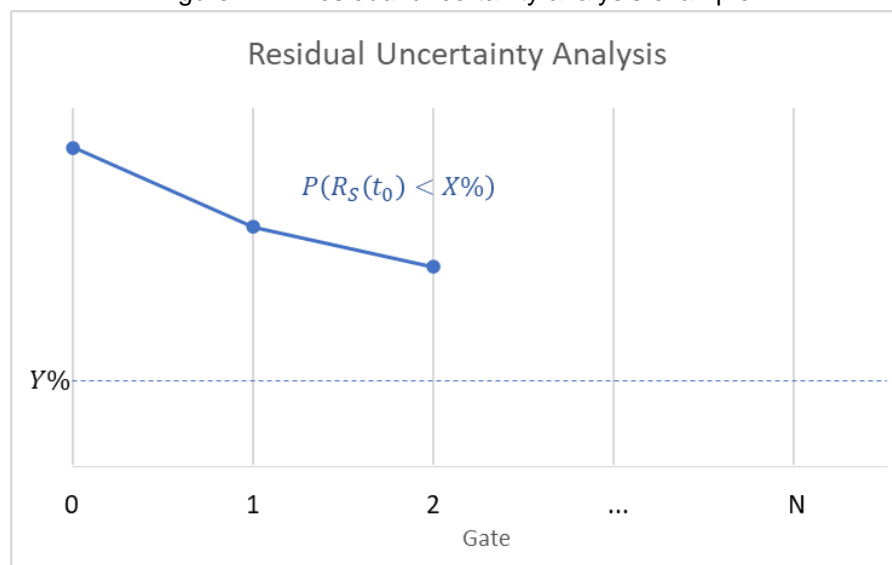
posterior distributions, then the distribution of  $R_S(t)$  is updated at each development stage.

As the reliability uncertainty is updated, it is possible to evaluate the behavior of the uncertainty levels at each gate. Thus, we can obtain uncertainty distributions over the system reliability as a function of the gates. The curve that illustrates the level of uncertainty of the reliability measure in  $t$  operating years, for each gate can be used to analyze the technological risk of the development project associated with reliability for including the new technology in the future production configurations. Indeed, the technological risk is related to the level of uncertainty regarding the technology attainment to a target reliability requirement (API 17N, 2017).

Let the target reliability requirement, stated according to section 2.1, be a minimum of  $X\%$  in  $t_0$  years, with a maximum uncertainty level of  $Y\%$ . The uncertainty level can be interpreted as the probability that the reliability of the new system in  $t_0$  years of operation is less than  $X\%$ , for a specific application, i.e.,  $P[R_S(t_0) < X\%]$ , which can be obtained by MC sampling at each stage.

Figure 14 shows an example of the residual uncertainty analysis; we visualize the distance between the estimated and targeted uncertainty levels over the gates. Figure 14 exemplifies a situation with two already carried out development stages out of  $N$ ; gate 0 corresponds to the prior analysis before the test runs, in which a high uncertainty level is expected.

Figure 14 – Residual uncertainty analysis example.



Source: The author



The behavior of the residual uncertainty is expected to decrease when a small number of failures (or no failures) is observed in the tests (or failures would have occurred long after  $t_0$ ). When the curve crosses the threshold of  $Y\%$ , the target is met, which is desired to occur until the last stage  $N$ . If the tests indicate a low system reliability, the residual uncertainty tends to increase over the gates. In this last case (or when the reduction is not significant enough from gate 0 to the current gate), design modifications can be implemented in the test plan or in the system design to improve the uncertainty level in which the system will meet the reliability requirements. The gates represent the points in the project evolution in which must be decided if the original planning will be followed or if modifications should be considered.

For equipment to be qualified using a TQP, planning for qualification should start as early as practicable. An early appreciation of qualification activities is especially important where there is a significant gap between the current technology maturity level, and the required one (API 17N, 2017). The residual uncertainty analysis proposed in this section emerges as a powerful tool in planning qualification tests, by assessing the tests protocols that contribute most satisfactorily to reducing residual uncertainty, and in defining changes in design, by identifying the failure mechanisms that most contribute to uncertainty.

### 3 PRIOR ANALYSIS FOR CONTINUOUSLY OPERATED EQUIPMENT BASED ON GENERIC DATA AND EXPERTS' OPINION

In the fourth step of the methodology proposed in Chapter 2 (Bayesian Inference of the MRM parameters), informative prior distributions  $\pi_0(\theta_i|E_{i,0})$  must be defined for the MRM parameters  $\theta_i$ , with  $i = 1, \dots, m$  and  $m$  being the number of basic events modeled in the MRM, based on indirect evidence  $E_{i,0}$  about the reliability of the new technology failure events. Indirect evidence comprise those obtained from sources other than direct observation of the performance of the equipment or its prototype (whether in the field or testing laboratory), such as expert opinions or data from similar systems.

This chapter presents a methodology for getting these informative prior distributions and is based on the paper titled “Bayesian prior distribution based on generic data and experts’ opinion: a case study in the O&G industry” (MAIOR et al., 2022), and published in the Journal of Petroleum Science and Engineering (JPSE) of which I am co-author. Below are my contributions to the paper:

- Direct conception and validation of the proposed methodology.
- Direct conception and validation of the models (Fault Tree Analysis, Top-down propagation of the events contribution, Method of Moments, Maximum Entropy, and Monte Carlo).
- Participation in the development and validation of questionnaires to elicit experts.
- Participation in the development and validation of the computational implementation of the models.
- Results analysis.

#### 3.1 INTRODUCTION

Often, expert opinions are the available knowledge to estimate the prior distribution for new technology (or its components), which is still preferable to non-informative prior distributions. In this case, experts can either provide direct parameter estimations of prior distributions or present key values of these distributions, such as an expected failure probability or reliability or a lower or upper percentile (GUO et al., 2018).

However, the direct elicitation of the parameters is not always straightforward its interpretation may be overly complicated. For instance, the Arrhenius-Weibull model is a three parameters Weibull model adopted to assess the probability of the time to failure at different temperatures. One of its parameters is given by  $B = E_a/k$ , where  $E_a$  is the activation energy and  $k$  is Boltzmann's constant ( $8.62 \times 10^{-5} \text{ eV} \cdot \text{K}^{-1}$ ). Thus, the experts must understand the activation energy concept, which may not always be true. Therefore, some parameters' elicitation might end up being a simple guess (MODARRES; AMIRI; JACKSON, 2017).

Distinct procedures have been proposed to establish informative prior distributions. From subjective information and historical data, PENG et al. (2013) proposed an approach applying an encoding method to elicit information through a series of questions in an interview process. However, the authors consider system-level information (i.e., aggregated data), which encompasses subsystems and components. Indeed, for complex systems, the direct elicitation performing interviews with several questions for each component may be unfeasible. Alternatively, GUO et al. (2018) applied a Bayesian melding approach using pooling operations on the system/subsystems' reliability to integrate the available information (e.g., qualitative or quantitative, fragmentary or extensive, expert knowledge-based or empirical-based), while KRIVTSOV (2017) determine the prior distribution through random sampling using prior data, in form of a random sample, about the parameters. However, these methods require raw equipment data (e.g., failure times) or direct elicitation of parameters, which may not be available or accessible. Indeed, different methods, like empirical Bayes and hierarchical Bayes (BAHOOTOROODY et al., 2020; GELMAN, 2006; LI et al., 2019) also make use of raw equipment data, which limit applicability.

In order to define the Bayesian prior distribution  $\pi_0(\theta|E_0)$  for the reliability of equipment under development, we propose a methodology that does not require direct elicitation of parameters to define informative distribution for FT's basic events (component level) but rather uses expert opinion and/or generic data for the top event (the system level). Thus, the proposed methodology allows keeping elicitation simple and intuitive. To that end, we adopted two estimation procedures, one of them is based on the method-of-moments (MM) (WANG et al., 2021) and the other relies on the maximum-entropy (ME) method (DUBEY; ABEDI; NOSHADRAVAN, 2021). Here, MM is applied to get the distribution of the probability of occurrence of the basic FTA events. If the probability of occurrence of the basic event is time dependent and a parametric

continuous distribution (e.g. Weibull) is assumed to model the variability of the time of occurrence of this event, then the ME method is applied to estimate the uncertainty about the parameters of this continuous distribution.

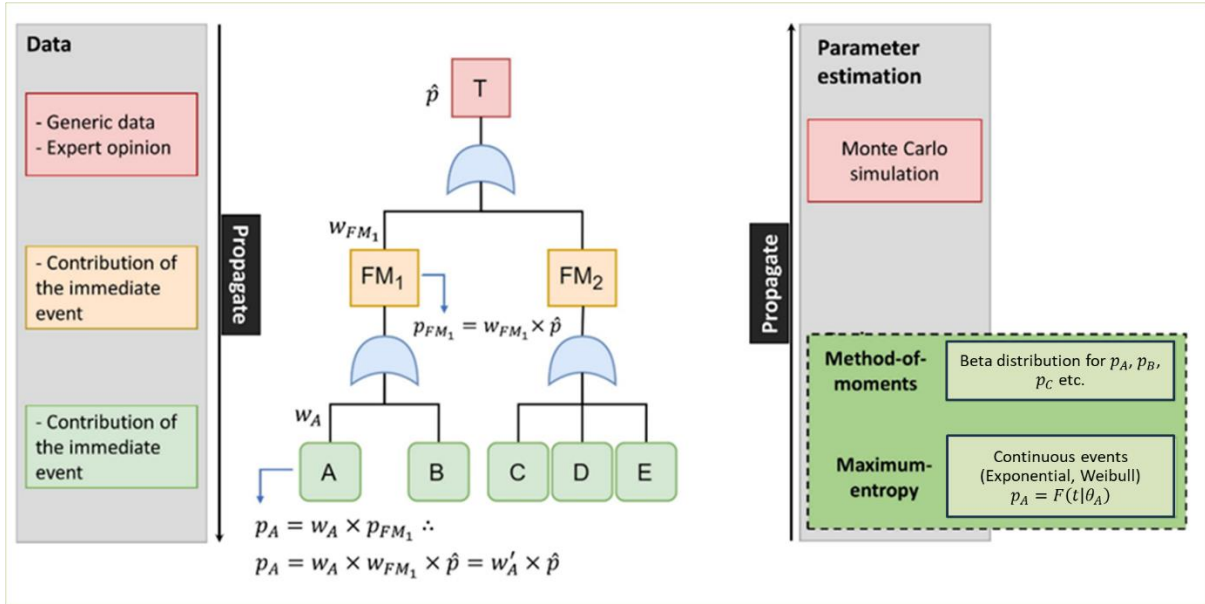
We apply the proposed methodology in a case study of a novel completion expansion packer that will operate in an open hole well of the O&G industry. We consider that failures may occur in two different moments: equipment (i) installation and (ii) operation. In each moment, an FT is used to model the logical relationships between the failure causes and mechanisms that lead to equipment failure. The goal is to propose a framework to determine the prior distributions of the failure events. The Bayesian analysis allows us to evaluate and monitor the reliability uncertainty throughout the equipment development stage as new information becomes available. To defined target for the prior reliability, we considered a reliability of 90% with a minimum confidence level of 80% (or maximum uncertainty level of 20%).

## 3.2 METHODOLOGY

### 3.2.1 Overview

Commonly, in the early stages of technology development, the only available data is from generic databases and engineering judgment. As it is frequently performed in risk and reliability analysis, we consider that after an initial investigation (e.g., FMEA), FTs are created to evaluate a limited number of top events, which may represent failure during specific periods of equipment life (e.g., installation and/or operation). Our proposed methodology is illustrated in Figure 15, in which the challenge is to propagate ‘downward’ this top event ( $E_T$ ), information gathered from generic database, throughout the failure modes ( $E_{FM_1}$  and  $E_{FM_2}$ ) until the basic events ( $E_A$ ,  $E_B$ ,  $E_C$ ,  $E_D$  and  $E_E$ ) of the novel technology. To that end, we consider expert opinions and two distinct approaches (MM and ME) to define the prior distribution for each basic event. Finally, these distributions are used in a Monte Carlo simulation algorithm to propagate ‘upward’ the uncertainty from the basic events and obtain a probability distribution of the system’s reliability. Then, the results may be compared to the desired target reliability measure to assess the risk associated with the equipment’s application. The next sub-sections detail each step of the proposed methodology.

Figure 15 – Overview of the proposed methodology and how the contributions of the basic events are computed.



Source: Maier et al. (2022)

### 3.2.2 Expert opinion for FT events

FT is a well-known graphical model commonly applied in reliability engineering to describe how failures propagate through the system and lead to its failure (RUIJTERS et al., 2019). To illustrate, consider the FT from Figure 15, which shows that  $E_A$  and  $E_B$  contribute to  $E_{FM_1}$  while  $E_C$ ,  $E_D$ , and  $E_E$  contribute to  $E_{FM_2}$ . Since the events are related to different consequences and probabilities, the event  $i$  contributes with a weight  $w_i$  to the immediate upper event (e.g., if  $E_{FM_1}$  has occurred,  $w_A$  represents the probability that this failure was caused by  $E_A$ ). These weights allow us to build relations between the top and basic events used to estimate the equipment reliability.

In this work, only the weights for each event are elicited, avoiding the direct estimation of parameters. Hence, to understand the experts' opinions about each failure event and its immediate causes, it is beneficial to consider two types of data:

- **Qualitative data:** by assuming that a failure has occurred (e.g.,  $E_T$ ,  $E_{FM_1}$  or  $E_{FM_2}$ ), the specialist indicates the relative frequency (very unlikely, unlikely, likely, very likely, or extremely likely) of the failure being due to each of the immediate lower events.

- Quantitative data: by assuming that the failure has occurred (e.g.,  $E_T$ ,  $E_{FM_1}$  or  $E_{FM_2}$ ), the specialist assigns numerical values (weights) to each of the immediate events representing the probability that the specific lower basic event has caused the failure.

In this case, it is possible to assess the consistency of the expert answers by comparing the qualitative vs. quantitative responses, which is paramount when considering subjective data evaluation such as expert opinion. In addition, as distinct experts may have different knowledge about the new equipment, one may assign specific relevance factors for each expert (i.e., the  $j$ -th specialist may receive a relevance factor,  $r_j$ , validated by other reliable sources such as senior experts or a consensus). Then, the quantitative responses of experts with  $r_j = x, \forall x \in Z_+^*$ , are considered  $x$  times to compute a weighted median value (CORMEN et al., 2009).

The elicited contributions define the relations between the system level and the other events. Since the failure probabilities are small, the probability of one event can be considered as the sum of the probabilities of its immediate causes (MODARRES; AMIRI; JACKSON, 2017). For example, in Figure 15, given  $\hat{p}$  (i.e., the estimate of the failure probability related to  $E_T$ ), one defines the probability of the failure mode  $E_{FM_1}$  as  $p_{FM_1} = 1 - (1 - \hat{p})^{w_{FM_1}}$  (I), where  $w_{FM_1}$  represents the contribution of  $E_{FM_1}$  to  $\hat{p}$ . Analogously, the failure probability of basic event  $E_A$ , an immediate cause of  $E_{FM_1}$ , can be defined as  $p_A = 1 - (1 - p_{FM_1})^{w_A}$  (II), where  $w_A$  is the weight of  $E_A$  to  $p_{FM_1}$ . Then, combining (I) and (II), and setting  $w'_A = w_{FM_1} \times w_A$  as the weight of  $E_A$  to  $\hat{p}$ , we get  $p_A = 1 - (1 - \hat{p})^{w'_A}$ . This procedure is numerically illustrated in the case study presented in Section 3.

### 3.2.3 Downward propagation

Due to the complexity when considering a multilevel hierarchical structure, the system's reliability can be represented by a multilevel reliability model (MRM), which consists of specific probabilistic models to describe the failure of basic components (GRISHKO et al., 2017; SWAMINATHAN & SMIDTS, 1999). These models can be parametric probability distributions (e.g., Bernoulli, Exponential, Weibull) or physics-

based reliability models, like Arrhenius-Weibull (MODARRES, 2021) and Gaussian Degradation Process (BAE et al., 2007). Here, the MRM model uses the logic gates of the FT, in which each basic event  $i$  ( $E_i$ ) has a set of parameters  $\theta_i$  that model the probability of occurrence of the corresponding mechanism/cause of failure. Then, the reliability function of the entire system is a function of  $\theta_i$ ,  $f[R_i(t|\theta_i)]$ ,  $\forall i$ , which translate the possible pathways leading to equipment, for example, failure during installation ( $t = 0$ ) or over a mission time (e.g.,  $t = 27$  years) (BOUDALI; DUGAN, 2005).

Here, the propagation through two types of FTs is discussed: (1) one related to a failure in equipment installation, and (2) the other associated with a failure during equipment operation for a defined mission time. We adopt distinct approaches depending on the characteristics of the basic event: the first approach is adopted if success/fail event (Bernoulli Distribution) are considered, and the second approach is adopted if continuous distributions describe the basic events, such as Exponential, Weibull, or Arrhenius-Weibull.

### 3.2.3.1 Method of Moments

The occurrence of an event  $E_i$  is assumed to be well described by a Bernoulli distribution (success/fail event) with parameter  $p_i$ . This probabilistic model is adequate, for example, to account for installation events typically related to operational procedures in which success and failure are the only two possible outcomes. Then,  $R(0|\theta)$ , the equipment reliability in installation (when  $t = 0$ ), is provided by the MRM and is given in Equation 25, where  $\theta$  is the set of MRM parameters.

$$R(0|\theta) = \prod_i (1 - p_i) \tag{25}$$

We assumed there is uncertainty in  $p_i$ , modeled by  $\pi(p_i)$  as a beta distribution  $B(\alpha_{p_i}, \beta_{p_i})$ ,  $\forall i$ . In this approach, in order to obtain the mean,  $\mu_{p_i}$ , and variance,  $\sigma_{p_i}^2$ , the PERT method is adopted, where a triangular distribution is first obtained from an optimistic estimate,  $a_{p_i}$ , a most likely estimate,  $m_{p_i}$ , and a pessimistic estimate,  $b_{p_i}$ , of  $p_i$ . Thus, the triangular distribution can be approximated to a Beta distribution by

estimating the expected value and variance of the Beta distribution of  $p_i$  from Equations 26 and 27, respectively (VOSE, 2008).

$$\mu_{p_i} = \frac{a_{p_i} + 4m_{p_i} + b_{p_i}}{6} \quad 26$$

$$\sigma_{p_i}^2 = \left( \frac{b_{p_i} - m_{p_i}}{6} \right)^2 \quad 27$$

The usage of (i) most likely, (ii) pessimistic, and (iii) optimistic values are adopted in order to make the elicitation process more intuitive when compared to directly estimating the hyperparameters of the beta distribution. Also, these values allow us to analytically estimate the prior distribution through MM using Equations 28 and 29 (MUNKHAMMAR; MATTSSON; RYDÉN, 2017). MM is an estimation technique in which the unknown parameters are estimated by matching theoretical moments (functions of the unknown parameters) with the appropriate sample moments. For details, see (KUERSTEINER; MATYAS, 2000; WOOLDRIDGE, 2001).

$$\alpha_{p_i} = \frac{\mu_{p_i}^2 \times (1 - \mu_{p_i})}{\sigma_{p_i}} - \mu_{p_i} \quad 28$$

$$\beta_{p_i} = \left( \frac{\mu_{p_i} \times (1 - \mu_{p_i})}{\sigma_{p_i}} - 1 \right) \times (1 - \mu_{p_i}) \quad 29$$

Then, based on the central limit theorem it is possible to consider confidence intervals obtained from a normal approximation to the Binomial distribution (WALLIS, 2013). The estimate  $\hat{p}$  is the most likely value and we assume that percentile 1,  $P_1$ , and percentile 99,  $P_{99}$ , are the optimistic and pessimistic values, respectively. Thus, we obtain the confidence interval using Equation 30.

$$(P_1; P_{99}) = \left( \hat{p} + Z_{1\%} \sqrt{\frac{\hat{p}(1 - \hat{p})}{n}}; \hat{p} + Z_{99\%} \sqrt{\frac{\hat{p}(1 - \hat{p})}{n}} \right) \quad 30$$



As mentioned, basic event  $E_i$  contributes with a weight  $w_i$  to upper event. Thus, the relations  $m_{p_i} = \hat{p} \times w'_i$ ,  $a_{p_i} = P_1 \times w'_i$ , and  $b_{p_i} = P_{99} \times w'_i$  were used to compute  $\mu_{p_i}$  and  $\sigma_{p_i}$ , where  $w'_i$  is the contribution of event  $i$  to the top event.

### 3.2.3.2 Maximum Entropy

Here, the occurrence of event  $E_i$  is time-dependent and described by a continuous distribution (e.g. Weibull). In these cases, the MM approach presented in previous section is applied to get the distribution of  $p_i = F_i(t|\theta_i)$ , the probability that event  $i$  will occur until  $t$  (normally, the mission time), where  $\theta_i$  is the set of parameters of the chosen distribution (e.g. Weibull). Then, the ME method is adopted to estimate the distribution of  $\theta_i$  from the distribution of  $F_i(t|\theta_i)$ . The ME method was first introduced in Jayne's information theory (JAYNES, 1957; KANG; KWAK, 2009) to assign probability incorporating information as constraints (MERUANE et al., 2017). ME method involves maximizing the entropy measure  $H$  (Equation 31), where  $\pi(\theta_i)$  is the probability density function (PDF) for the parameters of event  $i$  and  $\theta_i$  is the parameter space of  $\theta_i$  (WANG; LIU, 2020).

$$\text{maximize } H = \int_{\theta_i} -\pi(\theta_i) \times \log[\pi(\theta_i)] d\theta_i \quad 31$$

The constraints here are related to percentiles of the reliability function,  $R_i(t|\theta_i)$  (where  $R_i(t|\theta_i) = 1 - F_i(t|\theta_i)$ ). Specifically, we consider that the expected value as well as the percentiles 5 and 95 of each event  $i$  have to be equal to the expected value, percentiles 5 and 95 of the reliability  $R_T$  of the top event  $E_T$  weighted (exponentially) by its specific contribution  $w'_i$  (Equations 32 to 34).

$$E[R_i(t|\theta_i)] = E[R_T(t)^{w'_i}] \quad 32$$

$$P_5[R_i(t|\theta_i)] = P_5[R_T(t)^{w'_i}] \quad 33$$

$$P_{95}[R_i(t|\theta_i)] = P_{95}[R_T(t)^{w'_i}] \quad 34$$

Then, to define the model parameters,  $\theta_i$ , it is necessary to solve Equation 31 subject to constraints 32 to 34, for each event. Note that such an optimization problem may not be simple to solve analytically, becoming more difficult as the number of hyperparameters increases. In this context, we use a Particle Swarm Optimization (PSO) algorithm to obtain the solution of the maximization problem. PSO is a metaheuristic algorithm that mimics the social behavior of organisms (e.g., the bird flocking), and has been explored in many risk and reliability contexts to optimize functions (BAI et al., 2021; BEZERRA SOUTO MAIOR et al., 2016; GARCÍA NIETO et al., 2015; LINS et al., 2012; SOUTO; DAS CHAGAS MOURA; LINS, 2019).

PSO consists of several particles exploring a search space, each particle moves with an associated velocity and random position. At each iteration, these particles' movements are guided by their own best (i.e., the best position of each particle achieved so far among all iterations) and the global best (i.e., the best position that any particle has achieved so far among all the particles). When a better position is found, the best position(s) are updated to guide the particles' movements in the next iteration. This process is repeated and eventually converges to a solution (MASON; DUGGAN; HOWLEY, 2018; PAREEK et al., 2021). This seeking behavior artificially modeled by PSO provides useful results in the quest for solutions of non-linear optimization problems in a real-valued search space (BRATTON; KENNEDY, 2007). Here, PSO outcome is an estimate for the hyperparameters  $\{h_1, h_2, \dots, h_{n_i}\}$  that describe the prior distribution of the parameters  $\theta_i$ ,  $\pi_0(\theta_i | h_1, h_2, \dots, h_{n_i})$ , where  $n_i$  is the number of hyperparameters for each event

### 3.3 CASE STUDY

The proposed methodology is applied to a case study of a novel offshore expansible production packer, which is a common completion equipment of the O&G industry. In a simplistic view, the packer's function is to grip and seal, and it must remain anchored stationery with the casing, maintaining pressure sealing integrity with differential pressures, either below or above the tool (FOTHERGILL, 2003; LI, 2012). Production packers are complex equipment designed for a wide range of situations to cover the entire life of the well and resist the most diverse and hostile environments. Specifically, the equipment here analyzed is developed for open wells to isolate

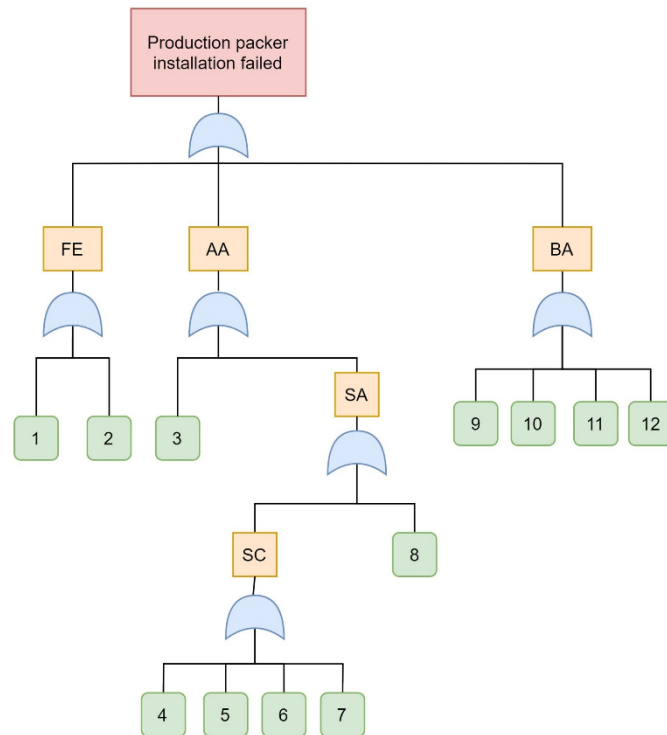
production zones working on an operational envelope of 25°C to 90°C of temperature and a maximum pressure differential of 5000 psi. As previously mentioned, in this paper, we discuss the new equipment installation and operation. Both approaches were implemented in Python programming language using the *SciPy* (VIRTANEN et al., 2020) and *Pyswarm* (MARINI; WALCZAK, 2015) libraries. More specifically, the module *scipy.stats* that contains a large number of probability distributions, summary and frequency statistics, and Monte Carlo functionality.

### 3.3.1 Equipment installation

The FT in Figure 16 is related to the equipment failure during its installation, in which there exist three failure modes: (i) unexpanded packer ( $E_{FE}$ ); (ii) annulus to annulus communication ( $E_{AA}$ ); and (iii) bore to annulus communication ( $E_{BA}$ ). These failure modes cover failure during either the equipment assembly, makeup (assembly of equipment in the production column to be introduced into the well), the run-in-hole (RIH) (introduction of the column into the well), or the failure to install the equipment system (equipment expansion). Intermediate events may be defined to facilitate the extrapolation for the basic events. Then, based on the equipment FMEA, twelve specific basic events ( $E_1, \dots, E_{12}$ ) were extracted, in which the occurrence of at least one of them causes one of the three previously mentioned failure modes. In addition, we define intermediate events failure of the seal assembly ( $E_{SA}$ ) and loss of sealing capacity of one seal unit ( $E_{SC}$ ) to facilitate elicitation. The descriptions of the basic events are given in Table 6, each one is designed to represent important characteristics.

For example, basic event 1 ( $E_1$ ) corresponds to the premature closing of the installation valve. From the engineering point of view, the installation valve is used to pressurize the inside of the packer by injecting fluid from the bore. The pressure build-up inside the packer causes the expansion sleeve to expand until a satisfactory contact pressure against the wall of the annular region is achieved. Then, differential pressure closes the installation valve, preventing it from continuing to expand until rupture. However, if an external event causes the annular pressure to suddenly drop (e.g., formation fracture required pressure to close), the installation valve closing may be reached prematurely, not sealing the annular region.

Figure 16 – FT diagram representing the equipment failure during its installation.



Source: MAIOR et al. (2022)

Table 6 – Description of basic events of the fault tree diagram for the failure during the packer installation.

Basic event	Description
$E_1$	Installation valve closes prematurely, during the RIH procedure, due to differential pressure in the annular region.
$E_2$	Leak in the weld of the bore packer, during the expansion, due to excessive loads.
$E_3$	Expansion sleeve rupture caused by wall-thinning, during expansion, due to material defect or due to the expansion operation in a larger diameter than specified.
$E_4$	Damage of one of the seals on the expansion sleeve during the makeup or RIH procedure.
$E_5$	The porosity of the formation in the contact region prevents the seal from obtaining sufficient compression.
$E_6$	Lack of uniformity of the expansion generates trapped pressure between the seals.
$E_7$	The occurrence of pressure trapped between the seal and the formation wall in an airtight region prevents the seal from obtaining sufficient compression.
$E_8$	Before expansion provides sufficient compression to the seals, the installation valve prematurely closes due to pin manufacturing defects.
$E_9$	The installation valve fails to close due to pin manufacturing defects.

Basic event	Description
$E_{10}$	The installation valve fails to close due to lock mechanism failure.
$E_{11}$	Contact with the debris during the RIH and/or expansion process causes the filter to clog, which prevents the installation valve from reaching the proper pressure to close.
$E_{12}$	Contact with the debris during RIH and/or expansion causes the filter to rupture, allowing the presence of debris inside the installation valve, which prevents it from closing

Source: MAIOR et al. (2022)

For the equipment installation, the MRM is easily obtained by the multiplication of the reliability models of the basic events since all logic gates of the FT are of the “OR” type, which is presented in Equation 35:

$$R(0|\theta) = \prod_{i=1}^{12} (1 - p_i) \quad 35$$

where the parameter set is  $\theta = \{p_1, p_2, p_3, p_4, p_5, p_6, p_7, p_8, p_9, p_{10}, p_{11}, p_{12}\}$ . In this case study, the only initially available information is for the system level (i.e., FT’s top event) accessible in generic database by Wellmaster report. The Wellmaster database provides information on completion equipment to improve reliability through systematic collection, analysis, and feedback of reliability data to participating O&G companies and equipment manufacturers (MOLNES; STRAND, 2000). Here, the relevant data for assessing the reliability of the novel equipment is related to the packer’s information from other open well applications. As a premise, we have considered the prior uncertainty about the reliability of the novel equipment to be equal to the uncertainty for the reliability of the similar equipment in database Wellmaster. In this case, the number of production packers installed ( $n$ ) and the number of failures during its installation ( $f$ ) are 573 and 16, respectively.

### 3.3.1.1 Elicitation results

In this phase, the weights  $w_i$  to perform the downward propagation are extracted. Six experts took part in this step, each of them assigned with  $r_j$  validated by the company: two specialists, involved in the equipment design since the very first

stages of its development, were assigned with  $r_j = 2$ ; two specialists with experience with the production packer installation and operation were assigned with  $r_j = 2$ ; two specialists with less time experienced with the equipment, were assigned with  $r_j = 1$ . The weighted median of the elicited values was used as  $w_i$  for each basic event to consider the opinion of all experts (see Figure 17).

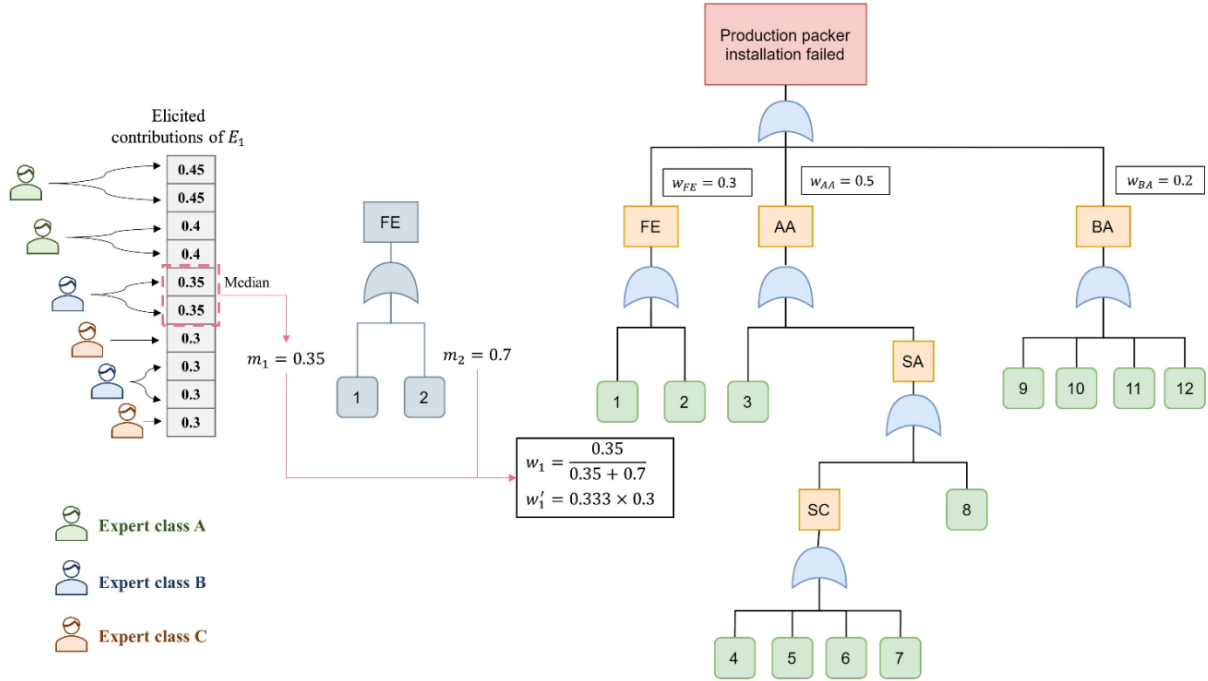
As previously mentioned, for each upper event, the median values of the lower events (e.g.,  $m_1$  and  $m_2$ ) were scaled between 0 and 1 (e.g.,  $w_k = \frac{m_k}{m_1+m_2}$ , for  $k = 1,2$ ) and, then, these values were adopted as the contributions (weights) of the events to the occurrence of the immediate event above. The weight calculations procedure is detailed in Figure 17 considering realistic values and preserving the original elicited order for the O&G application. For the failure mode, most experts believe that  $E_{AA}$  is the one that contributes most to the failure during installation (followed by  $w_{FE}$ , and  $w_{BA}$ ). Then, suppose that its weight  $w_{AA}$  has been assigned 0.5, the weight of the event  $E_{FE}$ ,  $w_{FE}$ , has been set as 0.3, and the contribution of  $E_{BA}$ ,  $w_{BA}$ , has been determined as 0.2. Then, the contribution for  $E_{FE}$  from the immediate causes are related to  $E_1$  and  $E_2$  and may be elicited. As shown in Figure 17, the median value assigned by the experts to  $E_1$  was  $m_1 = 0.35$  and to  $E_2$  was 0.7. Then, scaling the medians between 0 and 1 results in  $w_1 = \frac{0.35}{0.35+0.7} = 0.333$  and  $w_2 = \frac{0.7}{0.7+0.35} = 0.667$ . Thus, the contributions of these events to the installation failure are given by  $w'_i = w_{FE} \times w_i$ ; thus,  $w'_1 = 0.10$  and  $w'_2 = 0.20$ .

Analogously, the experts provide their opinions about the contribution of the immediate causes to  $E_{AA}$  (i.e.,  $E_3$ , and  $E_{SA}$ ). In fact,  $E_{SA}$  was unanimously considered as the most likely cause of the  $E_{AA}$ . Next, the experts analyze the immediate causes of  $E_{SA}$ , which are  $E_{SC}$  and  $E_8$ , assigning the same weight for both events. Then, the experts consider the events associated with  $E_{SC}$ , represented by  $E_4$ ,  $E_5$ ,  $E_6$ , and  $E_7$ , with most experts assigning greater weight to  $E_6$ . Finally, the experts evaluate the causes of  $E_{BA}$  (i.e.,  $E_9$ ,  $E_{10}$ ,  $E_{11}$ , and  $E_{12}$ ). All responses were validated by the senior expert of the company as well as the failure contribution of basic events ( $w'_i$ ).

In the end, the weights of the twelve previously mentioned basic events are defined. The descending order of the event weights is presented in Table 7. As one can see, based on expert opinion,  $E_8$  ('premature close due to pin manufacturing

defects') was the one with greater weight while  $E_{12}$  ('debris causing the filter to rupture') was considered the less influencing basic event.

Figure 17 – Example containing illustrative values



Source: Maior et al. (2022)

Table 7 – Failure contribution of basic events for the installation FT diagram

Order	1 <sup>st</sup>	2 <sup>nd</sup>	3 <sup>rd</sup>	4 <sup>th</sup>	5 <sup>th</sup>	6 <sup>th</sup>	7 <sup>th</sup>	8 <sup>th</sup>	9 <sup>th</sup>	10 <sup>th</sup>	11 <sup>th</sup>	12 <sup>th</sup>
Event $i$	$E_8$	$E_2$	$E_3$	$E_5$	$E_1$	$E_7$	$E_4$	$E_6$	$E_9$	$E_{10}$	$E_{11}$	$E_{12}$

Source: Maior et al. (2022)

### 3.3.1.2 Uncertainty propagation

As previously mentioned, we assumed that the failure occurrence of all basic events during installation ( $E_i, i = 1, \dots, 12$ ) are described by a Bernoulli model with parameter  $p_i$  with only two possible outcomes: success or failure. Therefore, the equipment reliability in installation,  $R(0|\theta)$ , given in Equation 35 have  $\theta = \{p_1, \dots, p_{12}\}$ , as set of MRM parameters. Given the generic database (Wellmaster) evidence, we can estimate  $p$  as  $\hat{p} = \frac{f}{n}$ , in which  $f$  is the number of reported failures for the  $n$  packers registered. We can also obtain the confidence intervals  $P_1$  and  $P_{99}$  (Equation 30). From the elicitation procedure, the contributions  $w'_i$  were used to obtain  $1 - (1 - \hat{p})^{w'_i} = m_{p_i}$ ,  $1 - (1 - P_1)^{w'_i} = a_{p_i}$ , and  $1 - (1 - P_{99})^{w'_i} = b_{p_i}$ . These estimates allow computing  $\mu_{p_i}$

and  $\sigma_{p_i}$  (Equations 26 and 27) for the PERT distribution. Because a beta distribution is assumed to model  $p_i, i = 1, \dots, 12$ , the hyperparameters  $\alpha_{p_i}$  and  $\beta_{p_i}$  can be estimated analytically using MM (Equations 28 and 29). Finally, the prior beta distributions  $\pi_0(p_i|\alpha_{p_i}, \beta_{p_i})$  for each event  $i$  are achieved, completing the downward propagation. The results are summarized in Table 8.

Table 8 – Prior distributions obtained through MM.

$E_i$	$p_i$	Hyperparameters	
		$\alpha_{p_i}$	$\beta_{p_i}(10^3)$
1	$p_1$	15.20	8.85
2	$p_2$	15.09	2.93
3	$p_3$	15.14	4.13
4	$p_4$	15.22	12.46
5	$p_5$	15.15	4.65
6	$p_6$	15.22	12.46

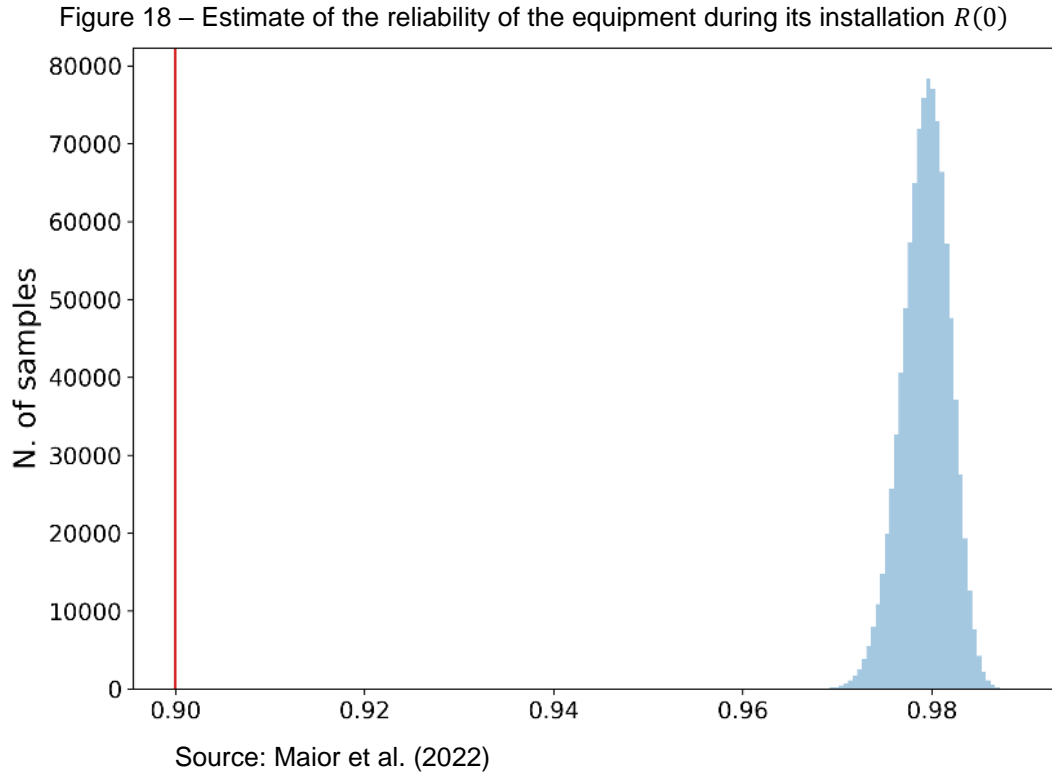
$E_i$	$p_i$	Hyperparameters	
		$\alpha_{p_i}$	$\beta_{p_i}(10^3)$
7	$p_7$	15.20	9.34
8	$p_8$	15.02	2.05
9	$p_9$	15.23	17.96
10	$p_{10}$	15.23	22.47
11	$p_{11}$	15.23	22.47
12	$p_{12}$	15.23	17.96

Source: Maier et al. (2022)

Then, in possession of all the basic event distributions, we used a Monte Carlo simulation algorithm to perform upward propagation, i.e., to propagate the uncertainty through the FT until the top event, determining the probability of failure in installation for the novel O&G equipment. The method consists of generating random samples of  $p_i$  from  $\pi_0(p_i|\alpha_{p_i}, \beta_{p_i})$ , for  $i = 1, \dots, 12$ , then, calculating the samples of  $R(0|\theta)$ , according Equation 35 (SINGH; MITRA, 1995).

Yet, the system's reliability is obtained as the probability of the complementary event. For the real case study, equipment reliability during its installation,  $R(0)$ , is represented in Figure 18. One can see that the simulation returned high reliability (close to 1) with low variability. The resulting narrow confidence/uncertainty intervals for  $R(0)$  reflect the low uncertainty about the parameters caused by the large number of packers installed with few failures (recall the information from the Wellmaster report). Indeed, the results meet the metric recommended by API 17 as the failure probability tends to 0.



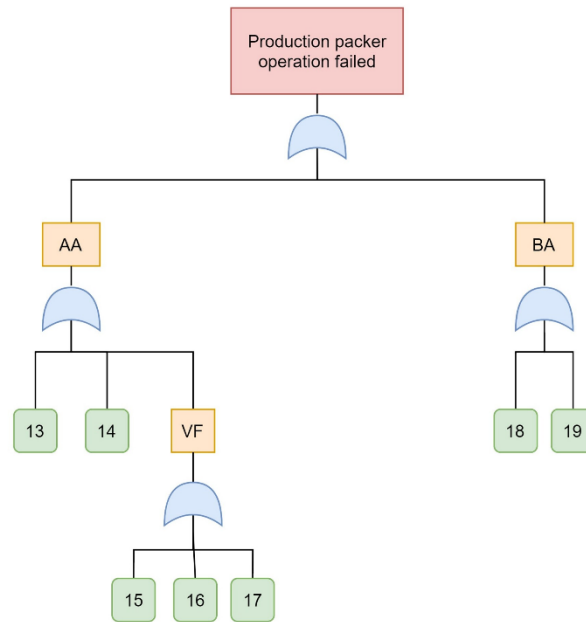


### 3.3.2 Equipment operation

Figure 19 shows the FT diagram related to the equipment failure during its operation. The related failure modes are: (i) annular-annular communication ( $E_{AA}$ ) and (ii) bore-annular communication ( $E_{BA}$ ). They represent the loss of annular isolation during the well production. Based on the equipment FMEA, seven specific basic events ( $E_{13}, \dots, E_{19}$ ) were extracted, in which the occurrence of at least one causes one of the two previously mentioned failure modes.  $E_{VF}$  is an intermediate event related to the valve failure, which may be caused by aging ( $E_{15}$ ), microparticle accumulation ( $E_{16}$ ), or loads ( $E_{17}$ ). Table 9 describes all the basic events for the operation FT.

Here, it is necessary to determine the most suitable statistical analysis for each basic event, regarding the event characteristics as well as possible tests to be performed. An Exponential model, with parameter  $\lambda_i$ , was adopted for basic events in which it is not expected degradation effects during the equipment's mission time. As a result, the Exponential model was selected for  $E_{13}$ ,  $E_{17}$ , and  $E_{19}$ , as the project avoids (verified by tests) the occurrence of fatigue in the equipment body and other failure mechanisms related to the incidence of cyclical load/stress.

Figure 19 – FT diagram representing equipment failure during well operation.



Source: Maior et al. (2022)

Table 9 – Description of basic events of the FT diagram for the equipment failure during well operation.

Basic Event	Description
$E_{13}$	The incidence of loads during operation/interventions in well production causes the expansion sleeve to buckle, which leads to annular-annular communication.
$E_{14}$	Aging of the mechanical properties of each of the expansion sleeve's seals causes leakage in the expansion sleeve's set of seals.
$E_{15}$	Aging of the compensation valve seal, due to long-term exposure to fluids and high temperatures, causes leakage through the pressure compensation valve.
$E_{16}$	The accumulation inside the pressure compensation valve of microparticles, which naturally pass through the filter, over time, blocks the movement of the valve piston, which prevents pressure compensation inside the production packer.
$E_{17}$	The load caused by pressure differentials mechanically deforms the sealing surfaces of the pressure compensation valve, which causes leakage through the valve.
$E_{18}$	Loss of the sealing capacity of the seals and sealing surfaces of the installation valve, over time, reopens communication with the bore.

Basic Event	Description
$E_{19}$	Load on the production packer causes a leak in the annular region with the bore.

Source: Maier et al. (2022)

For events in which degradation is expected, the Weibull model, with parameters  $\alpha_i$  and  $\beta_i$ , was adopted. Moreover, because  $E_{14}$  and  $E_{15}$  are tested at different temperatures, a particular Weibull model, the Arrhenius-Weibull model with parameters  $a_i$ ,  $b_i$ , and  $\beta_i$ , was considered. The Arrhenius-Weibull model is a 3-parameter Weibull model that allows assessing the probability of time to failure at different temperatures (MODARRES, 2021). Specifically, for this novel O&G packer, fifteen seal assemblies are arranged in parallel. Therefore, as the Arrhenius-Weibull model represents the failure distribution of one seal assembly, the reliability model for  $E_{14}$  is provided by Equation 36, where  $t$  is the mission time,  $\tau$  is the temperature and  $a_{14}$ ,  $b_{14}$ , and  $\beta_{14}$  are the Arrhenius-Weibull model parameters.

$$R_{14}(t, \tau | a_{14}, b_{14}, \beta_{14}) = 1 - \left[ 1 - e^{-\left(\frac{t}{b_{14} e^{\frac{a_{14}}{\tau}}}\right)^{\beta_{14}}} \right]^{15} \quad 36$$

Finally, the MRM of the equipment operation is given in Equation 37, where the parameter set is  $\theta = \{\lambda_{13}, a_{14}, b_{14}, \beta_{14}, a_{15}, b_{15}, \beta_{15}, \alpha_{16}, \beta_{16}, \lambda_{17}, \alpha_{18}, \beta_{18}, \lambda_{19}\}$ . Once again, the MRM was obtained by the multiplication of the reliability models of each basic event since all FT logic gates are of the “OR” type.

$$R(t|\theta) = \left\{ 1 - \left[ 1 - e^{-\left(\frac{t}{b_{14} e^{\frac{a_{14}}{\tau}}}\right)^{\beta_{14}}} \right]^{15} \right\} \times e^{-\lambda_{13}t - \left(\frac{t}{b_{15} e^{\frac{a_{15}}{363}}}\right)^{\beta_{15}} - \left(\frac{t}{\alpha_{16}}\right)^{\beta_{16}} - \lambda_{17}t - \left(\frac{t}{\alpha_{18}}\right)^{\beta_{18}} - \lambda_{19}t} \quad 37$$

As in the installation case, the only available information is the data presented by the Wellmaster. The report provides the scale ( $\alpha$ ) and shape ( $\beta$ ) parameters of the Weibull for the time to failure related to the failure modes annulus communication ( $E_{AA}$ ) and column-annulus communication ( $E_{BA}$ ) during the operation, which concerns the intermediate events for this FT. Table 10 summarizes this information.

Table 10 – Completion expansion packer Wellmaster report (operation of similar equipment).

Failure mode	Scale parameter (years)	Shape parameter
annular-annular communication ( $E_{AA}$ )	63,521.0	0.605
bore-annular communication ( $E_{BA}$ )	860.2	1.372

Source: Maier et al. (2022)

The ME method was applied (Equation 31) to aggregate this information as probability distributions for the parameters of each event  $E_i$ . As constraints of the ME method, we considered that each basic event  $i$  has a contribution  $w'_i$  to the corresponding failure mode ( $E_{AA}$  and  $E_{BA}$ ). The basic events 13 to 17 contribute to  $E_{AA}$ , and the occurrence of the basic events 18 and 19 cause  $E_{BA}$ .

### 3.3.2.1 Elicitation results

Five specialists took part to evaluate the events weights related to the operation of the novel equipment. Each of them was assigned with  $r_j$  validated by the company: two experts involved in the equipment design since the very first stages of its development had  $r_j = 2$ ; for the two specialists with experience with the production packer installation and operation,  $r_j = 2$ ; for one specialist with less time experienced with equipment,  $r_j = 1$ . The median values of the elicited weights were used as  $w_i$  to obtain the prior distributions for each basic event.

Once again, for each upper event (e.g.,  $E_{VF}$ ), the median values of the lower events ( $m_{15}$ ,  $m_{16}$  and  $m_{17}$ ) were scaled between 0 and 1 (e.g.,  $w_{15} = \frac{m_{15}}{m_{15}+m_{16}+m_{17}}$ ). For example, Table 11 shows hypothetical values for the opinions of the five experts regarding the weights of the events 15, 16 and 17 when the compensation valve fails ( $E_{VF}$ ). Following the procedure in Figure 17, the median values weighted by the

experts' relevance factors are  $m_{15} = 20\%$ ,  $m_{16} = 35\%$  and  $m_{17} = 35\%$ . Then  $w_{15} = \frac{20\%}{20\%+35\%+35\%} = 22\%$ , which is the contribution of event 15 to the valve failure.

Table 11 – Responses regarding the contribution of events 15, 16 and 17 to the valve failure ( $E_{VF}$ ).

Expert (relevance factor)	Contribution of events		
	15	16	17
1 (1)	10%	40%	50%
2 (2)	30%	35%	35%
3 (2)	25%	60%	15%
4 (2)	20%	35%	45%
5 (2)	50%	30%	20%

Finally, the weights of the seven previously mentioned basic events (Figure 19 and Table 9) are presented in descending order in Table 12. As one can see,  $E_{18}$  ('loss of the sealing capacity of the seals and sealing surfaces of the installation valve over time') was the one with greater weight while  $E_{17}$  ('mechanical deformation of the sealing surface of the compensation valve due to pressure differentials') was considered the less impacting basic event.

Table 12 – Failure contribution of basic events for the operation FT diagram

Order	1 <sup>st</sup>	2 <sup>nd</sup>	3 <sup>rd</sup>	4 <sup>th</sup>	5 <sup>th</sup>	6 <sup>th</sup>	7 <sup>th</sup>
Event $i$	$E_{18}$	$E_{14}$	$E_{15}$	$E_{19}$	$E_{13}$	$E_{16}$	$E_{17}$

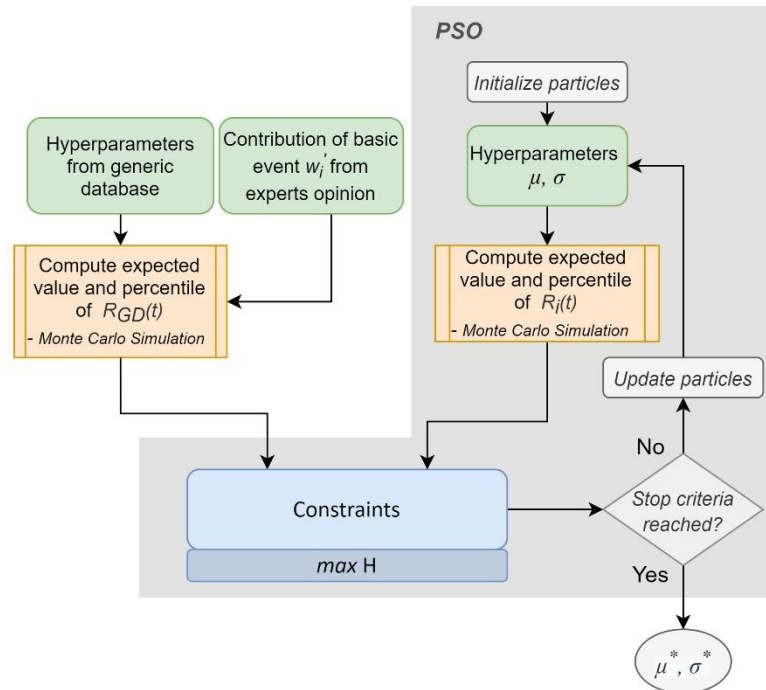
Source: Maïor et al. (2022)

### 3.3.2.2 Uncertainty propagation

Here, we assumed that each  $\pi_0(\theta_i)$ ,  $\forall i$ , is a lognormal distribution with independent hyperparameters  $\mu_{\theta_i}$ , and  $\sigma_{\theta_i}$ . Thus, Equation 31 was formulated as the sum of the entropies of each individual hyperparameter (JAYNES, 1957). and we compute the entropy of the random variables lognormally distributed. Then, the optimization problem (Equation 31) subject to the constraints in Equations 32-34 is solved through ME method and using the PSO algorithm.

A summarization of the process used to solve the optimization problem is illustrated in Figure 20. From the hyperparameters of Wellmaster (generic database) we calculate the expected value and percentiles of  $R_{GD}$  via Monte Carlo simulation, which define the problem constraints (the right side of the constraints Equations 32-34). Then, at each iteration, PSO searches a set of hyperparameters ( $\mu$  and  $\sigma$ ) that maximize the entropy ( $\max H$ ) and meet the constraints. Then, the left side of the constraints is also computed via Monte Carlo simulation: at each iteration of PSO, using the hyperparameters selected, we generate 100,000 random values for  $\theta_i$ , using *scipy.stats.lognorm.rvs*, which allows the estimation of the cumulative distribution function (CDF) of  $f(t|\theta_i)$  and its expected value and percentiles. This process is repeated until it reaches a minimum step size of swarm's best position of  $10^{-8}$  or a minimum of  $10^{-8}$  change of swarm's best objective value; thus, it converges until to an optimal solution ( $\mu^*$  and  $\sigma^*$ ).

Figure 20 – Procedure adopted to solve the constrained ME method.



Source: Maior et al. (2022)

For example, the maximum-entropy optimization problem related to  $E_{13}$ , which is governed by an Exponential distribution, to estimate the distribution of  $\lambda_{13}$  is presented in Equation 38 subject to the constraints 39-41. The right side of the

constraints is computed via Monte Carlo simulation using the Weibull parameters for the  $E_{AA}$  presented in Table 10.

$$\begin{aligned} \max_{\mu_{\lambda_{13}}, \sigma_{\lambda_{13}}} H \equiv & - \int \frac{\exp\left(-\frac{(\ln \lambda_{13} - \mu_{\lambda_{13}})^2}{2\sigma_{\lambda_{13}}^2}\right)}{\lambda_{13} \sigma_{\lambda_{13}} \sqrt{2\pi}} \\ & \times \left[ -\frac{(\ln \lambda_{13} - \mu_{\lambda_{13}})^2}{2\sigma_{\lambda_{13}}^2} - \ln(\lambda_{13} \sigma_{\lambda_{13}} \sqrt{2\pi}) \right] d\lambda_{13} \end{aligned} \quad 38$$

subject to:

$$E[R_{13}(27|\mu_{\lambda_{13}}, \sigma_{\lambda_{13}})] = E[R_{AA}(27|\alpha_{AA}, \beta_{AA})^{w_{13}}] \quad 39$$

$$P_5[R_{13}(27|\mu_{\lambda_{13}}, \sigma_{\lambda_{13}})] = P_5[R_{AA}(27|\alpha_{AA}, \beta_{AA})^{w_{13}}] \quad 40$$

$$P_{95}[R_{13}(27|\mu_{\lambda_{13}}, \sigma_{\lambda_{13}})] = P_{95}[R_{AA}(27|\alpha_{AA}, \beta_{AA})^{w_{13}}] \quad 41$$

In this case, PSO searches through a 2-dimension space (i.e.,  $\mu_{\lambda_{13}}$  and  $\sigma_{\lambda_{13}}$ ), and, at each iteration of PSO, another Monte Carlo simulation is executed using the current hyperparameters to compute the expected value and percentiles of the reliability  $R_{13}(27|\mu_{\lambda_{13}}, \sigma_{\lambda_{13}})$  that are the left side of the constraints. Thus, the solution provides the estimates of  $\mu_{\lambda_{13}}^*$  and  $\sigma_{\lambda_{13}}^*$  describing the prior lognormal distribution of  $\lambda_{13}$ , completing the downward propagation.

Note that for events dealing with a statistical distribution of more than one parameter (e.g., Weibull and Arrhenius-Weibull), the number of terms in the objective function increases, generating a more complex problem to be optimized. Despite being a difficult problem, the PSO algorithm achieved satisfactory solutions for all basic events in our case study. The results for our real case are summarized in Table 13.

Finally, in possession of the prior distributions for the basic events, we again used Monte Carlo simulation to propagate the uncertainty through the FT until the top event (probability of failure in operation) in the upward propagation, by generating random samples for  $\theta_i$  from  $\pi_0(\theta_i)$ , with  $i = 13, \dots, 19$ , and calculating the sample of  $R(t)$  from Equation 37. The considered mission time of operation is  $t = 27$  years (a common oil well concession period), and the reliability estimation,  $R(27)$ , is shown in

Figure 21. The mean value for the reliability of the MRM is 93.48%, while 28.1% is the probability that the reliability is less than 90% (red line).

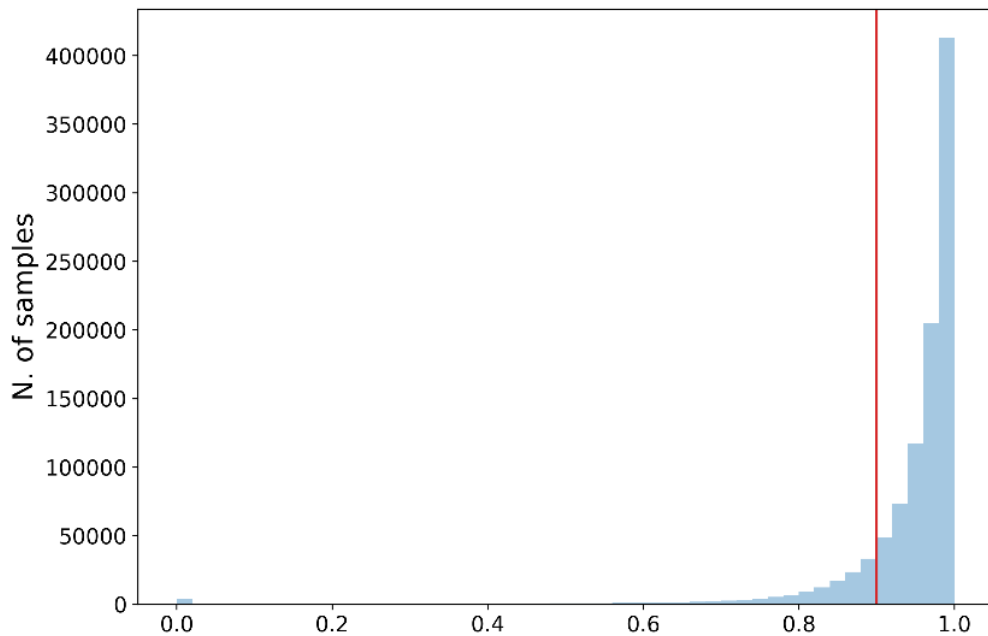
Table 13 – Prior distributions obtained through ME.

$E_i$	$\theta_i$	Hyperparameters	
		$\mu_{\theta_i}$	$\sigma_{\theta_i}$
<b>13</b>	$\lambda_{13}$	-16.378	4.082
	$a_{14}$	5.428	0.173
<b>14</b>	$b_{14}$	2.912	0.367
	$\beta_{14}$	0.185	0.240
<b>15</b>	$a_{15}$	5.670	0.824
	$b_{15}$	6.929	0.673
	$\beta_{15}$	0.348	0.310

$E_i$	$\theta_i$	Hyperparameters	
		$\mu_{\theta_i}$	$\sigma_{\theta_i}$
<b>16</b>	$\alpha_{16}$	6.924	0.694
	$\beta_{16}$	1.416	0.559
<b>17</b>	$\lambda_{17}$	-11.362	1.500
<b>18</b>	$\alpha_{18}$	6.944	0.208
	$\beta_{18}$	0.263	0.463
<b>19</b>	$\lambda_{19}$	-13.477	4.249

Source: Maior et al. (2022)

Figure 21 – Estimate of the equipment reliability for 27 years of operation,  $R(27)$



Source: Maior et al. (2022)

### 3.4 CONCLUSION

After the presented analysis, the level of uncertainty for  $R \geq 90\%$  is 28.82% and, thus, above the required maximum limit of 20%, resulting in a residual uncertainty



of 8.82% after prior analysis. This is somehow expected because we are only considering the prior distribution of the equipment based on generic data and expert opinion. Evidence related to specific tests (e.g., functional, degradation, accelerated, and numerical) from components, subsystems, and systems (many of them from mandatory standard tests) may become available during the equipment development. Therefore, it is possible to update the prior distribution considering this likelihood information. And, because we included more knowledge during the definition of the prior distribution, fewer empirical/physical tests may be required to overcome the residual uncertainty and confirm the feasibility of the novel equipment.

The posterior distribution is, then, required to meet the target at the end of the product development. In this sense, the methodologies presented in this work may be the starting point of a more comprehensive framework to update and monitor equipment reliability uncertainty during its development process.

## 4 PRIOR ANALYSIS FOR NON-CONTINUOUSLY OPERATED EQUIPMENT BASED ON EXPERTS' OPINION

This chapter is based on the paper titled “Using experts’ opinion for Bayesian prior reliability distribution of on-demand equipment: A case study of a novel sliding sleeve valve for open-hole wells” (MACEDO et al., 2023), and published in the Reliability Engineering and System Safety (RESS) journal, of which I am co-author. Below are my contributions to the paper:

- Direct conception and validation of the proposed methodology.
- Direct conception and validation of the models (Fault Tree Analysis, Top-down propagation of the events contribution, Population Variability Analysis, Method of Moments, Maximum Entropy, and Monte Carlo).
- Participation in the development and validation of questionnaires to elicit experts.
- Participation in the development and validation of the computational implementation of the models.
- Results analysis.

### 4.1 INTRODUCTION

In Chapter 3, it was proposed a methodology to define informative Bayesian prior distribution  $\pi_0(\theta_i)$  based on experts’ knowledge and generic data that does not require direct elicitation of parameters to define distribution for the equipment failure mechanisms but rather uses data at the system level. The proposed methodology was applied to estimate the prior distribution of a novel completion expansive packer that would operate in an open hole well of the O&G industry. However, that methodology is only suitable for equipment that operates continuously and does not consider the uncertainty related to the experts’ knowledge.

Knowledge of different experts varies from each other, and this leads to variations in estimates provided by different experts. Several methods have been proposed to aggregate different experts’ opinions. Linear or logarithmic pooling methods are intuitive and easy to apply, they construct an additive or multiplicative mixture across experts (associated with a specific weight) (GRIBOK; AGARWAL; YADAV, 2020). On the other hand, pooling techniques do not capture expert

differences from the consensus and the key output of a pooling approach may be an unparametrized distribution; however, to feed a further model a parametrized distribution is desired (BOLGER; HOULDING, 2017). Bayesian models treat the elicited information as data. Early Bayesian models treated experts as completely exchangeable, this often resulted in very narrow posterior distributions which demonstrate high overconfidence. The supra-Bayesian hierarchical approach has been applied for combining indirect elicitation across multiple experts. This approach allows us to model the imprecision and incoherence of individual experts as well as their variability (HARTLEY; FRENCH, 2021).

This chapter proposes a methodology to build informative prior distribution based on experts' knowledge about different failure mechanisms, i.e., modelled by distinct probability distributions, of novel equipment operating in standby mode and working on demand. To that end, we aggregated the failure probability estimates, provided by multiple experts via Population Variability Analysis (PVA) (DAS CHAGAS MOURA et al., 2016), to define the variability distribution of these estimates within a group of non-homogeneous experts. Then, the resulting variability distributions are used to estimate the probability distribution of all failure mechanisms of novel equipment.

We apply the methodology in a case study for a novel large-diameter sliding sleeve valve that operates in an open hole well in the O&G industry. Most of the time the valve remains on standby and is demanded during the well operations when it is necessary to isolate specific areas. Thus, the valve must be able to open and close multiple times under different pressures while maintaining the flow rate.

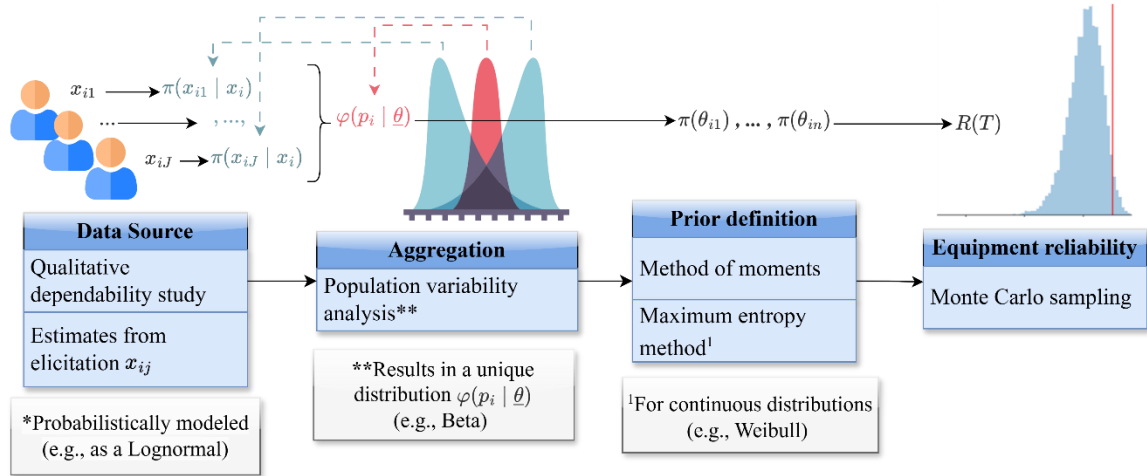
The main contribution of this section is the development of a Bayesian methodology to define an informative prior distribution for novel equipment that is flexible enough to consider events that degrade over time and/or with past demands and takes into account the uncertainty regarding different experts' opinions.

## 4.2 METHODOLOGY

Here, we propose a methodology to provide the prior reliability distribution, which is defined based on the distribution of all failure mechanisms leading to equipment failure. Figure 22 illustrates the main steps of the methodology, which are detailed in later sections.

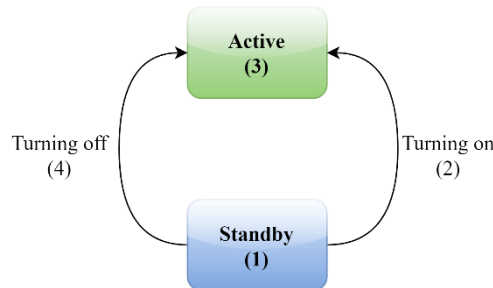
The input data considers a dependability study for the analyzed equipment and experts' opinions, which are extracted through elicitation. Since it is frequently performed in the early stages of risk and reliability analysis, we assume that FTs are created to evaluate a limited number of top events, which may represent failure during specific moments of the equipment life (e.g., during installation or operation). Each basic event,  $E_i$ , of the FT, relates a failure mechanism leading to the occurrence of the top event,  $E_T$ . Figure 23 illustrates the possible status for equipment that operates on-demand and remains on standby mode. We consider that failures may occur in two different moments: (i) during equipment actuation, when the equipment is demanded and in its transition state (i.e., status 2 and 4), and (ii) during operation (i.e., status 1 and 3) when the equipment is on standby (e.g., valve completely opened allowing fluid to flow) or working (e.g., valve actuated to close and, consequently, it blocks the flow).

Figure 22 – Main steps of the proposed methodology for obtaining an informative Bayesian prior distribution for on-demand equipment based on experts' opinions.



Source: Macedo et al. (2023)

Figure 23 – Possible status of on-demand equipment.



Source: Macedo et al. (2023)

### 4.2.1 Probabilistic Modeling

In this section, we describe how we specified the parametric distribution that can describe a given failure mechanism. We assume that failure mechanisms related to success/failure events are described by a demand ( $d$ ) and time ( $t$ ) dependent probability model. Equation 42 models the failure probability  $p_i(d, t)$  for basic event  $E_i$  based on MARTORELL et al., (2017), where  $\rho_i$  is the residual failure probability,  $\gamma_i$  is the degradation factor due to past demands ( $d$ ) associated with demand failures and  $\tau_i$  represents the degradation factor associated with time-related failures.

$$p_i(d, t) = \rho_i + \gamma_i \times d + \tau_i \times t \quad 42$$

Moreover, an Exponential model, with parameter  $\lambda_i$ , is adopted for failure mechanisms with unexpected degradation effects during the equipment's mission time, such as the ones related to the incidence of cyclical load/stress. For events in which degradation is expected, the Weibull model, with parameters  $(\alpha_i, \beta_i)$ , is used, and for failure mechanisms also influenced by temperature, the Arrhenius-Weibull model, with parameters  $(a_i, b_i, \alpha_i)$  is adopted (SHAKHATREH; LEMONTE; MORENO–ARENAS, 2019). Then, each FT event,  $E_i$ , follows a distribution with a set of parameters  $\theta_i$ . Thus, to determine the prior distributions of all  $E_i$ , one must estimate the respective  $\theta_i$ .

In the third step of Figure 22, the resulting distribution from experts' opinions is used to determine the parameters of the distributions that describe the failure mechanism of the basic events in the FTs. First, the Method of Moments (MM) is used to estimate the Beta distribution over the probability of occurrence of each event. If a continuous distribution describes the time in which  $E_i$  occurs, the Maximum Entropy Method (MEM) is applied to estimate its parameters. In the last step, the equipment reliability probabilistic model can be obtained through Monte Carlo (MC) sampling using the distributions obtained in the last step for all basic events (JIA; GUO, 2022).

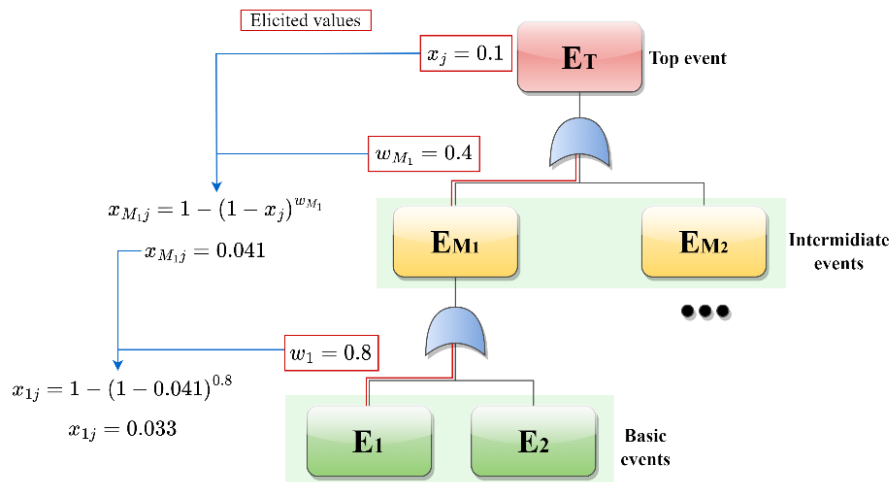
### 4.2.2 Data Source

As mentioned, for novel technologies reliability data from field or tests are scarce or non-existent. Here we consider that the only reliability information available

is the experts' opinion. Thus, to define the set of parameters  $\theta_i$  for all failure mechanisms we need to perform an elicitation process to build our prior evidence about  $\theta_i$ . If one directly elicits the parameters of a distribution, the information extracted from the experts might end up being a simple guess, since the interpretation of such parameters may be overly complicated (MODARRES; AMIRI; JACKSON, 2017). Therefore, to make the process more intuitive we adopted an indirect elicitation. The elicitation process involves asking the experts for estimates of the probability of failure at the system level only. In other words, expert  $j$  provides estimates of the probability of equipment failure,  $x_j$ , for the considered failure modes. In this sense, the elicitation process provides system-level information that is, in turn, used to estimate the probability of the basic events,  $x_{j,i}$ , which are related to failure mechanisms. Specifically, to propagate the information about the FT top event to the basic events ( $E_i$ ), we considered that each event contributes with a specific weight ( $w$ ) to the failure event immediately above.

For instance, as illustrated in Figure 24, expert  $j$  believes that the probability of occurrence of  $E_T$  is 10% and that the chance of  $E_T$  occurring due to  $E_{M_1}$  is 40% (i.e.,  $E_{M_1}$  contributes with  $w_{M_1} = 0.4$  to  $E_T$ ). Furthermore, according to the expert, the chance of  $E_{M_1}$  occurring due to a failure mechanism  $E_1$  is 80%. Thus, both events' contributions, i.e., all  $w_i$  and  $w_{M_i}$ , and estimates for the equipment probability of failure,  $x_j$ , are gathered from experts' opinions.

Figure 24 – Elicited values in red boxes and downward propagation methodology; how the contributions of the basic events are computed.



Source: Macedo et al. (2023)

Thus, we extract, through elicitation forms, estimates of the failure probability of the equipment during actuation and operation. More specifically, the form related to the failure mechanisms that may occur during the equipment actuation aims to elicit:

- An estimate of the probability of equipment failure during actuation given the number of actuations,  $d$ , at a specific time,  $t$ , i.e., an estimate for  $p(d, t)$ ;
- The contributions of the possible causes that lead to actuation failure.

In turn, the form related to the failure mechanisms that may occur during equipment operation intends to obtain:

- An estimate of the probability of equipment failure during operation for a given mission time,  $T$ , i.e., an estimate for  $p(t = T)$ ;
- The contributions of the possible causes that lead to operation failure.

Thus, we use the elicited information to estimate the failure mechanisms' probabilities of occurrence. The elicited contributions define the relations among the basic events and the information available at the system level and other events. Thus, given the estimate of the failure probability related to the top event provided by expert  $j$ , we compute  $x_{ij}$ , which is the probability estimate for the basic event  $E_i$  (recall Figure 24). We assume that all logic gates of the FT are "OR" type and all events are independent. Moreover, the reliability estimate of  $E_T$  ( $1 - x_j$ ) is the product of the reliability estimates of its immediate causes  $E_T = \prod^i (1 - x_{ij})$ . For instance, since the exemplified failure probability of  $E_T$  in Figure 24 is 10% and the contribution of  $E_{M_1}$  to  $E_T$  is  $w_{M_1} = 0.4$ , the probability  $x_{M_1j}$ , is given by  $x_{M_1j} = 1 - (1 - 0.1)^{0.4}$ . Similarly, one can compute  $x_{1j}$ . For further details, see MAIOR et al., (2022).

We consider that a distribution models the uncertainty of the estimate  $x_{ij}$  related to expert  $j$ . To account for the uncertainty in the expert opinion,  $x_{ij}$  is modeled as a continuous variable from 0 to 1. Since the elicitation process involves multiple experts, it results in various estimates, and, consequently, multiple distributions for each failure mechanism. Thus, after eliciting experts' opinions, an aggregation process based on PVA is performed to obtain a unique distribution describing the experts' uncertainty on the probability of occurrence of the basic events. This aggregation process is detailed in the following section.

### 4.2.3 Aggregation process

PVA provides a probability distribution to represent the variability of some measure of reliability between ‘populations’. In our case, ‘populations’ are the experts, and the measure is the failure probability. A representation of this variability of the failure probabilities, in the form of a probability distribution, is referred to as the population variability distribution. The assessment of such population variability distributions is referred to as population variability analysis (GRECO; PODOFILLINI; DANG, 2021a).

Let  $p_i$  be a continuous random variable that defines the failure probability of event  $i$  and  $\varphi(p_i|\underline{\theta}_i) = \varphi(p_i|\theta_1, \dots, \theta_n)$  denotes a parametric distribution with  $n$  parameters. In addition, a probability distribution  $\pi^{p_i}(\underline{\theta}_i) = \pi^{p_i}(\theta_1, \dots, \theta_n)$  over the parameters of the model describes the uncertainty over the unknown distribution  $\varphi(p_i|\underline{\theta}_i)$ . The posterior distribution of the population variability parameters based on  $\varepsilon^{p_i}$ ,  $\pi^{p_i}(\underline{\theta}_i|\varepsilon^{p_i})$ , is developed by applying Bayes' theorem (Equation 43).

$$\pi^{p_i}(\underline{\theta}_i|\varepsilon^{p_i}) = k^{-1} L_i(\varepsilon^{p_i}|\underline{\theta}_i) \pi_0^{p_i}(\underline{\theta}_i) \quad 43$$

where  $\varepsilon^{p_i} = \{x_{i1}, \dots, x_{ij}\}$  is the evidence that provides information about  $\pi^{p_i}(\underline{\theta}_i)$ ,  $\pi_0^{p_i}$  is the prior distribution over  $\underline{\theta}_i$ ,  $L_i(\varepsilon^{p_i}|\underline{\theta}_i)$  is the likelihood function of the evidence  $\varepsilon^{p_i}$ , given that the actual distribution of the quantity of interest,  $p_i$ , is a parametric distribution  $\varphi(p_i|\underline{\theta}_i)$ , and  $k = \int_{\underline{\theta}} L_i(\varepsilon^{p_i}|\underline{\theta}_i) \pi_0^{p_i}(\underline{\theta}_i) d\underline{\theta}_i$  is the normalization factor of the Bayesian equation (DAS CHAGAS MOURA et al., 2016; ZHAO, 2022).

Assuming that the experts' estimates,  $x_{ij}$ , are independent, the likelihood function for the entire set of evidence,  $L_i(\varepsilon^{p_i}|\underline{\theta}_i)$ , for the basic event  $i$  is the product of the likelihood functions for each expert  $j = 1, \dots, J$  (Equation 44).

$$L_i(\varepsilon^{p_i}|\underline{\theta}_i) = \prod_{j=1}^J L_{ij}(x_{ij}|\underline{\theta}_i) \quad 44$$



where  $L_{ij}(x_{ij}|\theta_i)$  is the probability density that expert  $j$  estimate  $x_{ij}$ . Note that  $x_{ij}$  is an estimate of  $x_i$  which is only one of the possible values of failure probability  $p_i$ , since  $p_i$  is distributed according to  $\varphi(p_i|\underline{\theta}_i)$ . Then,  $\pi^{x_{ij}} = \pi^{x_{ij}}(x_{ij}|x_i)$  is the probability density that the expert's estimate is  $x_{ij}$  when the expert is attempting to estimate is  $x_i$  (KELLY; SMITH, 2009). Thus, by allowing the failure probability to assume all possible values we write  $L_{ij}(\varepsilon^{p_i}|\theta_i)$  as  $\int_{p_i}^{\square} \pi^{x_{ij}}(x_{ij}|x_i)\varphi(p_i|\underline{\theta}_i)dp_i$ . Then, we can rewrite Equation 43 as:

$$\pi^{p_i}(\underline{\theta}_i|\varepsilon^{p_i}) = k^{-1}\pi_0^{p_i}(\underline{\theta}_i) \prod_{j=1}^J \int_{p_i}^{\square} \pi^{x_{ij}}(x_{ij}|x_i)\varphi(p_i|\underline{\theta}_i) dp_i \quad 45$$

To determine  $\underline{\theta}_i$  we adopted an Empirical Bayes that involved using to Maximum-Likelihood Method to fit the distribution to our evidence. The likelihood function to be maximized is given by Equation 44 (GRIBOK; AGARWAL; YADAV, 2020).

Thus, to perform a PVA of the failure probability of event  $i$ ,  $p_i$ , we need to select the appropriate distributions  $\varphi(p_i|\underline{\theta}_i)$  and  $\pi^{x_{ij}}(x_{ij}|x_i)$ . The specification of  $\varphi(p_i|\underline{\theta}_i)$  may be guided by the nature of the reliability measure; thus, we assume that the real value of  $p_i$  is modeled by a beta distribution  $(\underline{\theta}_i = a_i, b_i)$ ,  $Beta(p_i|a_i, b_i)$ , which is used to model continuous variables, like failure probabilities in the range  $[0, 1]$  (SABRI-LAGHAIE et al., 2022). On the other hand, the construction of  $\pi^{x_{ij}}(x_{ij}|x_i)$  depends on the type of available evidence. We know that the failure probability estimates,  $x_{ij}$ , are imprecise estimates of the real failure probability  $p_i$ . The uncertainty inherent in the experts' estimates about  $p_i$  can be represented using Error Factors with each estimate ( $EF_{ij}$ ) such that  $x_{ij} = EF_{ij} \times p_i$ . Thus, the error factors will be such that  $0 < EF_{ij} < \infty$ . The range of  $EF$  can be visualized to increase in more inconsistent experts' opinion representing lesser degrees of expertise and  $EF_{ij}$  will be 1 for a perfectly consistent judgment.

These characteristics are satisfied by many non-negative distributions, such as the log-normal, Weibull, beta, and gamma distributions. In this context, the log-normal model has been widely adopted (DAS CHAGAS MOURA et al., 2016; GRECO;

PODOFILLINI; DANG, 2021b, 2023; PANDYA et al., 2020; ZHAO, 2022). The  $EF$  range increases in more inconsistent experts' opinion, representing lesser degrees of expertise, and  $EF_{ij}$  will be 1 for a perfectly consistent judgment (PANDYA et al., 2020). Several non-negative distributions, including the log-normal, Weibull, beta, and gamma, meet the required characteristics for reliability analysis. In this context, the log-normal distribution is commonly used in this context, as it is effective in emulating the fact that experts, albeit inherently imprecise, should be able to provide the correct estimates in terms of median.

Thus, we adopted the log-normal error model (GRECO; PODOFILLINI; DANG, 2023) with parameters  $(\mu_{ij}, \sigma_{ij})$  to represent  $\pi^{x_{ij}}(x_{ij}|x_i)$ . Since  $p_i$  can only take values between 0 and 1 the log-normal is then truncated to meet this requirement (GRECO; PODOFILLINI; DANG, 2021b; ZHAO, 2022). In this case,  $x_{ij}$  is the median of the distribution and the standard deviation  $\sigma_{ij}$  reflects the analyst's confidence of the expert  $j$  and it can be expressed in terms of Error Factor ( $EF_{ij} = e^{1.645 \times \sigma_{ij}}$ ), where 1.645 is the 95th percentile of the standard normal distribution (PANDYA et al., 2020).

During elicitation the  $j$ -th expert provide  $x_j$  (estimate on system level, described in Section 4.2.2); then,  $EF_{ij} = EF_j$ . To make the methodology more practical, instead of assessing individual expert credibility we adopted degrees of expertise. Thus, the  $EF_j$  of each expert, which is related to the expert's knowledge about equipment, was assigned by the analyst. Experts with field experience (design and operational) are supposed to have low  $EF_j$  and experts involved with development (research and development qualification, or homologation) are supposed to have moderate  $EF_j$ . Here, we consider the values of 3 and 5 as the low and moderate  $EF_j$ , respectively. Those  $EF_j$  values are defined based on authors expertise and literature review (DAS CHAGAS MOURA et al., 2016; ZHAO, 2022).

Finally, the likelihood ( $L_{ij}$ ) that the expert provides an estimate  $x_{ij}$ , as a function of the values of  $a_i$  and  $b_i$ , is given by Equation 46 (KELLY; SMITH, 2009):

$$L_{ij}(x_{ij} | EF_j, a_i, b_i) = \int_{p_i}^{\square} \text{Lognormal}(x_{ij} | p_i, EF_j) \times \text{Beta}(p_i | a_i, b_i) dp_i \quad 46$$

Thus, we estimate  $a_i$  and  $b_i$  via the Particle Swarm Optimization (PSO) algorithm, which has been successfully applied in many reliability problems (BEZERRA SOUTO MAIOR et al., 2016; DROGUETT et al., 2015), as the values that maximize this likelihood (Equation 47) (SOUTO; DAS CHAGAS MOURA; LINS, 2019).

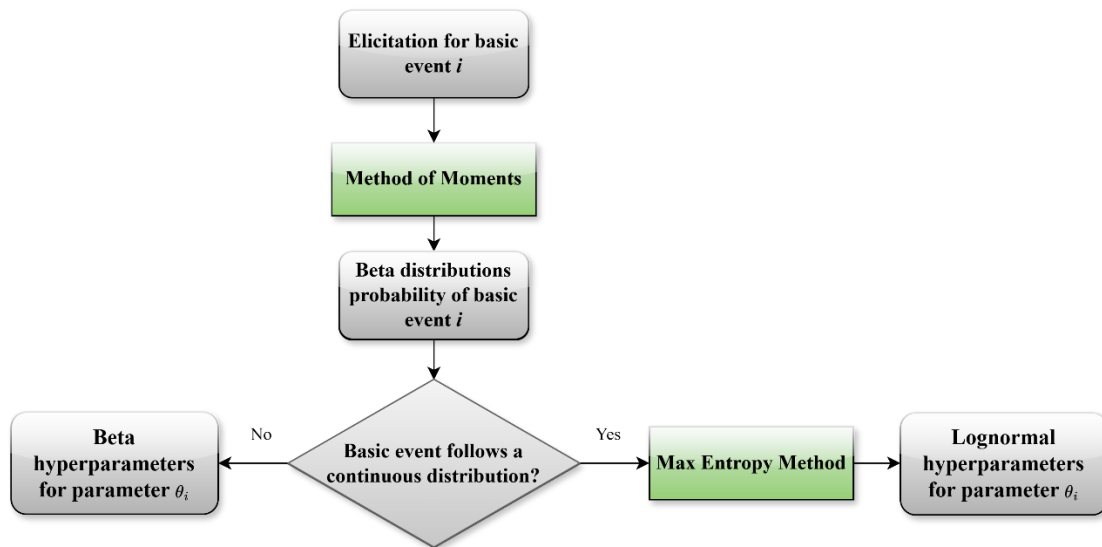
$$L_i(\varepsilon^{p_i}|EF_j, a_i, b_i) = \prod_{j=1}^n L_{ij}(x_{ij}|EF_j, a_i, b_i) \quad 47$$

Then, the aggregation results are the parameters of the beta distribution that described the probability  $p_i$ . The resulting beta distributions are used to define, for all basic events, the distribution of each parameter of  $\theta_i$ ,  $\pi(\theta_i) = \{\pi(\theta_{i1}), \dots, \pi(\theta_{in})\}$ , that define the distribution of the basic event  $i$ .

#### 4.2.4 Prior distribution definition

Depending on the probabilistic distribution of the basic event (defined according to Section 664.2.1), two approaches are proposed to determine the hyperparameters of the prior distribution: (i) MOM is adopted for getting the prior Beta distributions of  $p_i$ , (ii) MEM is adopted if the  $p_i$  is modeled by a continuous distribution (Figure 25).

Figure 25 – The approach applied to define the hyperparameters of the prior distributions.



Source: Macedo et al. (2023)

In a nutshell, when  $E_i$  follows a discrete distribution with a set of parameters  $\theta_i$  we apply MOM to estimate the hyperparameters that describe each parameter of  $\theta_i$ . For example, for a Bernoulli distribution with a parameter  $p_i$ , it (i.e.,  $p_i$ ) follows a log-normal distribution with hyperparameters  $\mu_i$  and  $\sigma_i$ ,  $Lognormal(\mu_i, \sigma_i)$ . Then, the beta distributions resulting from the aggregation process provide the expected value  $E[p_i]$  and variance  $var[p_i]$  of  $p_i$ . These values allow one to estimate the prior distribution through the MOM, in which the unknown parameters match the theoretical moments (functions of the unknown parameters) with the appropriate sample moments, by analytically solving Equations 48 and 49 (MUNKHAMMAR; MATTSSON; RYDÉN, 2017).

$$\mu_i = \log \left( \frac{E[p_i]^2}{\sqrt{(var[p_i] + E[p_i]^2)}} \right) \quad 48$$

$$\sigma_i^2 = \log \left( \frac{var[p_i]}{E[p_i]^2} + 1 \right) \quad 49$$

Similarly, when  $E_i$  follows a continuous distribution,  $f(t|\theta_i)$ , where  $\theta_i$  is a set of parameters, a constraint MEM is solved to obtain the hyperparameters that describe each parameter of  $\theta_i$ . For instance, if  $E_i$  follows an Arrhenius-Weibull distribution; then,  $\theta_i = (\alpha_i, \beta_i, a_i)$ . The maximization problem is given by Equations 50, 51 and 52, where  $\pi(\theta_i)$  is the probability density function for the parameters of event  $i$ ,  $\theta_i$  (MAIOR et al., 2022; WANG; LI, 2021). The constraints are related to the expected value and variance of the beta distribution from the aggregation process and the expected value and variance of the continuous distribution,  $E[f(t|\theta_i)]$  and  $var[f(t|\theta_i)]$ , respectively.

$$\text{maximize } H = \int_{\theta_i} -\pi(\theta_i) \times \log [\pi(\theta_i)] d\theta_i \quad 50$$

s.t.

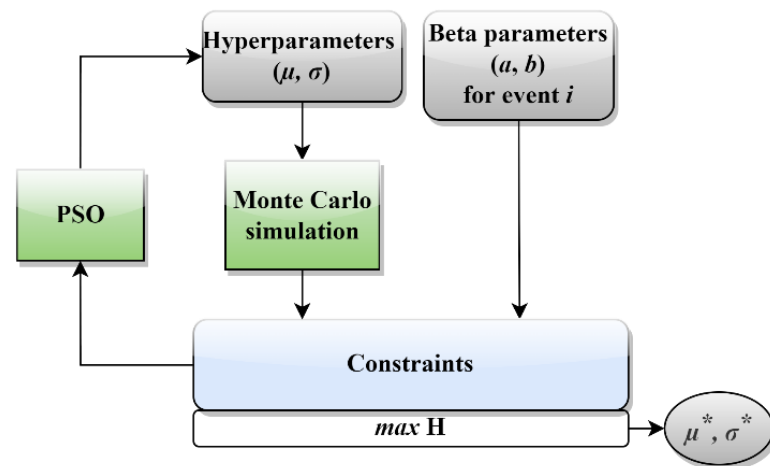
$$E[f(t|\theta_i)] = E[p_i] \quad 51$$

$$var[f(t|\theta_i)] = var[p_i] \quad 52$$

Here, the maximization problem presented in Equation 50 and subject to Equations 51 and 52, which are not solved analytically, is determined also using PSO. The hyperparameters provided by PSO at each iteration were used to generate 100,000 random values for each parameter of  $\theta_i$ , allowing the computation of  $f(t|\theta_i)$  and its moments  $E[f(t|\theta_i)]$  and  $var[f(t|\theta_i)]$ . The right sides of the constraints are computed via MC simulation. This process is repeated and eventually converges into a solution for the maximization problem  $(\mu^*, \sigma^*)$ . Thus, the outcome of the algorithm is the estimates for the hyperparameters that describe the prior distribution of the parameters of the set  $\theta_i$ . This process is illustrated in Figure 26. For details, see Maior *et al.* (2022).

The resulting distributions are used in another MC simulation algorithm to propagate ‘upward’ the uncertainty from the basic events and obtain a probability distribution of the system's reliability.

Figure 26 – The procedure adopted to solve the constrained maximum entropy method.



Source: Macedo et al. (2023)

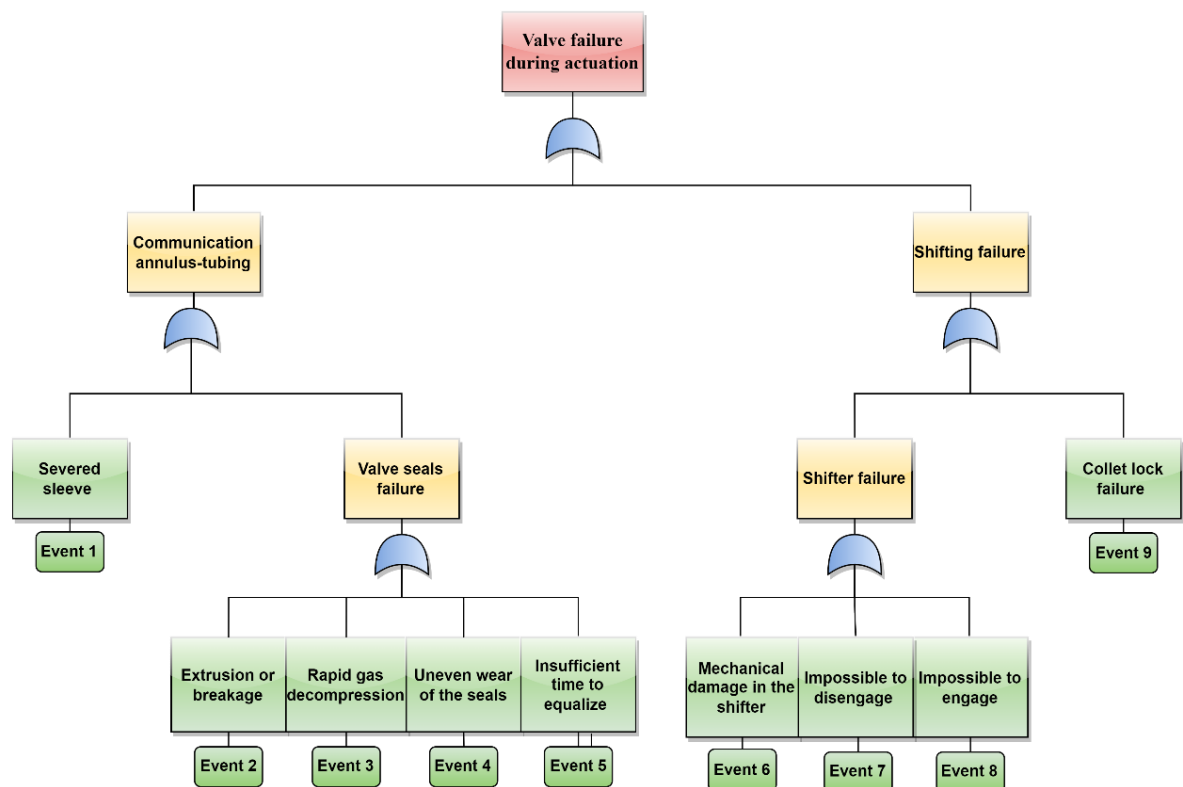
All steps described in Section 4.2 were implemented in Python programming language and, when possible, optimized with Numba (LAM; PITROU; SEIBERT, 2015). In the aggregation process, the SciPy (VIRTANEN et al., 2020) and Pyswarm (HAIR, 2015) libraries were adopted to maximize the likelihood function and to determine the hyperparameters of the beta distributions. In both approaches (i.e., MOM and MEM), we used the SciPy library (VIRTANEN et al., 2020), more specifically, the module *scipy.stats* (MARINI; WALCZAK, 2015) that contains a large number of probability distributions, summary and frequency statistics, and MC functionality.

### 4.3 CASE STUDY

The proposed methodology is applied to a sliding valve underdevelopment used to regulate the flow of material and to isolate areas of the well in the O&G industry. The valve may be adopted for both production or injection purposes and must be able to open and close multiple times under different pressures while maintaining the flow rate. For this system, the goal at the end of the development is to have 90% reliability for a time mission of 27 years. The desired confidence target is 60%.

As previously mentioned, we consider that failures may occur in two different moments: (i) valve actuation (i.e., opening or closing movement), and (ii) operation (i.e., the valve is completely closed or opened). In each moment, an FT is used to model the logical relationships between the failure causes and mechanisms that lead to equipment failure over a mission time of 27 years. The FT related to the equipment failure during its actuation (Figure 27) contains nine basic events ( $E_i, i = 1$  to 9), the description of each basic event is presented in Table 14.

Figure 27 – Fault tree diagram representing the valve failure during actuation, where green and yellow blocks represent basic and intermediate events, respectively.



Source: Macedo et al. (2023)

Table 14 – Description of basic events of the FT for the valve failure during actuation.

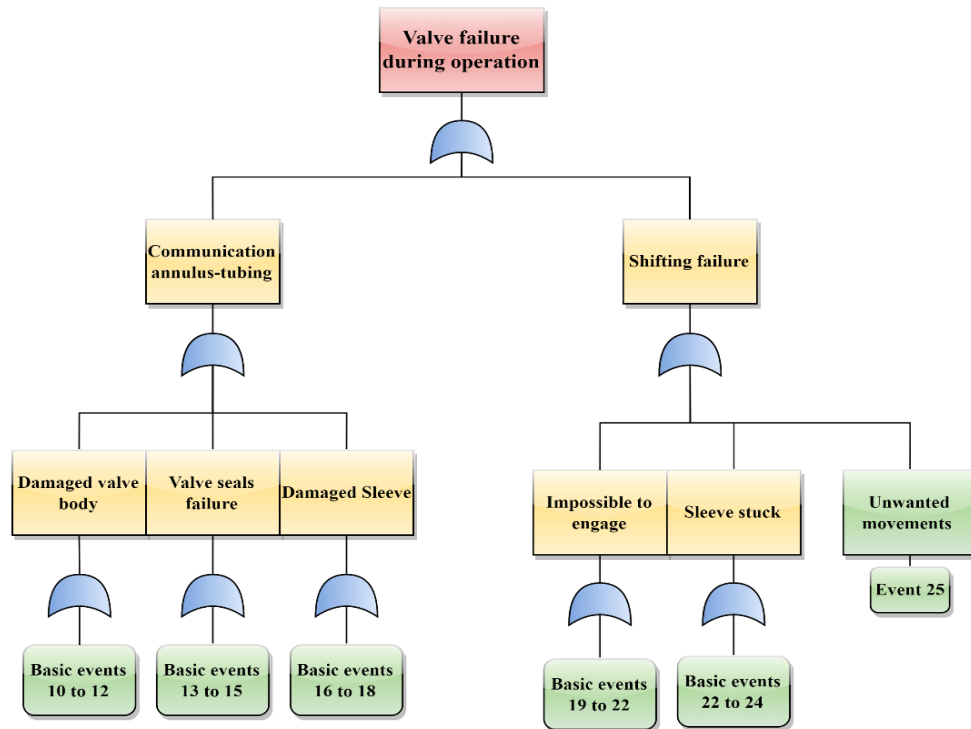
$E_i$	Description
1	The sleeve is severed, opening the connection to the annulus, due to mechanical damage due to excessive force applied.
2	The seals suffer extrusion or breakage during actuation, opening the connection to the annulus due to sealing failure when closed.
3	The seals are compromised by erosion due to rapid gas decompression, opening a connection to the annulus.
4	Uneven wear of the seals due to particle contamination.
5	The sliding seals suffer extrusion due to failure in the pressure equalization system caused by the insufficient time to equalize.
6	The shifter suffers mechanical due to excessive force applied. Such damage renders the valve closing impossible due to the damaged shifter profile.
7	The shifter suffers mechanical damage due to excessive force applied. Such damage renders the disengage of the valve impossible due to the damaged shifter profile.
8	It is impossible to engage the shifter due to wear caused by abrasion on the shifter profile, thus the opening/closing of the valve cannot be executed.
9	Undesired movement or no confirmation of valve status occurs due to excessive force applied in the collet lock.

Source: Macedo et al. (2023)

Since the resistance of a component to certain demand-induced stress can reduce over time and/or with previous demands, this probability is dependent on the time instant and on the index of the demand in question. Thus, each of these basic events is modeled by a time-and-demand-dependent probability of failure (Equation 42),  $p_i$  ( $i = 1$  to 9).

During operation, the valve is continuously subject to pressure, temperature, debris, friction, and chemical attack stresses, which can cause an accumulation of degradation in the valve components, and then lead them to a failed state. The FT related to the valve failure during operation has fifteen basic events ( $E_i$ ,  $i = 10$  to 25). A Weibull distribution with parameters  $\alpha_i$  and  $\beta_i$  is adopted to model the probability of the occurrence of  $E_i$ ,  $i = 10$  to 25 at time  $t$ , which can capture the failure rate degradation over time (if  $\beta_i > 1$ ) since these events are related to the ageing of components. Similar to the failure during actuation, there are two failure modes during operation: annulus-tubing communication and shifting failure, which represent the loss of isolation during a workover or the fault in the valve movement (open/close). A simplified version of the FT is depicted in Figure 28 and described in Table 15.

Figure 28 – Fault tree diagram representing the valve failure during operation, where green and yellow blocks represent basic and intermediate events respectively.



Source: Macedo et al. (2023)

Table 15 – Description of basic events of the FT for the valve failure during operation.

$E_i$	Description
10	The valve body is broken due to excessive loads, which cause communication annulus-tubing.
11	The valve body suffers a metal loss due to erosion over the operation mission time. Such loss causes communication annulus-tubing.
12	There is a compromise in the valve sealing surface on the flow trim in the valve body due to erosion along operation mission time, which causes communication annulus-tubing.
13	The valve seals fail due to plugged flow path, which causes communication annulus-tubing.
14	The valve seals fail due to abrasion, which causes communication annulus-tubing.
15	The seals fail to seal against the valve body due to ageing along operation mission time, which causes communication annulus-tubing.
16	Rupture of the sleeve due to excessive differential pressure.
17	Collapsed sleeve due to differential pressure.
18	Damaged sleeve due to erosion.
19	It is impossible to engage the sliding sleeve due to wear on the sleeve, which makes it impossible to open or close the valve.
20	It is impossible to engage the sliding sleeve due to the scale on the sleeve, which makes it impossible to open or close the valve.



$E_i$	Description
21	It is impossible to engage the shifter due to the scale on the shifter, which makes it impossible to open or close the valve.
22	It is impossible to engage the shifter due to debris on the shifter, which makes it impossible to open or close the valve.
23	The sleeve is stuck due to debris on the sleeve's exposed surfaces, which makes it impossible to open or close the valve.
24	The sleeve is stuck due to scale, which makes it impossible to open or close the valve.
25	There is a positioning failure due to the sleeve's unwanted movement not being locked in position because of wear on the collet lock.

Source: Macedo et al. (2023)

#### 4.4 RESULTS

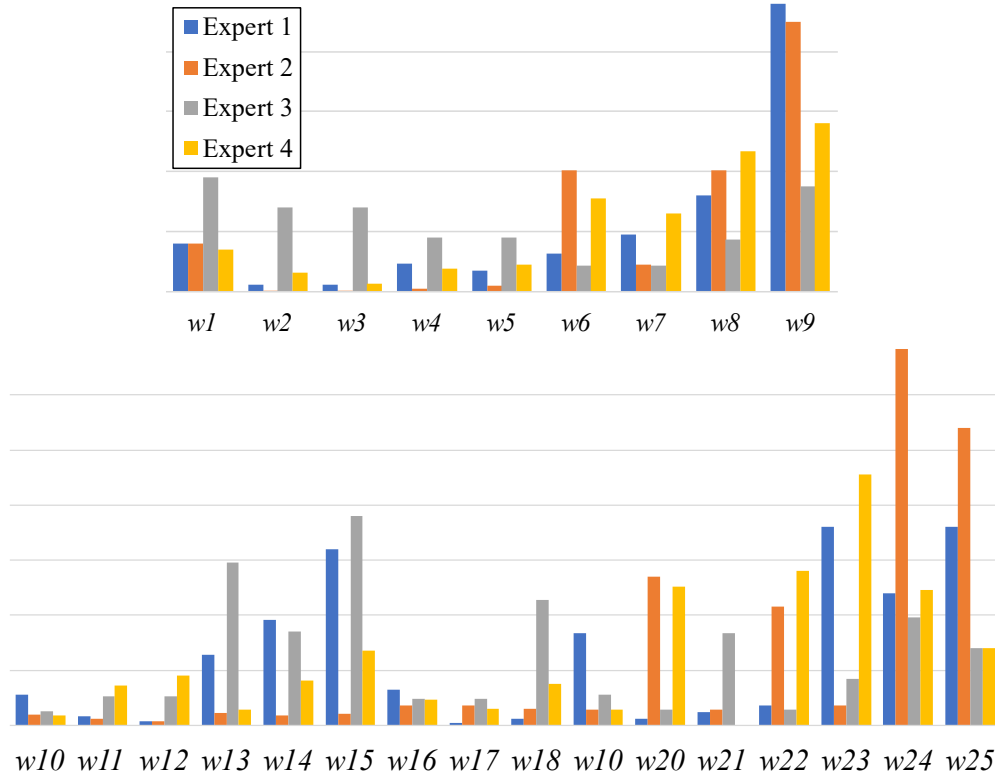
Four experts were involved in the elicitation process, two of them with high  $EF$  and the other two with moderate  $EF$ . First, the experts provided the contribution of the events that can lead to valve failure during actuation (Figure 27). Then, the experts provided the contribution of the events that can lead to valve failure during operation (Figure 28). The contributions,  $w_i$ , of each  $E_i$  to their respective top event (failure during actuation or failure during operation) were computed. The distribution of the values of  $w_i$  is presented in Figure 29.

In addition, the experts provided three estimates related to the failure during actuation (top event of Figure 27):

- The probability of failure in the first actuation at  $t = 0, d = 0$ ;
- The probability of failure in the fifth actuation at  $t = 0, d = 5$ ;
- The probability of failure in the first actuation at  $t = 10$  years,  $p(t = 10, d = 0)$ .

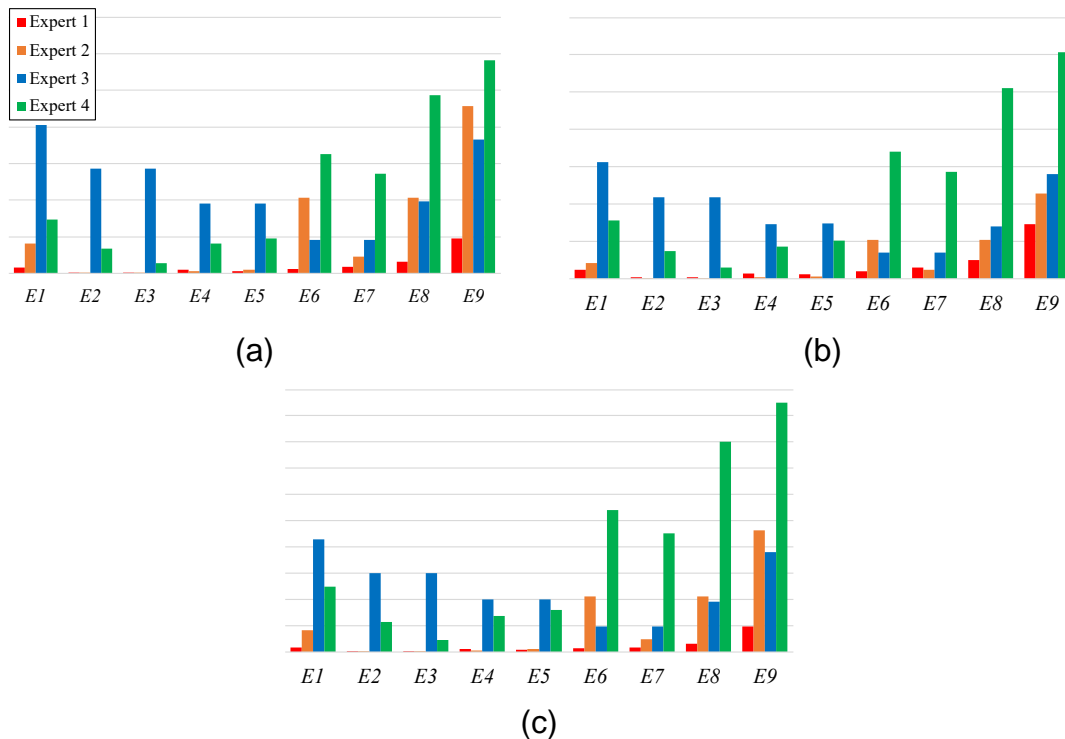
It is worth mentioning that the values of  $t$  and  $d$  were chosen based on the analyst's knowledge regarding the valve's expected lifetime and the expected number of actuations in the oil well. The probabilities estimate ( $x_j$ ) provided by the expert  $j$  and its contributions are used to compute the estimates ( $x_{ij}$ ) for each basic event  $i$  as described in Section 4.2.2. The distribution of the values of the probabilities estimate for  $E_i$  ( $x_{ij}$ ) related to the opinion of expert  $j$  about the failure during actuation is illustrated in Figure 30a, Figure 30b, and Figure 30c.

Figure 29 – Distribution of the contributions of each basic event,  $w_i$ , to actuation failure ( $i = 1$  to 9) and to operation failure ( $i = 10$  to 25).



Source: Macedo et al. (2023)

Figure 30 – Distribution of probability estimates of (a) failure during actuation for each basic event  $p_i(t = 0, d = 0)$ ; (b) failure during actuation for each basic event  $p_i(t = 0, d = 5)$ ; and (c) failure during actuation for each basic event  $p_i(t = 10, d = 0)$ .



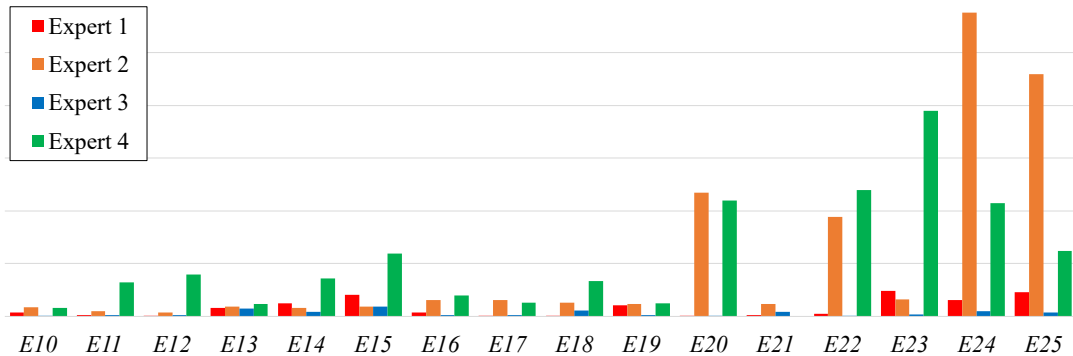
Source: Macedo et al. (2023)

Moreover, the experts provided one estimate related to the failure during operation:

- The probability of failure during its operations at 27 years,  $P(t = 27)$ .

Hence, the distribution of the values of the probabilities estimated for  $E_i(x_{ij})$  related to the opinion of expert  $j$  about the failure during operation is illustrated in Figure 31. Then, the estimates are adopted as modes of log-normal distributions with low or moderate  $EF$  are aggregated using PVA resulting in a single beta distribution, as described in Section 2.3. From Figure 31, note that the experts with low  $EF$  (more experience and knowledge about the project), represented in blue and grey, generally provide more optimistic estimates than the experts with moderate error factor. Then the aggregation process balances these views by considering the uncertainty related to the experience level of each expert.

Figure 31 – Distribution of estimates of the probability of failure in 27 years of operation  $p_i(t = 27)$ .



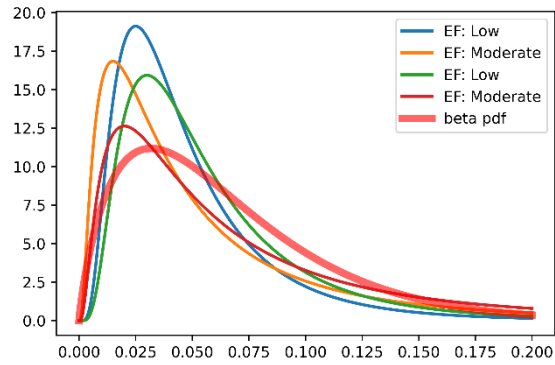
Source: Macedo et al. (2023)

Thus, the parameters and median of the beta distributions that describe  $p_i(d = 0, t = 0)$ ,  $p_i(t = 0, d = 5)$ ,  $p_i(t = 10, d = 0)$ , for  $i = 1$  to 9, and  $p_i(t = 27)$ , for  $i = 10$  to 25, were found via PSO. For instance, Figure 32 presents the log-normal distributions related to the expert's opinion about the probability of failure during actuation at  $t = 0$  and  $d = 0$  ( $P_0$ ) for  $E_9$  and the resulting beta distribution that has mode  $2.2 \times 10^{-2}$ , median  $2.5 \times 10^{-2}$ , and variance  $1.3 \times 10^{-4}$ .

The resulting beta distributions for the probability of failure during actuation are summarized in Table 16. Since all log-normal distributions from elicitation have a mode close to zero, values of  $\alpha$  less than 1 provide a likelihood function of greater value.

Thus, to ensure the bell shape of the Weibull distribution, we set the lower bound of the hyperparameter  $a$  as 1.1.

Figure 32 – Example of aggregation result, beta distribution for  $E_9$  obtained through PVA.



Source: Macedo et al. (2023)

Table 16 – Beta distribution that represents, for each basic event, the probability of the first actuation failure  $p_i(t = 0, d = 0)$ , the probability of actuation failure after 5 demands in  $t=0$ ,  $p_i(t = 0, d = 5)$ , and the probability of the first actuation failure in  $t=10$  without demands,  $p_i(t = 10, d = 0)$ .

$p_i(t = 0, d = 0)$										
Event		$E_1$	$E_2$	$E_3$	$E_4$	$E_5$	$E_6$	$E_7$	$E_8$	$E_9$
beta parameter	$a$	1.10	1.10	1.10	1.10	1.10	1.89	1.15	2.41	5.24
	$b$	75.69	85.40	85.40	96.95	96.95	159.93	123.01	149.22	192.90
Median (%)		1.04	0.92	0.92	0.81	0.81	0.98	0.68	1.38	2.48
$p_i(t = 0, d = 5)$										
beta parameter	$a$	1.10	1.10	1.10	1.10	1.10	1.96	1.35	1.85	5.24
	$b$	75.69	68.08	85.40	79.03	96.95	97.02	85.32	61.98	192.90
Median (%)		1.04	1.15	0.92	0.99	0.81	1.67	1.20	2.42	2.48
$p_i(t = 10, d = 0)$										
beta parameter	$a$	1.99	1.11	1.10	1.34	1.10	1.89	1.15	2.41	1.86
	$b$	72.22	58.23	58.09	69.45	96.95	159.93	123.01	149.22	27.23
Median (%)		2.27	1.36	1.35	1.46	0.81	0.98	0.68	1.38	5.41

Source: Macedo et al. (2023)

One can see, highlighted with a lighter color in Table 16 that the beta distributions for  $E_1$ ,  $E_3$ ,  $E_5$  and  $E_9$  remained the same as comparing  $p_i(t = 0, d = 0)$  to  $p_i(t = 0, d = 5)$ . This is because, according to the experts, the probability of failure due to  $E_1$ ,  $E_3$ ,  $E_5$  and  $E_9$  are not affected by previous demands. Similarly, the probabilities of failure due to  $E_5$ ,  $E_6$ ,  $E_7$  and  $E_8$  are not affected by time. Thus,  $p_i(t = 0, d = 0)$  and  $p_i(t = 10, d = 0)$  related to  $E_5$ ,  $E_6$ ,  $E_7$  and  $E_8$  remained the same, highlighted with a darker color in Table 16. As expected, the medians of the beta distributions related to the probabilities considering the degradation due to previous demands and to time were equal or higher than the median of the corresponding beta distribution of the initial probability of failure during actuation  $p_i(t = 0, d = 0)$ .

Moreover, the beta distributions for the probability of failure during operation over a mission time of 27 years are summarized in presented in Table 17.

Table 17 – Beta distributions of probability of failure during operation in 27 years for each event.

Event		$E_{10}$	$E_{11}$	$E_{12}$	$E_{13}$	$E_{14}$	$E_{15}$	$E_{16}$	$E_{17}$
beta parameter	$a$	1.12	1.15	1.15	1.15	1.14	1.15	1.14	1.15
	$b$	184.78	186.97	187.21	186.92	186.19	187.21	186.22	187.28
Median (%)		0.44	0.44	0.45	0.45	0.44	0.45	0.44	0.44
Event		$E_{18}$	$E_{19}$	$E_{20}$	$E_{21}$	$E_{22}$	$E_{23}$	$E_{24}$	$E_{25}$
beta parameter	$a$	1.14	1.15	1.16	1.11	1.13	1.13	1.15	1.15
	$b$	185.96	187.12	187.37	184.04	185.16	185.53	187.04	187.13
Median (%)		0.44	0.45	0.45	0.42	0.44	0.44	0.45	0.45

Source: Macedo et al. (2023)

As mentioned, the probability of failure during actuation follows Equation 42, and we assumed that the parameters  $\rho_i$ ,  $\gamma_i$ , and  $\tau_i$  follows a log-normal distribution with hyperparameters  $\mu_{\theta_i}$  and  $\sigma_{\theta_i}$  ( $\theta_i = \rho_i, \gamma_i$ , or  $\tau_i$ ). Considering the elicited values, we have the relations in Equations 53 - 55.

$$p_i(0,0) = \rho_i \quad 53$$

$$p_i(0,5) = \rho_i + \gamma_i \times 5 \quad 54$$

$$p_i(10,0) = \rho_i + \tau_i \times 10 \quad 55$$

In possession of the beta distributions of  $p_i(0,0)$ ,  $p_i(0,5)$ , and  $p_i(10,0)$  we can use their expected values and variances to obtain the expected value and variance for  $\rho_i$ ,  $\gamma_i$ , and  $\tau_i$ . For instance,  $E[p_i(0,5)] = E[\rho_i] + 5 \times E[\gamma_i]$  and, since we are assuming that the parameters are independent  $cov(\rho_i, \gamma_i) = 0$ ,  $var[p_i(0,5)] = var[\rho_i] + 25 \times var[\gamma_i]$ . Thus, we define the hyperparameters of log-normal distributions  $(\mu, \sigma)$  via MOM (MAIOR et al., 2022). The results are summarized in Table 18.

Table 18 – Hyperparameters of the prior distribution of the valve actuation failure.

$E_i$	Hyperparameter					
	$\mu_\rho$	$\sigma_\rho$	$\mu_\gamma$	$\sigma_\gamma$	$\mu_\tau$	$\sigma_\tau$
1	-4.56	0.80			-2.97	0.45
2	-4.68	0.80	-9.21	1.92	-5.17	1.13
3	-4.68	0.80			-4.65	1.00
4	-4.81	0.80	-9.50	1.95	-4.45	0.86
5	-4.81	0.80				
6	-4.66	0.65	-7.59	1.53		
7	-4.99	0.79	-7.98	1.62		
8	-4.31	0.58	-7.12	1.54		
9	-3.72	0.41			-2.05	0.47

Source: Macedo et al. (2023)

For  $E_1, E_3, E_5$ , and  $E_9$ ,  $\gamma = 0$  and for  $E_5, E_6, E_7$  and  $E_8$   $\tau = 0$ ; in these cases, there are no hyperparameters for  $\gamma$  and/or  $\tau$ .

Moreover, the beta distributions for  $p_i(t = 27)$  were used to define the constraints of the ME problem and the optimization problem was solved, as described in Section 4.2.4, to define the distributions of  $\alpha_i$  and  $\beta_i$ , for or all events  $E_i$   $i = 10$  to 25. The results are summarized in Table 19.

Table 19 – Hyperparameters of the log-normal distributions of Weibull parameters  $\alpha_i$  and  $\beta_i$ .

$E_i$	Hyperparameters			
	$\mu_\alpha$	$\sigma_\alpha$	$\mu_\beta$	$\sigma_\beta$
10	4.97	0.22	1.22	0.14
11	3.96	0.05	2.12	0.16
12	4.68	0.14	1.41	0.17
13	4.11	0.10	1.92	0.12
14	5.11	0.15	1.13	0.16

$E_i$	Hyperparameters			
	$\mu_\alpha$	$\sigma_\alpha$	$\mu_\beta$	$\sigma_\beta$
15	4.30	0.13	1.68	0.08
16	5.24	0.20	1.07	0.17
17	4.48	0.14	1.55	0.15
20	4.89	0.22	1.27	0.13
21	5.33	0.26	1.03	0.15
22	4.27	0.13	1.76	0.12
23	5.22	0.19	1.09	0.17
24	4.58	0.11	1.45	0.14
25	4.92	0.17	1.25	0.17

Source: Macedo et al. (2023)

Finally, in possession of basic events' prior distributions, MC simulation was performed to obtain the prior distribution of the valve reliability,  $R_V$  (Table 20).

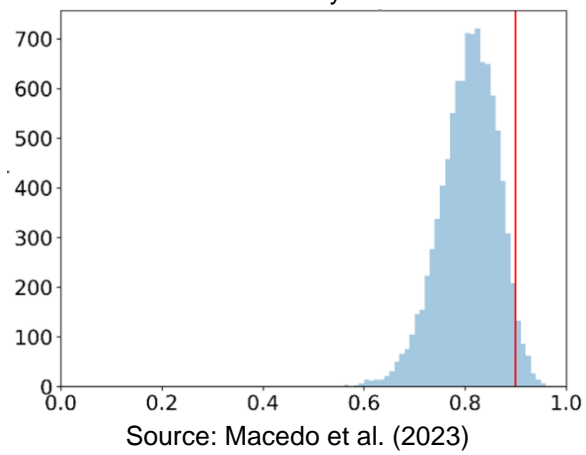
Table 20 – Prior reliability of the valve, values in percentage.

$P[R_V \geq 90\%]$	Mean	Median	Percentile	
			5	95
1.96	80.18	80.99	69.99	88.99

Source: Macedo et al. (2023)

Figure 33 shows that the confidence of  $R_V$  being greater than the required 90% (at the end of the development), for 27 years of mission time, is small as this is the first stage of development of the valve. Thus, the reliability confidence level obtained has not reached the target. Such a result agrees with the experts' expectations as data are rather scarce, and uncertainty is high at early development stages. In addition, the distributions obtained at this development stage of the novel valve were only based on experts' opinions, and one possible explanation for this result can be the pessimistic estimates provided by some of the experts. Nevertheless, the Bayesian methodology allows this first estimate to be updated as soon as test results during development or field data are available. In addition, it is believed that Bayesian updates, even with 'poor' likelihood functions, will result in posterior distributions with a lower bias since the prior distribution was carefully built with all the available information about the equipment.

Figure 33 – Prior reliability distribution of the valve; the vertical red line indicates the target reliability of 90% for 27 years.

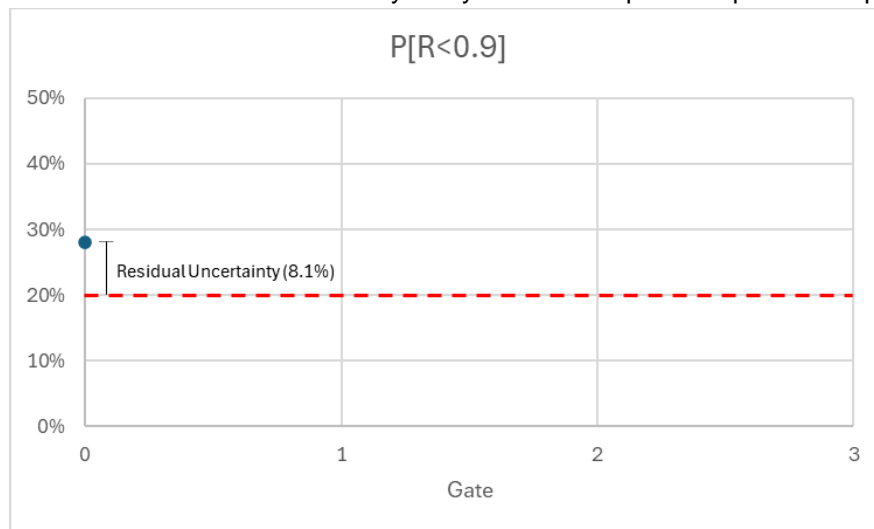




## 5 POSTERIOR ESTIMATES AND RESIDUAL UNCERTAINTY ANALYSIS FOR THE EXPANDABLE PRODUCTION PACKER CASE

In section 3.3, the Multilevel Reliability Model (MRM) was built for the novel offshore expansible production packer, and the reliability uncertainty distribution during operation was estimated for the mission time (Figure 21) based on the MRM parameters prior distributions obtained from generic data and expert opinions. This prior estimate provided a probability of 28.1% that the operating reliability is less than 0.9, i.e.  $P[R < 0.9] = 28.1\%$ , which is the uncertainty estimate at Gate 0, characterized by the blue dot in the graph in Figure 34, and corresponding to a residual uncertainty of 8.1% (the uncertainty level to be reduced in order to reach the target of  $P[R < 0.9] \leq 20\%$ , represented by the dashed red line).

Figure 34 – Gate 0 residual uncertainty analysis for the expansible production packer.



Source: The author.

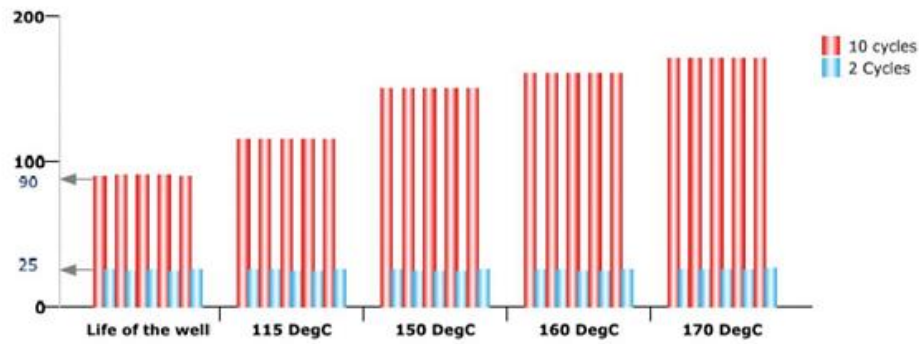
This section shows the updates to reliability uncertainty distributions estimated in Section 3 from the reliability tests carried out during equipment development phases, and the consequent reduction in residual uncertainty.

### 5.1 LIKELIHOOD FUNCTIONS

Some reliability tests performed for this equipment can be seen in JACINTO et al., (2015). For purposes of illustrating the methodology, the temperature and pressure cycle test for producer well, described in JACINTO et al., (2015), is considered. In this

test, temperature and pressure were varied on the compensation valve of the packer, as seen in Figure 35, thereby reproducing the well's life cycle in a conservative fashion. The cold temperature was set at 25°C with five temperature steps (90°C, 115°C, 150°C, 160°C, and 170°C) for the hot temperature. The temperature was changed between cold and hot temperatures five times in each step. During high temperatures, 10 pressure cycles were performed, while this was done only 2 times in cold temperatures. At the end of pressure cycles, before changing the temperature, a sealing test was carried out to check the functionality of compensation valve.

Figure 35 – Test sequence for producer well



Source: JACINTO et al., (2015)

In order to construct likelihood functions from this test, it is necessary to identify which failure events are covered by this test. As the test was carried out only on the compensation valve, only failure events associated with the compensation valve could be covered by the test. These are the events  $E_{15}$  (temperature ageing of the valve seals),  $E_{16}$  (debris preventing valve to move) and  $E_{17}$  (mechanical deformation on valve body due differential pressure) in Table 9. By analyzing the stressors, it is possible to check that only events  $E_{15}$  and  $E_{17}$  were stressed, since there is no debris applied during the test. Then, the data needed to feed the reliability models of these events must be extracted from the test. As seen in Section 543.3.2, the Arrhenius-Weibull and the Weibull models were chosen for events  $E_{15}$  and  $E_{17}$ , respectively.

The input data for Arrhenius-Weibull are the test times at the high temperatures (since the high temperature is the stressor for this event) and the high temperature levels applied during the test. Since the same item was subjected to all temperature steps, and no failure was observed during the sealing inspection, then the right-censored step-stress Arrhenius-Weibull model was used to formulate the likelihood function for the test data, as given in Equation 56 (MODARRES; AMIRI; JACKSON,

2017), where  $t_s$  is the total time that the valve was in the  $s^{th}$  temperature step,  $T_s$  is the temperature level of the  $s^{th}$  step,  $a_{15}, b_{15}$  and  $\beta_{15}$  are the Arrhenius-Weibull parameters for event  $E_{15}$ ,  $T_{use}$  is the expected use temperature of the valve, and  $t_e$  is the equivalent total test time at the use temperature (calculated according Equation 57). Due to the confidentiality of these data, the values of  $t_s$  and  $T_s$  will not be presented.

$$L(t_1, \dots, t_5, T_1, \dots, T_5 | a_{15}, b_{15}, \beta_{15}) = \prod_{s=1}^5 e^{-\left(\frac{t_e}{b_{15} e^{\frac{a_{15}}{T_{use}}}}\right)^{\beta_{15}}} \quad 56$$

$$t_e = \sum_{s=1}^5 t_s \times e^{a_{15} \times \left(\frac{1}{T_{use}} - \frac{1}{T_s}\right)} \quad 57$$

The event  $E_{17}$  models the mechanical deformation in the compensation valve due to pressure cycles. The expected number of cycles during the 27 years of mission is  $C$  (the real value of  $C$  is hidden for reasons of secrecy). In the test, a total of 300 pressure cycles were performed (10 at each hot temperature and 2 at each cold temperature), the equivalent time in field that the valve was subjected to the event  $E_{17}$  is  $300/C$ . Since the Weibull reliability model was assigned for event  $E_{17}$ , and no mechanical deformation had occurred during the test, then the right censored Weibull distribution is used to formulate the likelihood of Equation 58, where  $\alpha_{17}$  and  $\beta_{17}$  are the Weibull parameters for the event  $E_{17}$ .

$$L\left(\frac{300}{C} | \alpha_{17}, \beta_{17}\right) = e^{-\left(\frac{300/C}{\alpha_{17}}\right)^{\beta_{17}}} \quad 58$$

## 5.2 RELIABILITY UPDATE AND RESIDUAL UNCERTAINTY ANALYSIS

The procedure of extracting likelihood functions like the one described in previous section was accomplished for all tests performed during expandable packer development. Then, the posterior distributions for the reliability parameters  $\theta_i$  presented in Equation 33, and whose a priori distributions are shown in the Table 13, are calculated through the Bayesian equation (Equation 20) as tests are carried out.

For example, the posterior distribution for the parameters  $\alpha_{17}$  and  $\beta_{17}$  is obtained according to Equation 59 (by assuming independent prior distribution for  $\alpha_{17}$  and  $\beta_{17}$ , after running the test presented in previous section, where  $\mu_{\theta_{17}}$  and  $\sigma_{\theta_{17}}$  ( $\theta = \{\alpha, \beta\}$ ) are the hyperparameters of the Lognormal prior distribution of  $\alpha_{17}$  and  $\beta_{17}$ , estimated in section 3.3.2.2. To solve the Bayesian equations, the MCMC method was applied and implemented in the Stan language (BLEI; KUCUKELBIR; MCAULIFFE, 2017; ROSSI, 2018; SPADE, 2020).

$$\pi\left(\alpha_{17}, \beta_{17} \middle| \frac{300}{C}\right) \propto \pi_0(\alpha_{17} | \mu_{\alpha_{17}}, \sigma_{\alpha_{17}}) \times \pi_0(\beta_{17} | \mu_{\beta_{17}}, \sigma_{\beta_{17}}) \times L\left(\frac{300}{C} \middle| \alpha_{17}, \beta_{17}\right) \quad 59$$

Then, the MC process to generate samples for  $R(27)$  described in section 3.3.2.2 is repeated, but now using the posterior distributions to generate the samples of the parameters  $\theta_i$ . Firstly, component-level tests were carried out (such as the compensation valve test illustrated in the previous section) and a first update to the expandable packer reliability estimate was performed (Gate 1). In a second step, tests were carried out at the system level (packer), including qualification tests, making up the second update in the packer reliability estimate at gate 2. Figure 36 and Figure 37 show the uncertainty distributions of  $R(27)$  at Gates 1 and 2, where the red line marks the 90% target, and Figure 38 presents the residual uncertainty behavior.

The probability of  $R(27)$  being less than 90% target was 21.93% at Gate 1 and 17.89% at Gate 2, meaning a reduction in the residual uncertainty from 8.1% at prior analysis (see Figure 34) to 1.93% at Gate 1 and 0% at Gate 2 (in Gate 2, the target of  $P[R < 0.9] \leq 20\%$  was reached, so the residual uncertainty is 0%). This reduction in residual uncertainty along the gates is expected to be observed for reliable equipment design as more information is obtained about the reliability of the technology from the tests with no or little failure data.

In this specific application of the methodology for the new expandable packer, the target was reached after system level tests, configuring a successful development in terms of qualification against quantitative reliability requirements. This residual uncertainty analysis can be used to guide qualification efforts, supporting the planning of tests that will most contribute to reducing residual uncertainty and identifying, in case failures are observed in any test, failure mechanisms that need to be addressed through design improvements in the related component.

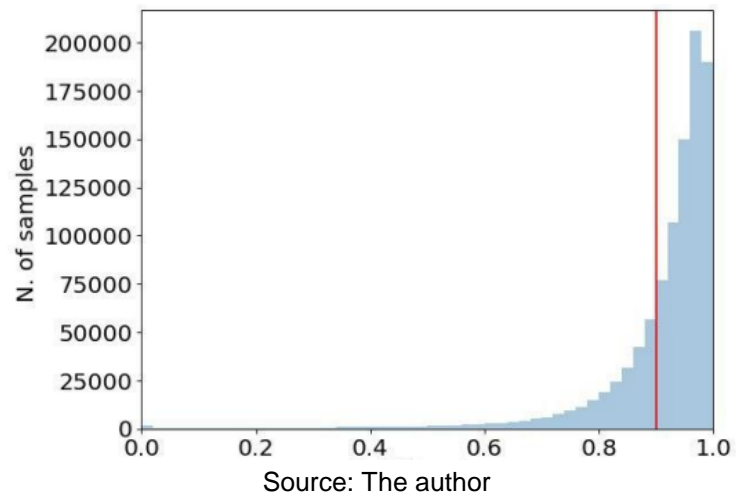
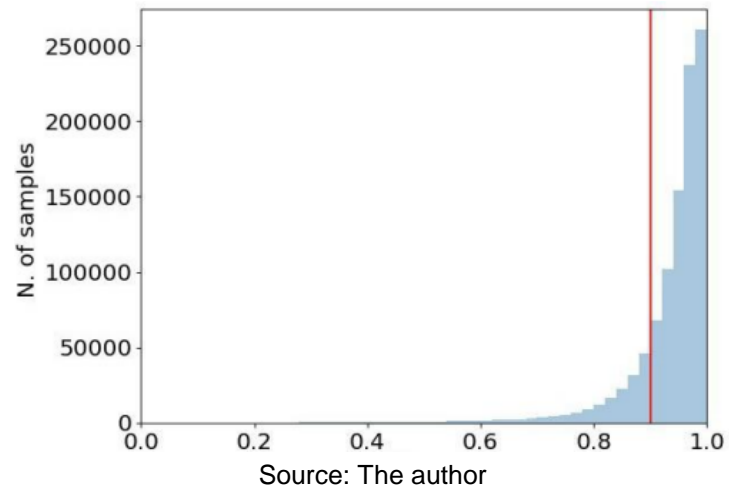
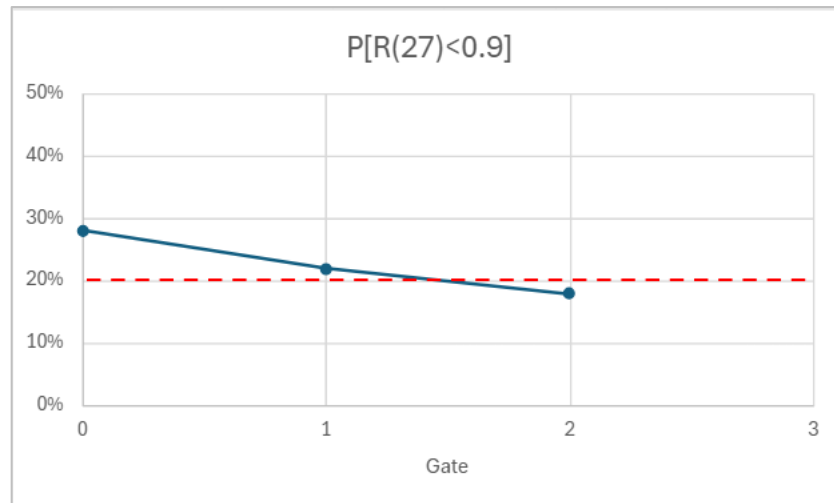
Figure 36 – Distribution of the samples of  $R(27)$  at Gate 1Figure 37 – Distribution of the samples of  $R(27)$  at Gate 2

Figure 38 – Gate 0-2 residual uncertainty analysis for the expansible production packer



## 6 CONCLUSIONS

This thesis has proposed a systematic methodology to predict and update reliability metrics and to perform uncertainty analysis of O&G equipment technologies that are under development. Effectively, the multilevel reliability model (MRM) formulation, the Bayesian framework and the residual uncertainty analysis comprise the modules of the methodology. They were presented in Chapter 2 and designed to be able to aggregate different types of data, allowing monitoring the evolution of uncertainty on reliability as tests and analyzes are carried out on each development phase. In this sense, the methodology solves part of the qualification problem of a technological development process in the oil and gas industry, namely the heterogeneity of information sources and the scarcity of long-term data available for new technologies.

In high reliable equipment of the O&G industry, failure and test data are rather scarce, especially for technologies under development. Therefore, limited prior knowledge on the system reliability is usually available in terms of generic databases, historic of similar heritage components and expert opinions only. Then, it was proposed two methods to get prior distributions for the MRM parameters in the Bayesian framework module. The first one is presented in Chapter 3 and can be applied for continuously operated system. The method described in Chapter 4 aims at the same objective but by considering non-continuously operated systems (on demand system). The approaches do not involve directly eliciting the expert opinion about the hyperparameters; this allows using different distributions to describe the basic events without hindering understanding during the elicitation process.

In Chapter 3, it was adopted an elicitation procedure to fit the Wellmaster (generic database) results in the specific scenarios for a novel expandable production packer of the O&G industry. The elicitation process engaged specialists from different areas involved in the equipment development process, allowing for a balance between pessimistic and optimistic analyses. Moreover, the procedure was based on the analysis of component failure mechanisms. Although the system is new, the components and materials are “old acquaintances” of the experts. The methodology considers distinct FTs to deal with different stages of equipment life cycle and, in the case study, the two analyzed stages were installation and operation. The results

obtained for the equipment installation and operation can be used to estimate the prior equipment reliability and to perform uncertainty analysis.

Chapter 4 proposed a methodology to define informative Bayesian prior distribution, based on experts' opinions, for novel equipment that works on demand. Specifically, it was considered mathematical models that ponder both time and on-demand degradation simultaneously. Furthermore, the methodology takes into account the uncertainty related to the experts' opinions by using multiplicative error and PVA to aggregate the different estimates provided by the experts. The elicitation process adopted does not involve directly eliciting the expert opinion about the parameters of the distribution. In addition, the process engaged specialists from different areas involved in the equipment development process, allowing for a balance between pessimistic and optimistic analyses. It was presented a case study in which distinct FTs were adopted to deal with different stages of the equipment life cycle and the two analyzed stages were actuation and operation. The results obtained for the equipment actuation and operation can be used to estimate the equipment reliability and evaluating the uncertainties.

Using a systematic procedure, the methodology was able to satisfactorily evaluate reliability metrics of O&G equipment technologies that are under development by aggregating the prior distributions obtained in Chapters 3 and 4 with the results of the tests performed through the process, providing a powerful tool to drive efforts in defining and running reliability tests as well as design changes. Compared to reliability methodologies currently used by service companies, which basically involve carrying out reliability demonstration tests, the proposed methodology allows control and monitoring of the technological process since earlier stages through the residual uncertainty analysis. In fact, having a target of reliability and uncertainty, it is possible to monitor, throughout the stages, the evolution of these values. The proposed methodology makes this feasible thanks to its Bayesian approach and likelihood solutions for the heterogeneous data set that gradually updates the reliability function as new information becomes available.

Applied to two practical cases, the proposed methodology was tested on different data types and operations, with overwhelming results, demonstrating flexibility and robustness. It is expected that it can be applied to an increasing amount of equipment under development, ensuring that the product ultimately meets the company's intended performance requirements.

## 6.1 IMPACTS OF THE THESIS

### 6.1.1 Economic Impacts

- Reduction of well operation and intervention costs, reduction of failures, operational interruptions, and unscheduled stops, since the reliability of the new technology for the mission time is previously known with a certain level of confidence.
- Increased efficiency, with the optimal definition of an oil and gas production development project.
- Reduction of development costs for new technologies, predicting and monitoring equipment reliability from the early stages of the development process, reducing the chances of changes to the design after the prototypes are completed.
- Support to an efficient and optimized tests planning, by indicating the residual uncertainty to be reduced for each alternative plan.

### 6.1.2 Social Impacts

- Increased worker safety, reducing the risk of failures and accidents during the installation and operation of new completion technologies.
- Negotiation stability for completion equipment manufacturers, as the operational efficiency of their technologies can result in continued demand.

### 6.1.3 Environmental impacts

- Minimization of environmental impacts, since the probability of the new technology causing or contributing to the occurrence of leaks, or other environmental incidents, is controlled since development, contributing to the preservation of ecosystems close to oil exploration sites.
- Compliance with environmental regulations, given the alignment of the proposed methodology with the standards and practical recommendations of



the petroleum industry, such as the RP API 17Q, mitigating possible negative impacts on the company's reputation and avoiding financial penalties.

## 6.2 LIMITATIONS AND FUTURE WORKS

The Bayesian model described in section 2.4 considers that all information collected to construct prior distributions and likelihood functions is 100% relevant. This may be unrealistic for information obtained during development, as it does not come from the actual application of the system, but from expert opinions, prototype tests and applications of similar systems, which can introduce additional uncertainties to the model and overestimate or underestimate reliability. A possible advance in the proposed Bayesian model consists in inserting a factor that weights the distributions and likelihood functions based on the relevance of the information used to construct them. For example, suppose that the data extracted from a certain test is considered 70% relevant, compared to the real application of the system, thus the likelihood function can be formulated by  $L(test|\theta_i)^{0.7}$ . It is worth mentioning that the implementation of this solution requires the conception of a procedure to define the relevance factors of each information collected throughout development.

Also, the informative a priori distributions obtained by the procedures proposed in chapters 3 and 4 are dependent only on data from expert opinions and generic databases (e.g.: Wellmaster), with no limitation on the shape of the resulting distributions. This means that "very informative" prior distributions can be obtained, with low uncertainty on  $\theta_i$ , so that little or no update is achieved with the likelihoods formulated from the test data. As future work, the methodologies described in chapters 3 and 4 can introduce additional uncertainty into the estimates extracted from generic databases and limits for the pessimistic and optimistic opinions of experts, so that the resulting distributions have a minimum acceptable dispersion to compose the a priori estimate of reliability.

Furthermore, the proposed methodology, despite being an operationalization of the qualification process defined in API 17Q, does not guarantee that the reliability target will be met at the end of development, as there is no process for defining the tests necessary for this. Thus, an additional module for optimal test planning can be developed and linked to the methodology so that the posterior reliability estimate obtained at the last Gate satisfies the reliability requirement of the technology.

## REFERENCES

ABBASZADEH, B. et al. Development of a Procedure for Risk-Based Qualification of Additively Manufactured Components: Adopting to Oil and Gas Industrial Applications. **Applied Sciences (Switzerland)**, v. 12, n. 20, 2022.

ADVANCED WELL EQUIPMENT STANDARD GROUP. **AWES Recommended Practice For Control Lines (CL)**. [s.l: s.n.].

AFUEKWE, A.; BELLO, K. Use of Smart Controls in Intelligent Well Completion to Optimize Oil & Gas Recovery. **Journal of Engineering Research and Reports**, 2019.

AMERICAN BUREAU OF SHIPPING. **Guidance Notes on Qualifying New Technologies**. [s.l: s.n.]. Disponível em: <[www.eagle.org](http://www.eagle.org)>.

AMERICAN PETROLEUM INSTITUTE. **API 17N - Recommended Practice on Subsea Production System Reliability, Technical Risk, and Integrity Management**. [s.l: s.n.].

AMERICAN PETROLEUM INSTITUTE. **API RP 17Q - Recommended Practice on Subsea Equipment Qualification**. [s.l: s.n.].

AMERICAN PETROLEUM INSTITUTE. **API SPEC 19V Subsurface Completion Isolation (Barrier) Valves and Related Equipment**. [s.l: s.n.].

AMERICAN PETROLEUM INSTITUTE. **API Specification 5CT, Casing and Tubing**. [s.l: s.n.].

AMERICAN PETROLEUM INSTITUTE. **API - SPEC 19G2 Flow-control Devices for Side-pocket Mandrels**. [s.l: s.n.].

AMERICAN PETROLEUM INSTITUTE. **API SPEC 11D1: Packers and Bridge Plugs**. [s.l: s.n.].

**API SPEC 14A: Subsurface Safety Valve and Annular Safety Valve Equipment**. 13. ed. [s.l.] International Organization for Standardization, 2024.

**API Standard 17F Standard for Subsea Production Control Systems**. 3. ed. [s.l.] American Petroleum Institute, 2014.

ARIF, J.; REHMAN-SHAikh, M. A.; EVANGELOU, S. Novel evaluation and testing of technology qualification process of subsea oil and gas products. **Journal of Petroleum Science and Engineering**, v. 208, 2022.

AVILA, J. C. **Forecasting intelligent-well completion production through a coupled reservoir model with custom functionality**. Proceedings of the Annual Offshore Technology Conference. **Anais...**2020.

AZEVEDO, R. et al. **Methodology for assessing the reliability of equipment under development**. Book of Extended Abstracts for the 32nd European Safety and Reliability Conference. **Anais...**2022a.

AZEVEDO, R. et al. **The use of Weibull-GRP Virtual Age Model for Addressing Degradation due to Demand Induced Stress in Reliability Analysis of On-demand Systems**. Book of Extended Abstracts for the 32nd European Safety and Reliability Conference. **Anais...**Singapore: Research Publishing Services, 2022b.

AZEVEDO, R. et al. **Methodology for Extracting Reliability from the Qualification Tests ISO 23936-2**. Proceeding of the 33rd European Safety and Reliability Conference. **Anais...**Singapore: Research Publishing Services, 2023.

AZEVEDO, R. V. et al. Technical assurance in new technology development projects: a reliability-based approach. **Rio Oil and Gas Expo and Conference**, v. 20, n. 2020, p. 135–136, 1 dez. 2020.

BAE, S. J.; KUO, W.; KVAM, P. H. Degradation models and implied lifetime distributions. **Reliability Engineering & System Safety**, v. 92, n. 5, p. 601–608, maio 2007.

BAHOOTOROODY, A. et al. On reliability challenges of repairable systems using hierarchical bayesian inference and maximum likelihood estimation. **Process Safety and Environmental Protection**, v. 135, p. 157–165, mar. 2020.

BAI, B. et al. Application of adaptive reliability importance sampling-based extended domain PSO on single mode failure in reliability engineering. **Information Sciences**, v. 546, p. 42–59, fev. 2021.

BEZERRA SOUTO MAIOR, C. et al. Remaining Useful Life Estimation by Empirical Mode Decomposition and Support Vector Machine. **IEEE Latin America Transactions**, v. 14, n. 11, p. 4603–4610, nov. 2016.

BLEI, D. M.; KUCUKELBIR, A.; MCAULIFFE, J. D. Variational Inference: A Review for Statisticians. **Journal of the American Statistical Association**, v. 112, n. 518, p. 859–877, 3 abr. 2017.

BOLGER, D.; HOULDING, B. Deriving the probability of a linear opinion pooling method being superior to a set of alternatives. **Reliability Engineering & System Safety**, v. 158, p. 41–49, fev. 2017.

BOUDALI, H.; DUGAN, J. B. A discrete-time Bayesian network reliability modeling and analysis framework. **Reliability Engineering & System Safety**, v. 87, n. 3, p. 337–349, mar. 2005.

BRATTON, D.; KENNEDY, J. **Defining a Standard for Particle Swarm Optimization**. 2007 IEEE Swarm Intelligence Symposium. **Anais...IEEE**, abr. 2007.

BRONI-BEDIAKO, E. et al. Application of intelligent well completion in optimising oil production from oil rim reservoirs. **Advances in Geo-Energy Research**, v. 3, n. 4, 2019.

CARVALHO, L. F.; DA SILVA, M. F. **Completação inteligente elétrica no pré-sal**. Disponível em: <<https://petroleohoje.editorabrasilenergia.com.br/completacao-inteligente-eletrica-no-pre-sal/>>. Acesso em: 5 fev. 2024.

CATELANI, M.; CIANI, L.; VENZI, M. Failure modes, mechanisms and effect analysis on temperature redundant sensor stage. **Reliability Engineering and System Safety**, v. 180, 2018.

CORMEN, T. H. et al. **Introduction to Algorithms**. 3. ed. [s.l.] The MIT Press, 2009.

DA SILVA, M. F. et al. **Cableless intelligent well completion development based on reliability**. OTC Brasil 2017. **Anais...2017**.

DAS CHAGAS MOURA, M. et al. Estimation of expected number of accidents and workforce unavailability through Bayesian population variability analysis and Markov-based model. **Reliability Engineering & System Safety**, v. 150, p. 136–146, jun. 2016.

DENNEY, D. Reliability Management of Deepwater Subsea Field Developments. **JPT, Journal of Petroleum Technology**, v. 55, n. 12, 2003.

DET NORSKE VERITAS. **DNVGL RP A203 - Technology Qualification**. [s.l.: s.n.]. Disponível em: <<http://www.dnvgl.com>>.

DROGUETT, E. L. et al. Variable selection and uncertainty analysis of scale growth rate under pre-salt oil wells conditions using support vector regression. **Proceedings of the Institution of Mechanical Engineers, Part O: Journal of Risk and Reliability**, v. 229, n. 4, p. 319–326, 14 ago. 2015.

DUBEY, V.; ABEDI, S.; NOSHADRAVAN, A. A multiscale modeling of damage accumulation and permeability variation in shale rocks under mechanical loading. **Journal of Petroleum Science and Engineering**, v. 198, p. 108123, mar. 2021.

EREN, T.; POLAT, C. Numerical investigation of the application of intelligent horizontal well completion. **Journal of Natural Gas Science and Engineering**, v. 83, 2020.

FEDER, J. Subsea Water-Treatment System Installed in Pilot Test at Ekofisk. **Journal of Petroleum Technology**, v. 71, n. 12, 2019.

FOTHERGILL, J. **Ratings Standardization for Production Packers**. All Days. **Anais...SPE**, 23 mar. 2003.

GAO, P.; XIE, L. Fuzzy Dynamic Reliability Models of Parallel Mechanical Systems Considering Strength Degradation Path Dependence and Failure Dependence. **Mathematical Problems in Engineering**, v. 2015, p. 649726, 2015.

GARCÍA NIETO, P. J. et al. Hybrid PSO–SVM-based method for forecasting of the remaining useful life for aircraft engines and evaluation of its reliability. **Reliability Engineering & System Safety**, v. 138, p. 219–231, jun. 2015.

GELMAN, A. Prior distributions for variance parameters in hierarchical models (comment on article by Browne and Draper). **Bayesian Analysis**, v. 1, n. 3, 1 set. 2006.

GELMAN, A.; SIMPSON, D.; BETANCOURT, M. The Prior Can Often Only Be Understood in the Context of the Likelihood. **Entropy**, v. 19, n. 10, p. 555, 19 out. 2017.

GRECO, S. F.; PODOFILLINI, L.; DANG, V. N. A Bayesian model to treat within-category and crew-to-crew variability in simulator data for Human Reliability Analysis. **Reliability Engineering & System Safety**, v. 206, p. 107309, fev. 2021a.

GRECO, S. F.; PODOFILLINI, L.; DANG, V. N. A Bayesian model to treat within-category and crew-to-crew variability in simulator data for Human Reliability Analysis. **Reliability Engineering & System Safety**, v. 206, p. 107309, fev. 2021b.

GRECO, S. F.; PODOFILLINI, L.; DANG, V. N. A Bayesian two-stage approach to integrate simulator data and expert judgment in human error probability estimation. **Safety Science**, v. 159, p. 106009, mar. 2023.

GRIBOK, A.; AGARWAL, V.; YADAV, V. Performance of empirical Bayes estimation techniques used in probabilistic risk assessment. **Reliability Engineering & System Safety**, v. 201, p. 106805, set. 2020.

GRISHKO, A.; YURKOV, N.; GORYACHEV, N. **Reliability analysis of complex systems based on the probability dynamics of subsystem failures and deviation of parameters**. 2017 14th International Conference The Experience of Designing and Application of CAD Systems in Microelectronics (CADSM). **Anais...IEEE**, 2017.

GRUNDLER, A.; DAZER, M.; HERZIG, T. Statistical Power Analysis in Reliability Demonstration Testing: The Probability of Test Success. **Applied Sciences (Switzerland)**, v. 12, n. 12, 2022.

GUO, J.; LI, Z.; KEYSER, T. A Bayesian approach for integrating multilevel priors and data for aerospace system reliability assessment. **Chinese Journal of Aeronautics**, v. 31, n. 1, p. 41–53, jan. 2018.

GUO, J.; (STEVEN) LI, Z.; (JUDY) JIN, J. System reliability assessment with multilevel information using the Bayesian melding method. **Reliability Engineering & System Safety**, v. 170, p. 146–158, fev. 2018.

HAGGAG, A. et al. Physical model for the power-law voltage and current acceleration of TDDb. **Microelectronics Reliability**, v. 45, n. 12, p. 1855–1860, 1 dez. 2005.

HARTLEY, D.; FRENCH, S. A Bayesian method for calibration and aggregation of expert judgement. **International Journal of Approximate Reasoning**, v. 130, p. 192–225, mar. 2021.

HU, J. et al. New Development of Intelligent Well Completion Technology in Oil Industry. **Journal of Innovation and Social Science Research**, v. 8, n. 7, 2021.

INTERNATIONAL ORGANIZATION FOR STANDARDIZATION. **ISO 14310 Petroleum and natural gas industries — Downhole equipment — Packers and bridge plugs**. [s.l: s.n.].

INTERNATIONAL ORGANIZATION FOR STANDARDIZATION. **ISO 14224 - Petroleum, petrochemical and natural gas industries - Collection and exchange of reliability and maintenance data for equipment**. [s.l: s.n.]. Disponível em: <[www.iso.org](http://www.iso.org)>.

INTERNATIONAL ORGANIZATION FOR STANDARDIZATION. **ISO 15156-1 Petroleum and natural gas industries — Materials for use in H<sub>2</sub>S-containing environments in oil and gas production. Part 1: General principles for selection of cracking-resistant materials**. [s.l: s.n.].

**ISO 11960 - Petroleum and natural gas industries — Steel pipes for use as casing or tubing for wells**. 6. ed. [s.l.] International Organization for Standardization, 2020.

**ISO 23936-2 Petroleum, petrochemical and natural gas industries — Non-metallic materials in contact with media related to oil and gas production. Part 2: Elastomers**. 1. ed. [s.l: s.n.].

JACINTO, C. C. et al. **World's First: Annular Barrier Installed in a Subsea, Deepwater Well without the Use of Cement**. Day 1 Tue, October 27, 2015. **Anais...OTC**, 27 out. 2015.

JACKSON, C.; MOSLEH, A. Bayesian inference with overlapping data: Reliability estimation of multi-state on-demand continuous life metric systems with uncertain evidence. **Reliability Engineering & System Safety**, v. 145, p. 124–135, 2016.

JAYNES, E. T. Information Theory and Statistical Mechanics. **Physical Review**, v. 106, n. 4, p. 620–630, 15 maio 1957.

JIA, X.; GUO, B. Reliability analysis for complex system with multi-source data integration and multi-level data transmission. **Reliability Engineering & System Safety**, v. 217, p. 108050, jan. 2022.

JIANG, P. et al. A reliability demonstration test plan derivation method based on subsystem test data. **Computers and Industrial Engineering**, v. 170, 2022.

KANG, H. Y.; KWAK, B. M. Application of maximum entropy principle for reliability-based design optimization. **Structural and Multidisciplinary Optimization**, v. 38, n. 4, p. 331–346, 19 maio 2009.

KELLY, D. L.; SMITH, C. L. Bayesian inference in probabilistic risk assessment—The current state of the art. **Reliability Engineering & System Safety**, v. 94, n. 2, p. 628–643, fev. 2009.

KIRAN, D. R. Failure Modes and Effects Analysis. **Total Quality Management**, p. 373–389, 1 jan. 2017.

KLEYNHANS, G. et al. **Development and qualification of a subsea compressor**. Proceedings of the Annual Offshore Technology Conference. **Anais...**2016.

KONG, B. et al. Bayesian probabilistic dual-flow-regime decline curve analysis for complex production profile evaluation. **Journal of Petroleum Science and Engineering**, v. 195, p. 107623, dez. 2020.

KRIVTSOV, V. A Bayesian Estimation Procedure of Reliability Function for Lifetime Distributions. **International Journal of Performability Engineering**, 2017.

KUERSTEINER, G. M.; MATYAS, L. Generalized Method of Moments Estimation. **Journal of the American Statistical Association**, v. 95, n. 451, p. 1014, set. 2000.

LAM, S. K.; PITROU, A.; SEIBERT, S. **Numba**. Proceedings of the Second Workshop on the LLVM Compiler Infrastructure in HPC. **Anais...**New York, NY, USA: ACM, 15 nov. 2015.

LI, M. et al. Bayesian modeling of multi-state hierarchical systems with multi-level information aggregation. **Reliability Engineering & System Safety**, v. 124, p. 158–164, 2014.

LI, X. et al. Dynamic risk assessment of subsea pipelines leak using precursor data. **Ocean Engineering**, v. 178, p. 156–169, abr. 2019.

LI, Z. Mechanical analysis of tubing string in well testing operation. **Journal of Petroleum Science and Engineering**, v. 90–91, p. 61–69, jul. 2012.

LIANG, Q. et al. Experimental study on the local drag of completion string with packers in horizontal wells. **Coatings**, v. 10, n. 7, 2020.

LINS, I. D. et al. A particle swarm-optimized support vector machine for reliability prediction. **Quality and Reliability Engineering International**, v. 28, n. 2, p. 141–158, 22 mar. 2012.

LIU, S. J. et al. **One Innovative Intelligent Completion Intermediate String Design for Deepwater Gas Well Completions: The Installation Case Study from L Gas Field, China**. International Petroleum Technology Conference, IPTC 2022. **Anais...**2022.

LLOYD'S REGISTER. **Guidance Notes for Certification through Technology Qualification**. [s.l: s.n.].

MACEDO, J. et al. **A Bayesian prior distribution for novel on-demand equipment based on experts' opinion: A case study in the O&G industry**. Book of Extended Abstracts for the 32nd European Safety and Reliability Conference. **Anais...**2022.

MACEDO, J. B. et al. Using experts' opinion for Bayesian prior reliability distribution of on-demand equipment: A case study of a novel sliding sleeve valve for open-hole wells. **Reliability Engineering & System Safety**, v. 238, p. 109430, 1 out. 2023.

MAIOR, C. B. S. et al. Bayesian prior distribution based on generic data and experts' opinion: A case study in the O&G industry. **Journal of Petroleum Science and Engineering**, v. 210, p. 109891, 1 mar. 2022.



MAIOR, C. S. et al. **Physics-Based Accelerated RDT Testing for High Reliable Equipment**. Proceedings of the 31st European Safety and Reliability Conference (ESREL 2021). **Anais...**Singapore: Research Publishing Services, 2021.

MARINI, F.; WALCZAK, B. Particle swarm optimization (PSO). A tutorial. **Chemometrics and Intelligent Laboratory Systems**, v. 149, p. 153–165, dez. 2015.

MARTORELL, P. et al. Unavailability model for demand-caused failures of safety components addressing degradation by demand-induced stress, maintenance effectiveness and test efficiency. **Reliability Engineering & System Safety**, v. 168, p. 18–27, dez. 2017.

MASON, K.; DUGGAN, J.; HOWLEY, E. A meta optimisation analysis of particle swarm optimisation velocity update equations for watershed management learning. **Applied Soft Computing**, v. 62, p. 148–161, jan. 2018.

MCGEORGE, D. et al. **Hybrid and composite risers for deep waters and aggressive reservoirs**. Offshore Mediterranean Conference and Exhibition 2019, OMC 2019. **Anais...**2019.

MCPHERSON, J. **Reliability Physics and Engineering Time-To-Failure Modeling Third Edition**. [s.l: s.n.].

MENEZES, E. et al. **Proposal of a Test Protocol for Reliability Evaluation of O&G Equipment**. Book of Extended Abstracts for the 32nd European Safety and Reliability Conference. **Anais...**Singapore: Research Publishing Services, 2022.

MERUANE, V. et al. Impact Location and Quantification on an Aluminum Sandwich Panel Using Principal Component Analysis and Linear Approximation with Maximum Entropy. **Entropy**, v. 19, n. 4, p. 137, 25 mar. 2017.

MODARRES, M. Probabilistic Physics-of-Failure Approach in Reliability Engineering. Em: MISRA, K. B. (Ed.). **Handbook of Advanced Performability Engineering**. Cham: Springer International Publishing, 2021. p. 479–500.

MODARRES, M.; AMIRI, M.; JACKSON, C. Summary of Mechanisms of Failure and Associated PoF Models. Em: **Probabilistic Physics of Failure Approach to Reliability**. [s.l.] John Wiley & Sons, Ltd, 2017. p. 13–99.

MOLNES, E.; STRAND, G.-O. **Application of a Completion Equipment Reliability Database in Decision Making**. All Days. **Anais...**SPE, 1 out. 2000.

MUHAMMAD, N. et al. Reliability and remaining life assessment of an electronic fuze using accelerated life testing. **Micromachines**, v. 11, n. 3, 2020.

MUNKHAMMAR, J.; MATTSSON, L.; RYDÉN, J. Polynomial probability distribution estimation using the method of moments. **PLOS ONE**, v. 12, n. 4, p. e0174573, 10 abr. 2017.

NI, S. et al. Risk identification and quantitative assessment method of offshore platform equipment. **Energy Reports**, v. 8, 2022.

O'CONNOR, A.; MODARRES, M.; MOSLEH, A. **Probability Distributions Used in Reliability Engineering**. [s.l: s.n.].

OHGATA, K. et al. **Universality of power-law voltage dependence for TDDb lifetime in thin gate oxide PMOSFETs**. 2005 IEEE International Reliability Physics Symposium, 2005. Proceedings. 43rd Annual. **Anais...**2005.

PAGGI, A. et al. **Prediction by means hazard rate occurrence is a deeply wrong approach**. 2017 IEEE International Workshop on Metrology for AeroSpace (MetroAeroSpace). **Anais...**2017.

PANDYA, D. et al. Quantification of a human reliability analysis method for radiotherapy applications based on expert judgment aggregation. **Reliability Engineering & System Safety**, v. 194, p. 106489, fev. 2020.

PAREEK, C. M. et al. Optimizing the seed-cell filling performance of an inclined plate seed metering device using integrated ANN-PSO approach. **Artificial Intelligence in Agriculture**, v. 5, p. 1–12, 2021.

PATEL, H. et al. Review of elastomer seal assemblies in oil & gas wells: Performance evaluation, failure mechanisms, and gaps in industry standards. **Journal of Petroleum Science and Engineering**, v. 179, p. 1046–1062, 1 ago. 2019.

PENG, W. et al. Life cycle reliability assessment of new products—A Bayesian model updating approach. **Reliability Engineering & System Safety**, v. 112, p. 109–119, abr. 2013.

POURGOL, M. et al. Probabilistic Physics of Failure (PPOF) Reliability Analysis of RF-MEMS Switches under Uncertainty. **International Journal of Reliability, Risk and Safety: Theory and Application**, 2018.

RAHIMI, M.; RAUSAND, M. Prediction of failure rates for new subsea systems: A practical approach and an illustrative example. **Proceedings of the Institution of Mechanical Engineers, Part O: Journal of Risk and Reliability**, v. 227, n. 6, 2013.

RANE, S. B.; POTDAR, P. R.; RANE, S. Accelerated life testing for reliability improvement: a case study on Moulded Case Circuit Breaker (MCCB) mechanism.

**International Journal of System Assurance Engineering and Management**, v. 10, n. 6, p. 1668–1690, 19 dez. 2019.

RAOUFI, M. H.; FARASAT, A.; MOHAMMADIFARD, M. Application of simulated annealing optimization algorithm to optimal operation of intelligent well completions in an offshore oil reservoir. **Journal of Petroleum Exploration and Production Technology**, v. 5, n. 3, 2015.

RATNAYAKE, R. M. C.; SAMARAKOON, S. M. S. M. K.; GUDMESTAD, O. T. **Use of technology qualification in offshore oil and gas operations: An FMECA analysis for mitigating potential failures**. Proceedings of the International Conference on Offshore Mechanics and Arctic Engineering - OMAE. **Anais...**2014.

REGATTIERI, A. et al. Reliability Assessment of a Packaging Automatic Machine by Accelerated Life Testing Approach. **Procedia Manufacturing**, v. 11, 2017.

ROSSI, R. **Mathematical Statistics: An Introduction to Likelihood Based Inference**. [s.l: s.n.].

RUIJTERS, E. et al. Rare event simulation for dynamic fault trees. **Reliability Engineering & System Safety**, v. 186, p. 220–231, jun. 2019.

SABRI-LAGHAIE, K. et al. A novel reliability monitoring scheme based on the monitoring of manufacturing quality error rates. **Reliability Engineering & System Safety**, v. 217, p. 108065, jan. 2022.

SANTANA, J. M. et al. **Reliability-based Guidelines for Elaborating Technical Specifications of New Technologies**. Book of Extended Abstracts for the 32nd European Safety and Reliability Conference. **Anais...**Singapore: Research Publishing Services, 2022.

SANTANA, J. M. et al. **Development of a Software Tool to Implement Reliability Assessment of Developing Technologies**. Proceeding of the 33rd European Safety and Reliability Conference. **Anais...**Singapore: Research Publishing Services, 2023.

SCHAEFER, B. D. C.; SAMPAIO, M. A. Efficient workflow for optimizing intelligent well completion using production parameters in real-time. **Oil and Gas Science and Technology**, v. 75, 2020.

SHAKHATREH, M. K.; LEMONTE, A. J.; MORENO–ARENAS, G. The log-normal modified Weibull distribution and its reliability implications. **Reliability Engineering & System Safety**, v. 188, p. 6–22, ago. 2019.

SINGH, C.; MITRA, J. **Monte Carlo simulation for reliability analysis of emergency and standby power systems**. IAS '95. Conference Record of the 1995 IEEE Industry Applications Conference Thirtieth IAS Annual Meeting. **Anais...IEEE**, 1995.

SOLOVYEVA, V. A.; ALMUHAMMADI, K. H.; BADEGHAISH, W. O. **Current Downhole Corrosion Control Solutions and Trends in the Oil and Gas Industry: A Review**. **Materials**, 2023.

SOUTO, M.; DAS CHAGAS MOURA, M.; LINS, I. Particle swarm-optimized support vector machines and pre-processing techniques for remaining useful life estimation of bearings. **Eksploatacja i Niezawodność – Maintenance and Reliability**, v. 21, n. 4, p. 610–618, 31 dez. 2019.

SPADE, D. A. Markov chain Monte Carlo methods: Theory and practice. Em: [s.l: s.n.]. p. 1–66.

SWAMINATHAN, S.; SMIDTS, C. The Event Sequence Diagram framework for dynamic Probabilistic Risk Assessment. **Reliability Engineering & System Safety**, v. 63, n. 1, p. 73–90, jan. 1999.

VIRTANEN, P. et al. SciPy 1.0: fundamental algorithms for scientific computing in Python. **Nature Methods**, v. 17, n. 3, p. 261–272, 2 mar. 2020.

VOSE, D. **Risk Analysis: A Quantitative Guide**. 3. ed. [s.l.] John Wiley & Sons, Ltd, 2008.

WALLIS, S. Binomial Confidence Intervals and Contingency Tests: Mathematical Fundamentals and the Evaluation of Alternative Methods. **Journal of Quantitative Linguistics**, v. 20, n. 3, p. 178–208, 4 ago. 2013.

WANG, F.; LI, H. On the use of the maximum entropy method for reliability evaluation involving stochastic process modeling. **Structural Safety**, v. 88, p. 102028, jan. 2021.

WANG, L. et al. A Bayesian reliability evaluation method with integrated accelerated degradation testing and field information. **Reliability Engineering & System Safety**, v. 112, p. 38–47, 1 abr. 2013.

WANG, L. et al. A Bayesian reliability evaluation method with different types of data from multiple sources. **Reliability Engineering & System Safety**, v. 167, p. 128–135, 1 nov. 2017.

WANG, W. et al. Model averaging based on generalized method of moments. **Economics Letters**, v. 200, p. 109735, mar. 2021.

WANG, Y.; LIU, Y. Bayesian entropy network for fusion of different types of information. **Reliability Engineering & System Safety**, v. 195, p. 106747, mar. 2020.

WEI, X.; WANG, Z.; GUO, J. Reliability assessment of transformer insulating oil using accelerated life testing. **Scientific Reports**, v. 12, n. 1, 2022.

WILKINS, J. **Qualification of thermoplastic composite pipes**. Proceedings of the International Conference on Offshore Mechanics and Arctic Engineering - OMAE. **Anais...**2018.

WILSON, A. G.; FRONCZYK, K. M. Bayesian Reliability: Combining Information. **Quality Engineering**, p. 0–0, 26 ago. 2016.

WOOLDRIDGE, J. M. Applications of Generalized Method of Moments Estimation. **Journal of Economic Perspectives**, v. 15, n. 4, p. 87–100, 1 nov. 2001.

WOSOWEI, J.; SHASTRY, C. An Efficient Intelligent Oil Well Monitoring System for Niger Delta Oil Fields. **International Journal of Advanced Research in Science, Communication and Technology**, 2023.

WRIGHT, E. J. **Enabling materials and corrosion technologies for optimizing offshore developments**. Proceedings of the Annual Offshore Technology Conference. **Anais...**2017.

XIE, C.; HUANG, H. Z. A Probabilistic Physics of Failure Approach for Structure Corrosion Reliability Analysis. **International Journal of Corrosion**, v. 2016, 2016.

YANG, L.; GUO, Y.; KONG, Z. On the performance evaluation of a hierarchical-structure prototype product using inconsistent prior information and limited test data. **Information Sciences**, v. 485, p. 362–375, jun. 2019.

YONTAY, P.; PAN, R. A computational Bayesian approach to dependency assessment in system reliability. **Reliability Engineering & System Safety**, v. 152, p. 104–114, 2016.

ZAHARIA, S. M.; POP, M. A.; UDROIU, R. Reliability and lifetime assessment of gliderwing's composite spar through accelerated fatigue life testing. **Materials**, v. 13, n. 10, 2020.

ZHAO, Y. A Bayesian approach to comparing human reliability analysis methods using human performance data. **Reliability Engineering & System Safety**, v. 219, p. 108213, mar. 2022.

ZHANG, J.; YANG, M.; XU, B.; DING, R.; CHENG, M.; DONG, P. A novel intelligent sliding sleeve for shale oil and gas mining equipment. **Journal of Petroleum Science and Engineering**, v. 158, p. 1-10, sep. 2017.